ผลการเสริมฤทธิ์ของซิตรอลเมื่อให้ร่วมกับยารักษามะเร็งดอกโซรูบิซิน
วินคริสติน หรืออีโทโปไซด์ ต่อเซลล์มะเร็งชนิดบีลิมโฟมาของมนุษย์

นางสาวดารินี ดังก้อง

POTENTIATING EFFECT OF CITRAL IN COMBINATION WITH DOXORUBICIN,
VINCRISTINE OR ETOPOSIDE ON HUMAN B-LYMPHOMA CELLS

Miss Darinee Dangkong

A Dissertation Submitted in Partial Fulfillment of the Requirements
for the Degree of Doctor of Philosophy Program in Pharmacology
(Interdisciplinary Program)
Graduate School
Chulalongkorn University
Academic Year 2013

| | |
|---|---|
| Thesis Title | POTENTIATING EFFECT OF CITRAL IN COMBINATION WITH DOXORUBICIN, VINCRISTINE OR ETOPOSIDE ON HUMAN B-LYMPHOMA CELLS |
| By | Miss Darinee Dangkong |
| Field of Study | Pharmacology |
| Thesis Advisor | Assistant Professor Wacharee Limpanasithikul, Ph.D. |

Accepted by the Graduate School, Chulalongkorn University in Partial Fulfillment of the Requirements for the Doctoral Degree

............................................................Dean of the Graduate School

(Associate Professor Amorn Petsom, Ph.D.)

THESIS COMMITTEE

............................................................Chairman

(Assistant Professor Naowarat Suthamnatpong, D.V.M., Ph.D.)

............................................................Thesis Advisor

(Assistant Professor Wacharee Limpanasithikul, Ph.D.)

............................................................Examiner

(Sireerat Sooampon, D.D.S., Ph.D.)

............................................................Examiner

(Piyanuch Wonganan, Ph.D.)

............................................................External Examiner

(Pongpun Siripong, Ph.D.)

ดารินี ดังก้อง : ผลการเสริมฤทธิ์ของซิตรอลเมื่อให้ร่วมกับยารักษามะเร็งดอกโซรูบิซิน วินคริสติน หรืออีโทโปไซด์ ต่อเซลล์มะเร็งชนิดบีลิมโฟมาของมนุษย์. (POTENTIATING EFFECT OF CITRAL IN COMBINATION WITH DOXORUBICIN, VINCRISTINE OR ETOPOSIDE ON HUMAN B-LYMPHOMA CELLS) อ.ที่ปรึกษาวิทยานิพนธ์หลัก: ผศ. ดร.วัชรี ลิมปนสิทธิกุล, 109 หน้า.

การศึกษานี้มีวัตถุประสงค์เพื่อศึกษาผลของซิตรอลต่อฤทธิ์ทำลายเซลล์มะเร็งของยาเคมีบำบัดดอกโซรูบิซิน วินคริสติน และอีโทโปไซด์ ในเซลล์มะเร็งเม็ดเลือดขาวของมนุษย์หรือรามอสเซลล์ จากการศึกษาความเป็นพิษโดยการย้อมเซลล์ด้วยรีซาซูริน พบว่า ซิตรอล ดอกโซรูบิซิน วินคริสติน และอีโทโปไซด์ มีความเป็นพิษต่อรามอสเซลล์หลังจากได้รับสารเหล่านี้นาน 24 ชั่วโมง โดยซิตรอลมีค่าความเข้มข้นที่ทำให้เซลล์ตายร้อยละ 50 (IC50) เท่ากับ 75.9 ไมโครโมลาร์ ซิตรอลที่ความเข้มข้น 10-40 ไมโครโมลาร์ เพิ่มความเป็นพิษของยาเคมีบำบัดทั้งสามชนิดต่อรามอสเซลล์ ทำให้ค่า IC50 ของยาแต่ละตัวมีค่าลดลง เมื่อให้ซิตรอลร่วมกับยาดังกล่าวในเซลล์เม็ดเลือดขาวจากคนปกติไม่พบการเพิ่มความเป็นพิษของยาเหล่านี้ ในการศึกษาผลของซิตรอลต่อการเหนี่ยวนำให้เซลล์ตายแบบเอพอพโตซิสโดยยาเคมีบำบัดทั้งสามชนิด โดยย้อมเซลล์ด้วย annexin V-FITC และ 4', 6-diamidino-2-phenylindole (DAPI) และวัดผลด้วยฟลูออเรสเซนโฟลไซโตมิเตอร์พบว่าซิตรอลเพิ่มความสามารถในการชักนำให้รามอสเซลล์เกิดเอพอพโทซิส ของดอกโซรูบิซิน วินคริสติน และอีโทโปไซด์ การศึกษานี้ได้ทำการตรวจสอบผลของซิตรอลต่อการแสดงออกในระดับ mRNA ของโปรตีนในกลุ่ม BCL-2 ในรามอสเซลล์ที่ได้รับยาเคมีบำบัดด้วยวิธี real time RT-PCR ซึ่งโปรตีนกลุ่ม BCL-2 มีความสำคัญในการควบคุมกระบวนการเอพอพโตซิส ผ่านทางไมโตคอนเดรีย พบว่าซิตรอลที่ความเข้มข้น 40 ไมโครโมลาร์ ชักนำให้การแสดงออกของ BAK ที่เหนี่ยวนำให้เซลล์ตายแบบเอพอพโทซิสเพิ่มขึ้น ในเซลล์รามอสที่ได้รับซิตรอลเพียงอย่างเดียว และในเซลล์ที่ได้รับซิตรอลร่วมกับยาเคมีบำบัดทั้งสามชนิด ซิตรอลทำให้การแสดงออกของ BCL-XL ที่ยับยั้งการตายแบบเอพอพโทซิสลดลงอย่างมีนัยสำคัญทางสถิติ เมื่อเทียบกับการให้ดอกโซรูบิซินเพียงอย่างเดียว ซิตรอลอาจเสริมฤทธิ์ของดอกโซรูบิซินในการชักนำให้เซลล์เกิดเอพอพโทซิส โดยผ่านการยับยั้งการแสดงออกของ BCL-XL นอกจากนี้พบว่าซิตรอลไม่มีผลต่อฤทธิ์ยับยั้งการแบ่งเซลล์มะเร็งของยาเคมีบำบัดทั้งสามตัว ผลจากการศึกษานี้สรุปได้ว่า ซิตรอลมีฤทธิ์เพิ่มความเป็นพิษของยาดอกโซรูบิซิน วินคริสติน และอีโทโปไซด์ ต่อเซลล์รามอส โดยเพิ่มความสามารถของยาเคมีบำบัดในการเหนี่ยวนำให้เซลล์มะเร็งเกิดการตายแบบเอพอพโทซิส ผลที่ได้รับจากการศึกษานี้อาจเป็นข้อมูลเบื้องต้นว่าซิตรอลที่เป็นส่วนประกอบในพืชหลายชนิดที่เป็นส่วนประกอบในอาหารอาจเสริมฤทธิ์กับยาเคมีบำบัดข้างต้น ที่นิยมใช้รักษาผู้ป่วยเซลล์มะเร็งชนิดบีลิมโฟมา ซึ่งผลดังกล่าว อาจนำมาใช้เป็นประโยชน์ในการใช้ยาร่วมกับการรับประทานอาหารหรือเครื่องดื่มที่มีซิตรอลเป็นองค์ประกอบในอนาคตได้ต่อไป

| | |
|---|---|
| สาขาวิชา เภสัชวิทยา | ลายมือชื่อนิสิต ........................................... |
| ปีการศึกษา 2556 | ลายมือชื่อ อ.ที่ปรึกษาวิทยานิพนธ์หลัก ............. |

# # 5187164120 : MAJOR PHARMACOLOGY

KEYWORDS: CITRAL / POTENTIATING EFFECT / CHEMO-POTENTIATION / HUMAN B-LYMPHOMA / RAMOS CELLS

DARINEE DANGKONG: POTENTIATING EFFECT OF CITRAL IN COMBINATION WITH DOXORUBICIN, VINCRISTINE OR ETOPOSIDE ON HUMAN B-LYMPHOMA CELLS. ADVISOR: ASST. PROF. WACHAREE LIMPANASITHIKUL, Ph.D., 109 pp.

This study intended to evaluate the potentiating effect of citral on anticancer effects of doxorubicin, vincristine, and etoposide against human lymphoma Ramos cells. Cytotoxicity of citral and anticancer drugs was determined by resazurin reduction assay. The results demonstrated that citral and these drugs had cytotoxicity on Ramos cells at 24 hours incubation. The IC50 value of citral was 75.9 µM. Citral at 10-40 µM significantly increased the cytotoxic effects of doxorubicin, vincristine, and etoposide on Ramos cells, leading to the decrease in the IC50 value of each drug. It did not increase the effect of these anticancer drugs on normal human peripheral blood mononuclear cells (PBMCs). This study also evaluated the effect of citral on apoptosis induction activity of the anticancer drugs by annexin V-FITC and 4', 6-diamidino-2-phenylindole (DAPI) staining monitored by fluorescence flow cytometer. The result demonstrated that citral increased anticancer drug-mediated apoptosis against human B lymphoma cells. BCL-2 family proteins play a pivotal role in the regulation of the mitochondrial pathway of apoptosis. Modulation of the mRNA expression of these proteins in the treated Ramos cells was also performed by real time RT-PCR. The mRNA expression of pro-apoptotic BAK was dramatically increased in Ramos cells treated with either 40 µM citral alone or in combination with anticancer drug. On the other hand, it significantly decreased the mRNA expression of anti-apoptotic BCL-XL when compared to the effect of the doxorubicin alone. Thus, it is possible that citral may potentiate apoptotic effect of doxorubicin by reducing the expression of anti-apoptotic BCL-XL. Citral did not change anti-proliferative effect of the drugs. In conclusion, citral potentiated cytotoxicity of doxorubicin, vincristine, and etoposide by increasing in apoptotic effect of these drugs. The results from this study may be an initial information about the possible potentiating anticancer activity of citral which is a component in several edible plants. This additive effect of citral may be useful for consuming food containing citral while using these anticancer drugs.

Field of Study:   Pharmacology          Student's Signature .........................................

Academic Year:   2013                  Advisor's Signature .........................................

# ACKNOWLEDGEMENTS

# CONTENTS

# LIST OF TABLES

Table                                                                                    Page

# LIST OF FIGURES

Figure Page

Figure                                                                                                          Page

# LIST OF ABBRIVIATIONS

| | |
|---|---|
| µg | Microgram |
| µg/ml | Microgram per milliliter |
| µm | Micrometre |
| µM | Micromolar |
| A 1 | BCL-2-related protein A1 |
| AIF | Apoptosis-inducing factor |
| ANOVA | Analysis of variance |
| APAF-1 | Apoptosis protease-activating factor 1 |
| ATCC | American Type Cell Culture |
| ATP | Adenosine triphosphate |
| BAD | BCL-2 antagonist of cell death |
| BAK | BCL-2-antagonist killer 1 |
| BAX | BCL-2 associated x protein |
| BCL-2 | B-cell lymphoma 2 |
| BCL-2A1 | BCL-2-related protein A1 |
| BCL-W | BCL2 like 2 protein |
| BCL-XL | BCL-2 related gene, long isoform |
| BH | BCL-2 homology domain |
| BH3 | BCL-2 homology 3 domain |
| BID | BH3 interacting domain death agonist |
| BIK | BCL-2-interacting killer |
| BIM | BCL-2-like-11 |

| | |
|---|---|
| BMF | BCL-2 modifying factor |
| $CaCl_2$ | Calcium chloride |
| CAD | Caspase-activated DNase |
| CD | Cluster-of-differentiation molecules |
| cDNA | Complementary deoxyribonucleic acid |
| CHOP | Cyclophosphamide, doxorubicin, vincristine, and prednisone |
| CHOPE | Cyclophosphamide, doxorubicin, vincristine, prednisone, and etoposide |
| CI | Combination index |
| $CO_2$ | Carbon dioxide |
| COX-2 | Cyclooxygenase 2 |
| $C_T$ | Cycle threshold |
| DAPI | 4', 6-diamidino-2-phenylindole |
| dATP | Deoxyadenosine triphosphate |
| $ddH_2O$ | Double-distilled water |
| DEPC | Diethyl pyrocarbonate |
| DIABLO | Direct IAP-binding protein with low isoelectric point |
| DLBCL | Diffuse large B-cell lymphoma |
| DMBA | 7, 12- dimethylbenz (a) anthracene |
| DNA | Deoxyribonucleic acid |
| dNTP | Deoxyribonucleotide |
| EDTA | Ethylenediaminetetraacetic acid |
| EndoG | Endonuclease G |

| | |
|---|---|
| EPOCH | Etoposide, prednisone, vincristine, cyclophosphamide, and doxorubicin |
| ER | Endoplasmic reticulum |
| FADD | Fas associated death domain |
| FasL | Fas ligand |
| FBS | Fetal bovine serum |
| g | Gram |
| GAPDH | Glyceraldehyde 3-phosphate dehydrogenase |
| HCl | Hydrochloric acid |
| HEPES | Hydroxyethyl piperazineethanesulfonic acid |
| HIF-1 | Hypoxia-inducible factor-1 |
| HRK | Harakiri |
| Htra2 | High temperature requirement A2 |
| IAPs | Inhibitors of apoptosis proteins |
| $IC_{50}$ | Inhibitory concentration 50 percent |
| ICAD | Inhibitor of caspase-activated DNase |
| IL | Interleukin |
| iNOS | Indicible nitric oxide synthase |
| KCl | Potassium chloride |
| Kg | Kilogram |
| $KH_2PO_4$ | Potassium dihydrogen phosphate |
| $LD_{50}$ | Lethal dose 50 percent |
| LPS | Lipopolysaccharide |
| M | Molar (mole per liter) |

| | |
|---|---|
| MCL-1 | Myeloid cell leukemia sequence-1 |
| mg | Milligram |
| $MgCl_2$ | Magnesium chloride |
| ml | Milliliter |
| mM | Millimolar |
| MOMP | Mitochondrial outer membrane permeabilization |
| mRNA | Messenger ribonucleic acid |
| MRSA | Methicillin-resistant *Staphylococcus aureus* |
| $Na_2HPO_4$ | Disodium hydrogen phosphate |
| NaCl | Sodium chloride |
| $NaHCO_3$ | Sodium bicarbonate |
| NaOH | Sodium hydroxide |
| NF-κB | Nuclear factor kappa B |
| NHL | Non-Hodgkin's lymphoma |
| nm | Nanometre |
| NO | Nitric oxide |
| NOXA | Phorbol-12-myristate-13-acetate-induced protein 1 |
| °C | Degree Celsius |
| PBMCs | Peripheral blood mononuclear cells |
| PBS | Phosphate buffer saline solution |
| pH | The negative logarithm of hydrogen ion concentration |
| ppm | Parts per million |
| PS | Phosphatidylserine |
| PUMA | P53-upregulated modulator of apoptosis |

| | |
|---|---|
| R-CHOP | Rituximab, cyclophosphamide, doxorubicin, vincristine, and prednisone |
| rpm | Revolution per minute |
| RPMI | Roswell Park Memorial Institute medium |
| RQ | Relative quantification |
| SDF-1 | Stromal cell-derived factor 1 |
| SEM | Standard error of mean |
| SMAC | Second mitochondria-derived activator of caspases |
| STAT3 | Signal transducer and activation of transcription 3 |
| tBID | BH3 interacting domain death agonist |
| TM | Transmembrane domain |
| VEGF | Vascular endothelial growth factor |
| $\Delta\psi m$ | Mitochondrial membrane potential |

# CHAPTER I

# INTRODUCTION

## 1.1 Background and rationale

Non-Hodgkin's lymphoma (NHL) is one of the most common hematologic malignancies worldwide. More than 80% of all NHL cases are B-cell lymphoma. The incidence is still rising with an estimated 355,900 new cases and 191,400 deaths from NHL occurred in 2008 (1). Although the treatment by CHOP regimen (cyclophosphamide, doxorubicin, vincristine, and prednisone) has been the standard front-line therapy for NHL patients, especially aggressive or advanced stage types such as diffuse large B-cell lymphoma which is the most common types of this disease, treatment failure is a major concern. Clinical studies have reported that the combination of etoposide and CHOP (EPOCH or CHOPE) for more efficacy of chemotherapy was intolerated in aggressive NHL patients with poor-prognostic disease and in the elderly patients (2; 3). Thus, strategies to decrease drug toxicity and improve its efficacy are urgently needed.

Over the past decade, medicinal plants have played an important role in the cancer therapy research. Many natural compounds such as curcumin, genistein, resveratrol, proanthocyanidin, emodin, silymarin, and flavopiridol have been reported to potentiate cytotoxicity of chemotherapeutic drugs in various cancer cell lines by enhancing chemotherapy-induced apoptosis (4-7). Citral or 3,7-dimethyl-2,6-octadienal is a volatile oil found in essential oils from several herbs and edible plants such as lemongrass (*Cymbopogon citratus*), lemon balm (*Melissa officinalis*), and *Litsea cubeba*. It is the main component (70-85%) in lemon grass essential oil (8).

Several pharmacological activities of citral have been documented such as anti-inflammatory effects, antimicrobial activities against Gram-positive and Gram-negative bacteria, fungi, and some protozoa, and anticancer activities against some cancer cell lines including leukemic, breast, and lymphoma cells. Treatment with citral resulted in an activation of caspase-3, leading to apoptosis in human (U937, HL60, and NB4), and mouse (RL12 and BS-24-1) leukemic cell lines (9). Moreover, it inhibited human breast cancer cells MCF-7 growth and induced cycle arrest in G2/M phase (10). Recently, an apoptotic activity of citral on acute promyelocytic leukemia cell line (NB4 cells) has been found and this effect was attributed to activation of caspase-3, and down-regulation of nuclear factor kappa B (NF-$\kappa$B) expression (11). Similarly, previous works have found that citral induced human lymphoma Ramos cell apoptosis by activating caspase activity in a concentration- and time-dependent manner but has no effect on the cell distribution in the cell cycle (12). It would be a better strategy if we combine citral with potent existing cytotoxic therapeutic agents. To our knowledge, the effect of citral on anticancer activities of chemotherapeutic agents has never been investigated. Therefore, this study was carried out to examine potentiating effect of citral on anticancer activities of commonly used cytotoxic drugs in NHL patients, doxorubicin, vincristine, and etoposide, on Ramos cells. Cytotoxic activity, anti-proliferative effect, apoptosis induction as well as the modulation of mRNA expression of BCL-2 family proteins responsible for intrinsic pathway of apoptosis of citral in drug-treated cells were elucidated in this study.

## 1.2 Research question

Does citral increase anticancer effects of doxorubicin, vincristine, and etoposide on human B lymphoma Ramos cells?

## 1.3 Objectives

1. To examine the potentiating effect of citral on cytotoxic activities of doxorubicin, vincristine, and etoposide in Ramos cells.

2. To determine the potentiating effect of citral on cytotoxicities of these drugs on normal white blood cells.

3. To elucidate molecular effect of citral to potentiate apoptotic effects of doxorubicin, vincristine, and etopposide in Ramos cells.

4. To study the effect of citral on anti-proliferative activities of doxorubicin, vincristine, and etoposide in Ramos cells.

## 1.4 Hypothesis

Citral potentially enhances anticancer effects of doxorubicin, vincristine, and etoposide on Ramos cells.

## 1.5 Expected benefits and applications

The results from this study may extended basic information about anticancer activity of citral which is a major constituent of several Thai spices. The information from this study may be useful for increasing therapeutic activity of chemotherapeutic agents. The strategy of combining citral with chemotherapy may represent an alternative approach to reduce the dose of the drugs as well as enhance the safety profile of such potent anticancer agents in NHL patients.

## 1.6 Keywords

Citral / potentiating effect / chemo-potentiation / human B-lymphoma / Ramos cells

# CHAPTER II

# LITERATURE REVIEWS

## 2.1 Non-Hodgkin's lymphoma

Non-Hodgkin's lymphoma (NHL) is a heterogeneous group of B- and T lymphocyte derived hematological malignances, and the most common cancer of the lymphatic system usually occurred in middle-aged and older people. This disease is more often found in men than women, and associated with increasing age. Approximately, 90% of all NHL cases are derived from B-lymphocytes at various stages of differentiation contributing to different types of B-cell neoplasms (13).

Clinically, NHL can be classified as indolent (low grade, intermediate) or aggressive (high grade) lymphoma. World Health Organization (WHO) categorizes NHL into more than 30 subtypes (Table 1) according to original types of cancer stimulating-lymphoid cells, morphological characteristics, immunophenotypes, and clinical features (14). Moreover, the Ann Arbor staging system is also used to divide the clinical stages of NHL into stage l-lV. Stage I is an early disease that the cancer is found only in a single lymph node in one organ or area outside the lymph node. Stage II is the locally advanced disease that cancer is found in two or more lymph node regions on one side of the diaphragm. Stage III is the advanced disease that the cancer involves lymph nodes on both sides of diaphragm. Stage IV is widespread disease that the cancer is found in several parts of one or more organs or tissues (15). The appropriate staging and classification of lymphomas are necessary to make the accurate diagnosis and treatment (16).

**Table 1:** Non-Hodgkin's lymphoma classification by WHO (14).

| WHO category |
| --- |
| B-cell lymphomas: single B-cell codes |
|     Small lymphocytic lymphoma or CLL |
|     Lymphoplasmacytic lymphoma / Waldenstrom's macroglobulinemia |
|     Mantle cell lymphoma |
|     DLBCL |
|     Burkitt's lymphoma / leukemia |
|     Splenic marginal zone lymphoma |
|     Follicular lymphoma |
|     Extranodal marginal zone B-cellb (MALT) lymphoma |
|     Nodal marginal zone lymphoma |
|     Precursor B-lymphoblastic lymphoma or leukemia |
|     Hairy cell leukemia |
| B-cell lymphomas: combined B-cell codes |
|     Small lymphocytic lymphoma or CLL and DLBCL |
|     Lymphoplasmacytic lymphoma / Waldenstrom's macroglobulinemia and plasma cell myeloma |
|     B-cell prolymphocytic leukemia + small lymphocytic lymphoma or CLL and DLBCL |
|     DLBCL and splenic marginal zone lymphoma |
|     DLBCL and follicular lymphoma |
|     DLBCL and MALT lymphoma |
|     DLBCL and nodal marginal zone lymphoma |
|     DLBCL and  precursor B-lymphoblastic lymphoma or leukemia |
|     Follicular lymphoma and Langerhans cell histiocytosis |
| T-cell, null, and NK lymphomas |
|     T-cell prolymphocytic leukemia |
|     Mycosis fungoides |
|     Sezary syndrome |
|     Peripheral T-cell lymphoma unspecified |
|     Angioimmunoblastic T-cell lymphoma |
|     Subcutaneous panniculitis-like T-cell lymphoma |
|     Anaplastic large-cell lymphoma |
|     Extranodal NK / T-cell lymphoma, nasal type |
|     Precursor T lymphoblastic lymphoma or leukemia |

Chronic lymphocytic leukemia (CLL)
Diffuse large B-cell lymphoma (DLBCL)

Diffuse large B-cell lymphoma (DLBCL) is the most common type of aggressive NHL around the world. From the International Lymphoma Study Project, DLBCL patients were founded 34% of all NHL cases (17). It has been found that more than 50% of DLBCL patients are older than 60 years old (15). Approximately 75% of patients are highly moderate to high risk (stage lll-lV) associated with worse prognosis.

At present, NHL is the fifth most common cancer in the United States and the eighth most common in Thailand (18). The incidence of this disease is still rising over years. In Thailand, it is also the most frequently found hematological cancer. However, the NHL's etiology is still unclear (16). Several risk factors are associated with an increased incidence of NHL including exposure to chemicals, organ transplantation, viral infection, blood transfusion, family history, and lifestyle factors.

## 2.2 Non-Hodgkin's lymphoma therapy

Treatment options for NHL patients are surgery, radiotherapy, immunotherapy and chemotherapy (16; 19). Because of the unlimited proliferation of B-cells in NHL, these tumors tend to be more chemo-sensitive and radio-sensitive. Radiotherapy is an effective treatment for NHL patients with localized disease. However, it is unsuccessful for advanced stages of the cancer (19). Combination chemotherapy has been standard treatment for NHL patients, especially aggressive or advanced stage types such as DLBCL which is the most common type of this disease (15; 19). Several chemotherapeutic regimens used in NHL patients are shown in table 2 (20).

**Table 2:** Common NHL chemotherapy regimens (15; 20).

| Regimens | |
|---|---|
| Primary treatment | |
| CHOP | Cyclophosphamide/ hydroxyldaunorubicin or doxorubicin/ vincristine/ prednisone |
| R-CHOP | Rituximab/ cyclophosphamide/ hydroxyldaunorubicin or doxorubicin/ vincristine/ prednisone |
| m-BACOD | Methotrexate/ bleomycin/ doxorubicin/ cyclophosphamide/ vincristine/ dexamethasone |
| ProMACE-CytaBOM | Cyclophosphamide/ doxorubicin/ etoposide cytozar/ bleomycin/ vincristine/ methotrexate/ prednisone |
| MACOP-B | Methotrexate with leucovorin rescue/ doxorubicin/ cyclophosphamide/ vincristine/ prednisone/ bleomycin |
| ProMACE-MOPP | Prednisone/ methotrexate/ cyclophosphamide/ etoposide/ doxorubicin/ rnechlorethamine/ vincristine/ procarbazine |
| CVP | Cyclophosphamide/ vincristine/ prednisone |
| COPA | Cyclophosphamide/ vincristine/ doxorubicin/ prednisone |
| COPADM | Cyclophosphamide/ vincristine/ prednisolone/ doxorubicin/ methotrexate |
| CHVP | Cyclophosphamide/ doxorubicin/ teniposide/ prednisone |
| COPP | Cyclophosphamide/ vincristine/ procarbazine/ prednisone |
| VACOP-B | Etoposide/ doxorubicin/ cyclophosphamide/ vincristine/ prednisone/ bleomycin |
| Salvage treatment | |
| IMVP-I 6 | Ifosfamide/ methotrexate/ etoposide |
| MIME | Methyl-gag/ ifosfamide/ methotrexate/ etoposide |
| ESHAP | Etoposide/ cytosine arabinoside/ cisplatin/ methylprednisolone |

## 2.3 Chemotherapy in non-Hodgkin's lymphoma

CHOP regimen is composed of cyclophosphamide, doxorubicin (hydroxydaunorubicin), vincristine (oncovin) and prednisone. This regimen is the front-line therapy for NHL and a gold standard regimen for DLBCL patients (15). It is a three-week cycle regimen which the number of cycles depends on the extent of the disease. The pharmacological properties of the drugs in CHOP regimen are as follows;

Cyclophosphamide

Cyclophosphamide is an alkylating agent which acts as a cell cycle non-specific anticancer drug. Chemical structure of this drug is shown below (Figure 1).
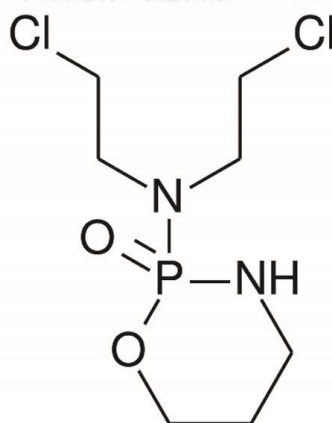


**Figure 1:** Chemical structure of cyclophosphamide.

Cyclophosphamide is a prodrug metabolized by cytochrome P450 mixed-function oxidase enzyme in the liver to 4-hydroxycyclophosphamide and aldophosphamide. Aldophosphamide is then cleaved to the cytotoxic form, phosphoramide mustard which acts as an antitumor agent and acrolein which causes

hemorrhagic cystitis. Phosphoramide mustard transfers its alkyl groups to various cellular proteins and DNA. Alkylation of DNA leads to cell death. The major site of alkylation within DNA is the N7 position of guanine but other bases, N1 and N3 of adenine, N3 of cytosine, and O6 of guanine, are also alkylated to lesser degrees. Cyclophosphamide has two alkyl groups so that DNA alkylation can occur on either a single strand or on double strands of DNA through cross-linking. Alkylation of guanine can result in miscoding through abnormal base pairing with thymine or in depurination by excision of guanine residues, leading to DNA strand breakage (21).

Cyclophosphamide is the most widely used alkylating agent in combined chemotherapy with other chemotherapeutic agents for several solid and hematologic tumors as well as for NHL. It is administered orally or intravenously. Its major side effects are bone marrow suppression, gastrointestinal ulceration and hemorrhagic cystitis which can be prevented by 2-mercaptoethane sulfonate (mesna) and diuresis (22).

Doxorubicin

Doxorubicin is an anthracycline antibiotic derived from *Streptococcus peucetius* var. *caesius*. It is a cell cycle non-specific drug. Chemical structure of this drug is shown below (Figure 2).
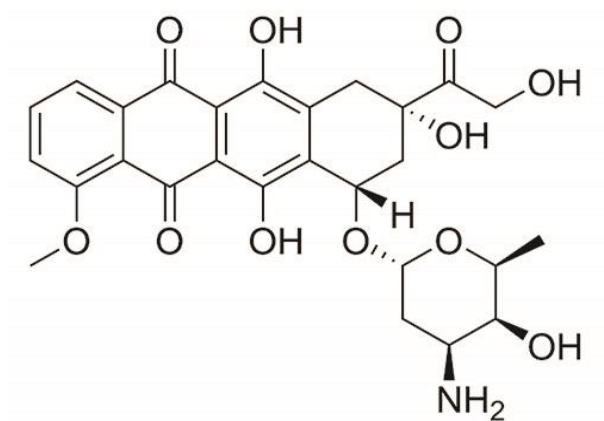
**Figure 2:** Chemical structure of doxorubicin.

Doxorubicin acts as a cytotoxic drug mainly via three mechanisms; 1) intercalate DNA which leads to inhibition of replication and transcription processes, 2) form a tripartite complex with topoisomerase II and DNA which causes the inhibition of the relegation of the broken DNA strands, leading to apoptosis, 3) form semiquinone radical intermediates which react with oxygen to generate cytotoxic free radicals [hydrogen peroxide ($H_2O_2$) and hydroxyl radicals ($\cdot OH$)] in both normal and malignant tissues. These free radicals attack DNA, oxidize DNA bases and lead to DNA damage, triggering apoptotic pathways of cell death (22).

Moreover, it has been reported that doxorubicin binds the proteasomes at cytoplasm after entering the cells. The binding of doxorubicin to proteasomes also inhibits the protease activity, suppressing the degradation of proteins involved in cell growth and metabolism and thus inducing apoptosis of these cells (23). A recent study shows that doxorubicin inhibits hypoxia-inducible factor-1 (HIF-1) from binding to DNA in hypoxic human cells and inhibited tumor growth in human prostate cancer xenografts. An inhibition of HIF-1 transcriptional activity leads to decreased vascular

endothelial growth factor (VEGF), and stromal cell-derived factor 1 (SDF-1) expression resulting in decreased tumor vascularization and growth (24).

Doxorubicin is a chemotherapeutic drug widely used in many combined regimens for several cancers as well as lymphomas. However, serious side effect often limits its use. Similar to cyclophosphamide, its common side effects are bone marrow suppression and gastrointestinal ulceration. The most important side effect of this drug is cardiotoxicity mediated by free radical which can be fatal (22).

Vincristine

Vincristine, an alkaloid derivative of *Vinca rosea*, is predominantly an M phase specific drug. Chemical structure of this drug is shown below (Figure 3).
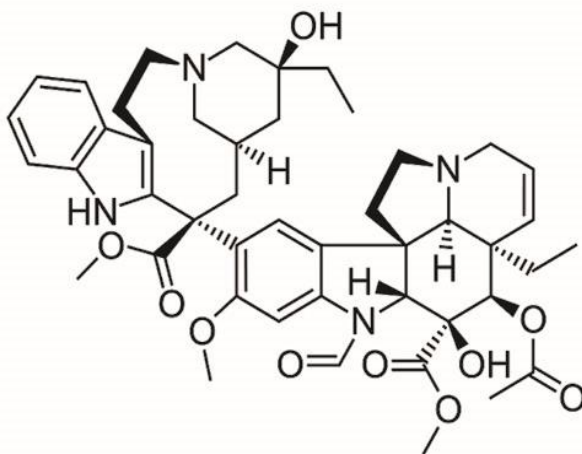


**Figure 3:** Chemical structure of vincristine.

Vincristine binds to $\beta$-tubulin and blocks the polymerization of the tubulin with $\alpha$-tubulin, leading to cell division arrest in metaphase of mitosis. Microtubules are also found in high concentration in the brain and are essential to other cellular functions

such as movement, phagocytosis, and axonal transport. Therefore, inhibition of microtubule polymerization disrupts microtubule functions, causing neurotoxicity (22). Vincristine is also widely used intravenously in various hematologic malignancies such as Hodgkin's and non-Hodgkin's lymphoma, multiple myeloma and several pediatric tumors including rhabdomyosarcoma, neuroblastoma, Ewing's sarcoma and Wilms' tumor (21).

Prednisone

Prednisone is a synthetic corticosteroid drug which is rapidly metabolized to the active metabolite prednisolone by liver enzyme. This drug is commonly used for various cancers as well as hematologic malignancies. Chemical structure of this drug is shown below (Figure 4).
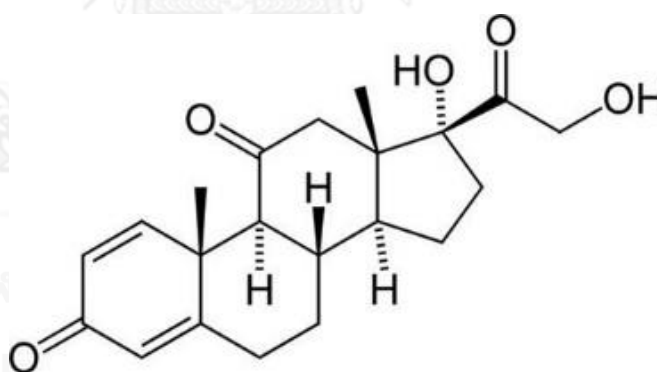


**Figure 4:** Chemical structure of prednisone.

Prednisone is a lipid-soluble drug that can cross the phospholipid bilayers of the cell membrane and binds to glucocorticoid receptor in the cytosol to form drug-receptor complex. The complex can translocate into the nucleus and acts as a transcription factor to turn on various target genes as well as genes associated with

the cell cycle of activated lymphoid cells leading to inhibition of proliferation, activation and migration of these cells. This drug affects on the expression of several genes so that many side effects are observed such as weight gain, fluid retention, mood swings, bone mineral loss, and thinning of the skin (25).

CHOP regimen remains the front-line therapy for NHL patients although the unsuccessful outcomes of this therapy have been frequently observed and concerned to be a major burden in these patients. Many clinical studies reported the occurrence of inadequate complete-response rate, poor long-term survival and relapse in DLBCL patients who received CHOP regimen with standard-dose treatment, with a cure rate less than 50% in the patients (26-28). Enhancing the dose of doxorubicin in CHOP regimen improved survival rate in cancer patients but fatal cardiotoxicity was a major limitation (29; 30). Addition of other cytotoxic drug, etoposide into CHOP, CHOPE or EPOCH leads to increasing cytotoxicity of conventional CHOP. Etoposide is an essential drug in salvage regimens for NHL patients (3). It is a semisynthetic derivative of podophyllotoxin extracted from *Podophyllum peltatum*. It is cell-cycle–specific agents, block cell division in the late S-G2 phase. Chemical structure of this drug is shown below (Figure 5).
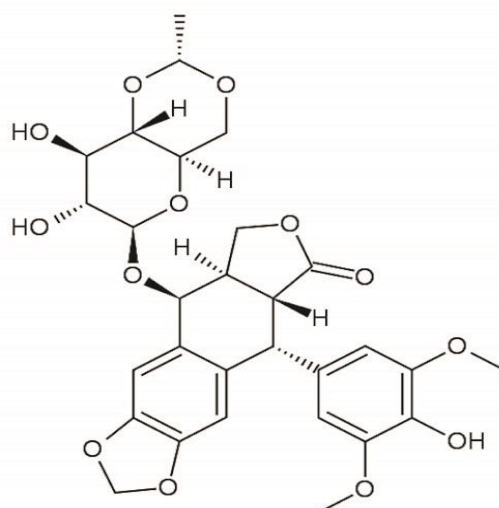
**Figure 5:** Chemical structure of etoposide.

Epotoside acts as a topoisomerase ll inhibitor by forming ternary complex with DNA and enzyme. This mechanism causes DNA damage through strand breakage, leading to cell death. Clinical studies have reported that the use of CHOP regimen with etoposide to provide more efficacy of chemotherapy was unsuccessfully tolerated toward aggressive NHL patients with poor-prognostic disease and the elderly patients (2). Side effects of this drug commonly found are alopecia, and bone marrow depression (21; 22). Thus, the effective strategies to improve treatment efficacy and reduce drug-associated toxicities in the patients are required.

## 2.4 Apoptosis

It has been widely accepted that apoptosis pathway is the key mechanism to eradicate tumor cells. Many currently used anticancer drugs are developed under the basic that they kill cancer cells by apoptosis induction.

Apoptosis or programmed cell death is an essential physiological process that plays a crucial role in controlling the number of cells in development and throughout the life by removal of cells at the appropriate time. It is also involved in a broad range of pathological conditions include neurodegenerative diseases, cardiovascular diseases, immunological diseases, and cancer (31). Apoptosis is characterized by cellular biochemical and morphological changes. These include cell shrinkage, chromatin condensation, multiple of 200 base pair DNA fragmentation, plasma membrane convolutes or blebbing, and the formation of membrane bound vesicles named as apoptotic bodies, but most organelles remain intact. These apoptotic bodies are recognized and engulfed by phagocytes without initiating any inflammatory response (Figure 6) (32).

There are three different pathways to initiated apoptosis (Figure 7) (33). 1) extrinsic apoptotic pathway which can be trigger by binding of death ligands to death receptors and consequent caspase-8 activation; 2) intrinsic apoptotic pathway, which is initiated by cellular stress followed by activation of caspase-9; or 3) perforin/granzyme pathway, where the cytotoxic T cell produces protease enzyme and delivers to sensitize target cells. Each of these pathways converges to a common execution step that requires proteolytic cleavage and activation of caspases-3 and/or caspases-7 (34).
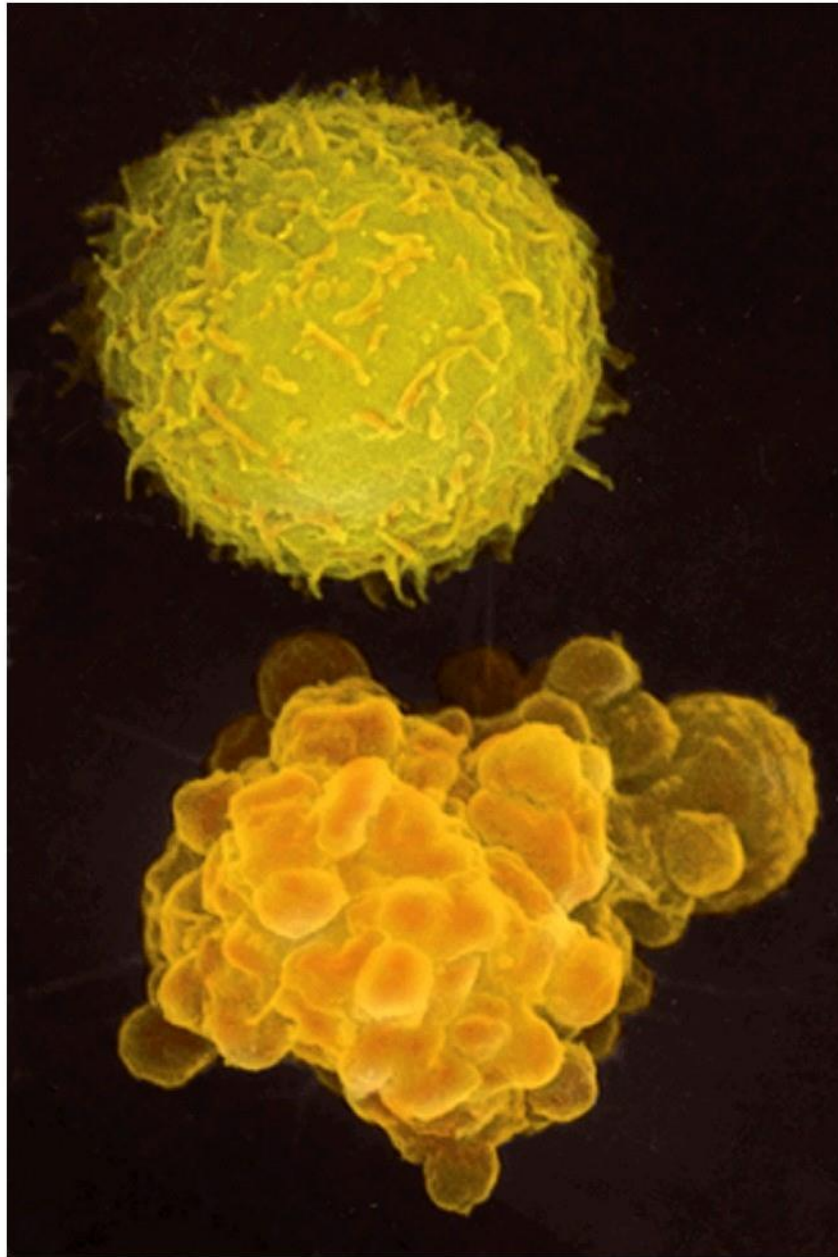
**Figure 6:** Photomicrographs comparing a normal lymphocyte (top) and apoptotic lymphocyte (bottom) (32).
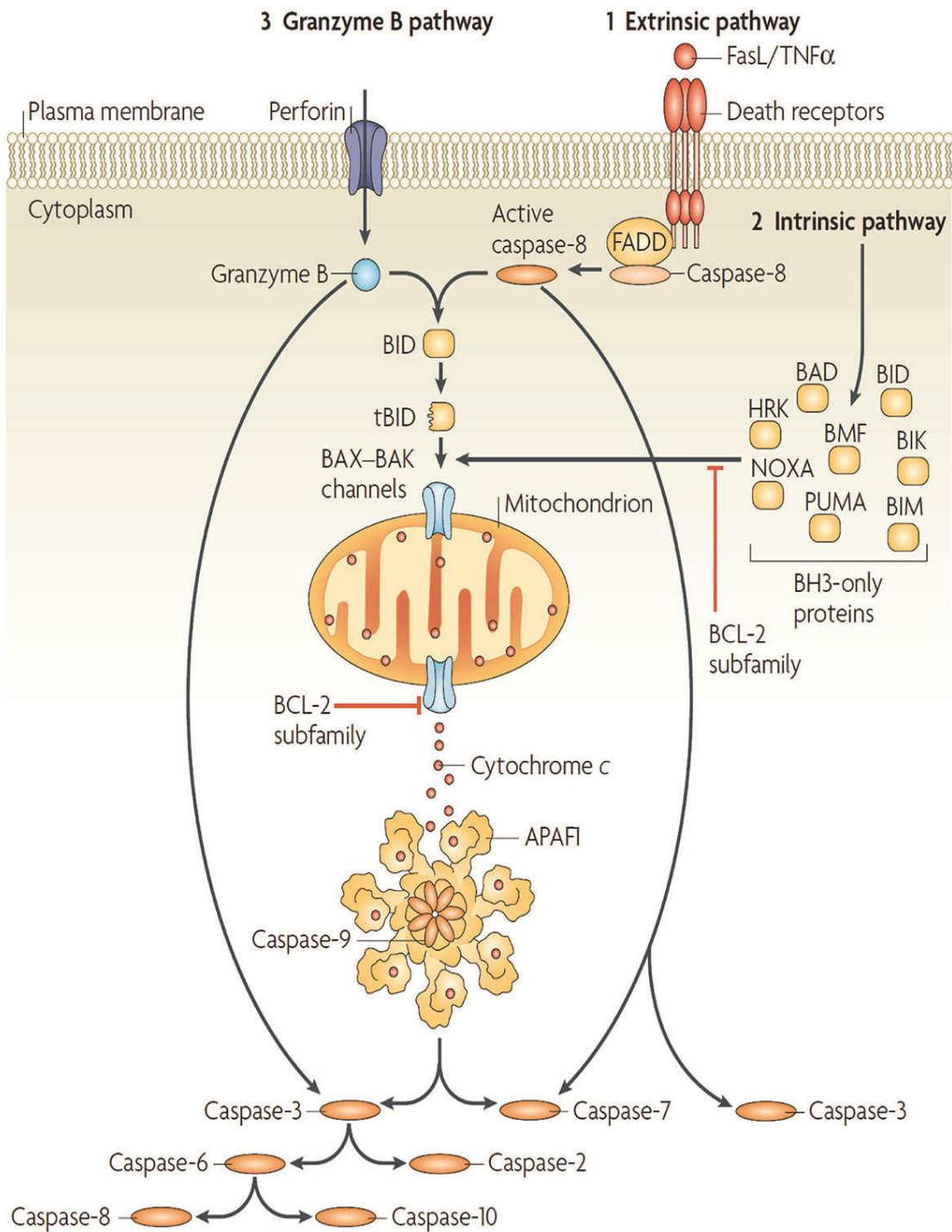
**Figure 7:** Pathways of apoptosis signaling (33).

## 2.5 Mitochondrial pathway of apoptosis

The mitochondria or intrinsic pathway originates from apoptotic stimuli such as ultraviolet radiation, reactive oxygen and reactive nitrogen species, chemotherapeutic agents, heat shock, growth factor withdrawal and DNA damage (35), resulting in a perturbation of intracellular homeostasis. The activation occurred by these apoptotic signals causes changes in the inner mitochondrial membrane permeabilization leading to the loss of the mitochondrial transmembrane potential ($\Delta\psi$m) and release of pro-apoptotic proteins from intermembrane space of mitochondria into the cytosol (Figure 8). Mitochondrial apoptogenic factors are divided into two groups. The first group activates caspase-dependent mitochondrial pathway of apoptosis. It is composed of cytochrome c, second mitochondria-derived activator of caspase/direct IAP-binding protein with low isoelectric point (SMAC/DIABLO), and the high temperature requirement protein HtrA2/Omi, which is the mitochondrial serine protease (36; 37). The second group consists of apoptosis-inducing factor (AIF), endonuclease G (EndoG) and caspase-activated DNase (CAD), which are released from the mitochondria at a late phase of apoptosis after the cell has committed to die. They play role in apoptosis in either a caspase-independent or -dependent manner. The major weapon in the mitochondrial arsenal is cytochrome c, which, when introduced into the cytosol, incorporates with cytosolic adaptor proteins, apoptotic protease-activating factor-1 (APAF-1), ATP/dATP, and procaspase-9 forming an apoptosome (36). Interaction of cytochrome c and APAF-1 in the presence of ATP/dATP, APAF-1 undergoes a conformational change by self-aggregation, and induces the recruitment of procaspase-9 which is subsequently autoproteolytic cleaved to active caspase-9 (37). Caspase-9 then directly activates effector caspases, caspases-3, -6 and -7, which results in the

sequentially cell death by proteolytic clevage of multiple downstream targets (Figure 8) (32). SMAC/DIABLO which is also released from the mitochondria into the cytosol, can bind to the inhibitor of apoptosis proteins (IAPs) interfering its association with active caspase-9, thus allowing caspase-9 to activate caspase-3, resulting in apoptosis (38).
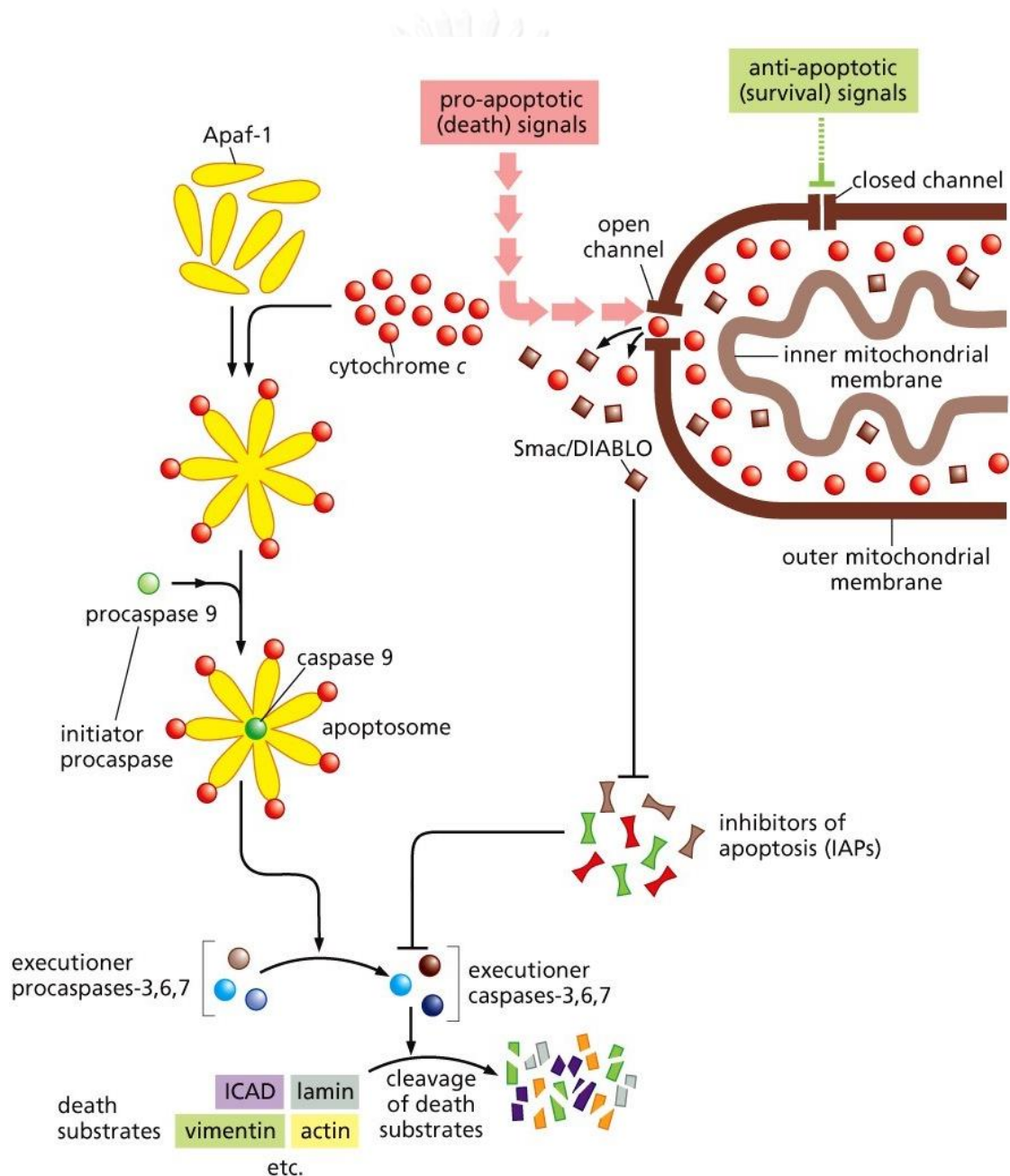


**Figure 8:** The intrinsic pathway of apoptosis (32).

## 2.6 BCL-2 family proteins

Proteins in BCL-2 (B-cell lymphoma 2) family are essential regulators for mitochondrial or intrinsic pathway of apoptosis. They play a pivotal role in mitochondrial outer membrane permeabilization (MOMP) which is a crucial phenomenon in the process of intrinsic pathway of apoptosis. These proteins are sub-divided into three groups, based on their BCL-2 homology domains (BH1–4 domains) and their pro- or anti-apoptotic action, the pro-apoptotic BCL-2, the anti-apoptotic BCL-2, and the BH3-only proteins (Figure 9) (39; 40). The pro-apoptotic BCL-2 proteins, BCL2 associated X protein (BAX) and BCL2 antagonist killer 1 (BAK), contain BH 1-3 domains. Their functions are essential for MOMP through the creation of proteolipid pore in mitochondria by forming a dimer or oligomers. The pore formation leads to the release of pro-apoptotic proteins, cytochrome c and DIABLO/SMAC from the mitochondrial inter-membrane space into the cytosol that subsequently initiates caspase activation (40; 41). BCL-2, BCL2 like 2 protein (BCL-W), BCL2 related protein, long isoform (BCL-XL), BCL-2-related protein A1 (A1 or BCL-2A1) and myeloid cell leukaemia sequence-1 (MCL-1) are the members of the anti-apoptotic BCL-2 proteins which contain BH domains 1-4. Most of them contain transmembrane domains (TM) and normally associate with membranes. They are integrated in the endoplasmic reticulum (ER), the nuclear envelope and the outer mitochondrial membrane. The roles of these proteins contribute to an inhibition of apoptosis. On mitochondria, they prevent cytochrome c release from mitochondria through directly bind to and inhibit the pro-apoptotic BCL-2 proteins. This event preserves cell survival (40).

**Figure 9:** The BCL-2 family of proteins (41).
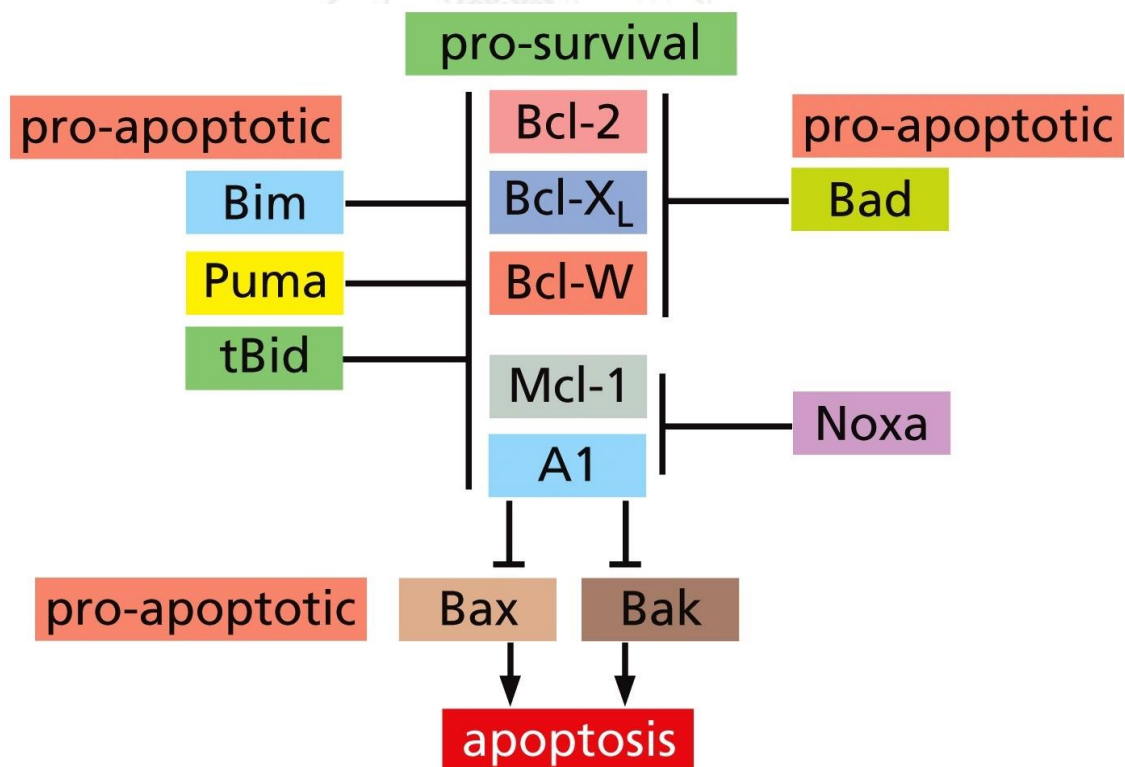


**Figure 10:** BH-3 only proteins and their regulation to promote apoptosis (32).

BH3-only proteins contain a conserved BH3 domain that can bind and regulate the anti-apoptotic BCL-2 proteins to promote apoptosis. BCL-2 antagonist of cell death (BAD), BH3-interacting domain death agonist (BID), BCL-2-interacting killer (BIK), BCL-2-like-11 (BIM), BCL-2 modifying factor (BMF), Harakiri (HRK), Phorbol-12-myristate-13-acetate-induced protein 1 (NOXA) and p53-upregulated modulator of apoptosis (PUMA) are the members of proteins in this group. BH3-only proteins are pro-apoptotic members and function as initial sensors of apoptotic signals that emanate from various cellular processes such as tumor suppressor p53 in response to DNA damage (42). An activation of these proteins is vital for overcoming the function of anti-apoptotic BCL-2 proteins promoting MOMP. BID, BIM and PUMA engage MOMP because they bind and neutralize all anti-apoptotic BCL-2 members. BAD and NOXA neutralize BCL-2/BCL-XL/BCL-W and MCL-1/A1, respectively (Figure 10) (32). Furthermore, activated BH-3 only proteins, BID and BIM, can interact with BAX and BAK to induce their activation or oligomerization and apoptosis (Figure 11) (43; 44).
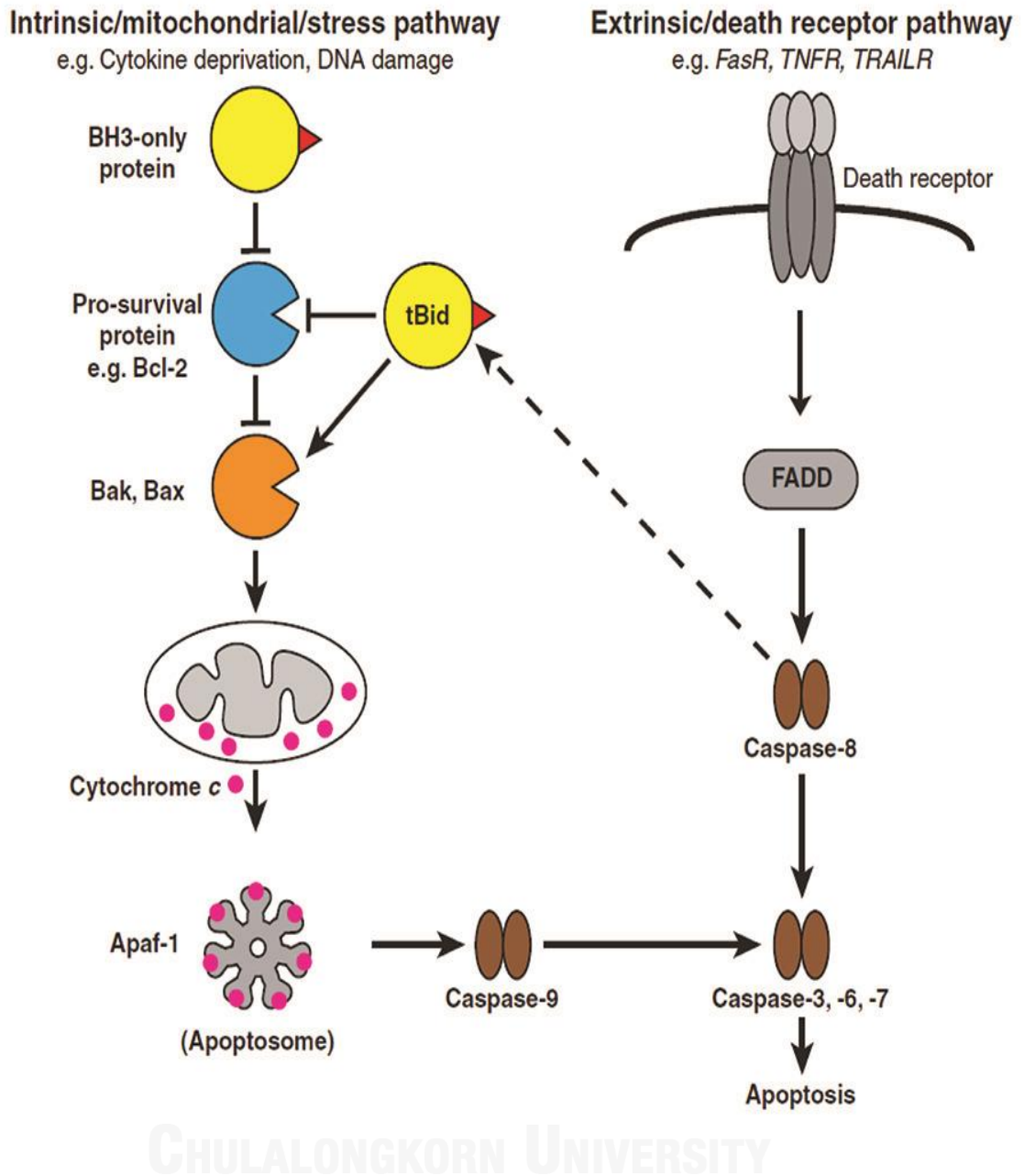
**Figure 11:** The BCL-2 protein family controls the mitochondrial pathway of apoptosis (43).

## 2.7 Potentiation of chemotherapy

Potentiation of chemotherapy or chemo-potentiation has been suggested since an ineffective chemotherapy was observed in cancer patients. It is defined as the use of other agents or low-dose radiation to potentiate killing effects of chemotherapeutic drugs. This event leads tumor cells more responsive to conventional chemotherapy without increasing in side-effects from drug combination in the cancer patients (45; 46). The existence of advanced knowledge on apoptosis and molecular characteristics of the cancer cells contributes to understanding the function of BCL-2 family. The over-expression of anti-apoptotic BCL-2 and BCL-XL is observed in many solid tumors as well as NHL (47). The over-expression of these proteins emerges an evasion of apoptosis leading to chemotherapy failure (48). An activation of pro-apoptotic molecules and/or suppression of anti-apoptotic molecules are possible mechanisms to enhance chemotherapy-induced apoptosis (49).

Rituximab (Rituxan®, Mabthera®) is a chimeric monoclonal antibody against the cluster-of-differentiation molecules 20 (CD20) over-expressed on the B-lymphocytes. Benefits of combining one targeted cancer drug such as rituximab with a gold standard CHOP regimen have highlighted the success of combination anticancer therapy (13; 15-17; 19). The addition of rituximab with conventional CHOP (R-CHOP) generated potentially increasing apoptotic activity of CHOP without a significant increase in toxic effects from drug combination. This synergistic effect was the consequence of inhibition of anti-apoptotic BCL-2 family by the suppression of interleukin-10 (IL-10), and inactivation of the signal transducer and activation of transcription 3 (STAT3) (50; 51). This combination therapy, R-CHOP, has shown to be an effective strategy and become the standard treatment for elder patients (51),

however, high cost of target-based antibody restricts its use. Taken together, the development of new compounds that exhibit the potential activity for enhancing the killing effect of chemotherapeutic drugs, lacking an increased toxicity to normal cells, and being affordable towards all patients have been explored.

Over the past decade, medicinal plants have played an important role in the cancer therapy research. The benefits of natural-derived products are is resourceful and economical. Numbers of natural compounds such as curcumin, genistein, resveratrol, proanthocyanidin, emodin, silymarin, and flavopiridol have been reported to potentiate cytotoxicity of chemotherapeutic drugs in various cancer cell lines by enhancing chemotherapy-induced apoptosis via the modulation of BCL-2 family proteins (4). Potentiating effect of genistein in combination of CHOP regimen has been elucidated in NHL *in vitro* as well as *in vivo*. The treatment of genistein followed by CHOP resulted in significantly higher an antitumor activity of CHOP than CHOP alone. The in-depth mechanism was also elucidated and shown that genistine completely attenuated increasing NF-κB activity induced by CHOP treatment (7). The study of chemo-potentiation activity of resveratrol in paclitaxel-refractory NHL cell line, Ramos cells, has reported that resveratrol synergistically increased apoptosis activity of the chemotherapeutic drug via the modulation of apoptotic regulatory proteins participating in the mitochondrial pathway, leading to an increasing level of cytosolic SMAC/DIABLO and cytochrome c. The potential effect of resveratol mediated paclitaxel-induced apoptosis was the consequence of BCL-XL down-regulation (5). BCL-XL inhibitor gossypol has shown the beneficial effect to potentiate chemotherapeutic drugs frequently used in NHL both *in vitro* and *in vivo* models (6; 52). Gossypol enhanced apoptosis and growth inhibition induced by etoposide, adriamycin, and

paclitaxel in Ramos cells (6). Further researches and studies examined the potentiating effect of natural-derived compounds in NHL cells are interested.

## 2.8 Citral

Citral or 3,7-dimethyl-2,6-octadienal is an essential oil found in several herbs and edible plants such as lemon grass (*Cymbopogon citratus*), lemon balm (*Melissa officinalis*), and *Litseacubeba*. It is the mixture of two isomeric acyclic monoterpene aldehydes, the *trans*-isomer geranial or citral A and the *cis*-isomer neral or citral B (53). Both isomers have the same molecular formula $C_{10}H_{16}O$, but their structures are different. Its chemical structure is shown below (54).
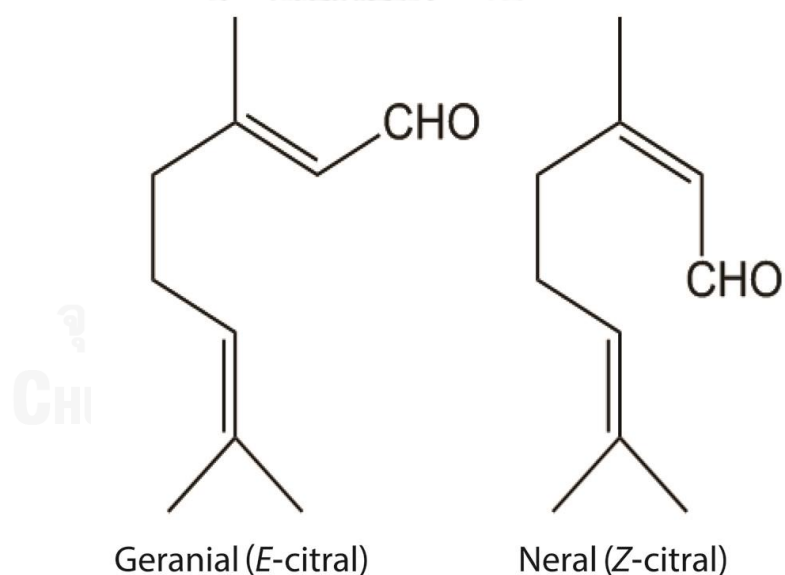


**Figure 12:** Chemical structure of the citral.

Citral is used as a flavor additive and ingredients for cooking. It is the main component (70-85%) in lemon grass essential oil (8) which is commonly used as a food additive in several Thai dishes. The study has revealed that a cup of tea prepared from one gram of lemon grass contained 44.5 μM of citral (9). Citral has a long history of acceptance by US and European regulatory bodies and has been accorded GRAS (generally recognized as safe) status. The average daily intake of citral in humans was estimated to be 5 mg/kg (55). The pharmacokinetic properties of citral were studied in rats and mice. It had rapid metabolism and complete within 72 hours mainly in the urine but also via the lungs and in the feces. Two major metabolites detected were 2, 6-dimethyl-2,6-octadiendioic acid and 2,6-dimethyl-2-octendioic acid (56). The toxicological studies have demonstrated that citral has no major toxicity and carcinogenic potential in both rats and mice. It has low acute toxicity, with variation in the lethal dose 50 percent ($LD_{50}$) values depending on the strains and species of animals used and the route of administration. The oral $LD_{50}$ in rats is 4.96 g/kg body weight and the dermal $LD_{50}$ in rabbits is 2.25 g/kg body weight. There was no macroscopic change in rats after administration of citral to rats at levels of 10,000, 2500 or 1000 ppm in the diet for 13 week (57). The short-term (28-day) studies on citral given by gavage to rats revealed a maximum non-lethal daily dose of 2.4 g/kg body weight. At this dose, citral caused hepatomegaly, microsomal enzyme induction and peroxisome proliferation (58). It was also reported that citral had no mutagenic effect in *in vitro* studies (59).

Pharmacological properties of citral have been investigated in many aspects. The examples of pharmacological effects of citral are shown in the following;

Antimicrobial effects

Citral has *in vitro* broad spectrum activities against many microorganisms including Gram-positive and Gram-negative bacteria, fungi, and some protozoa. It has been reported to have antimicrobial activities against *Staphylococcus aureus*, *Escherichia coli*, *Pseudomonas aeruginosa*, *Candida albicans*, methicillin-resistant *S. aureus* (MRSA), *Aspergillus niger*, *Klebsiella pneumonia*, *Propionibacterium acnes* (60), *Bacillus sp.*, *L. monocytogenes*, *S. aureus*, *A. hydrophila*, *E. faecalis* (61), *S. aureus*, *Bacillus cereus*, *B. subtilis*, *E. coli*, *K. pneumonia* (62), MRSA, *Penicillium italicum* and *Rhizopus stolonifer* (63). It also had potent *in vitro* antifungal activities against several *Candida* species (*C. albicans*, *C. glabrata*, *C. krusei*, *C. parapsilosis* and *C. tropicalis*) (64), *Colletotrichum coccodes*, *Botrytis cinerea*, *Cladosporium herbarum*, *R. stolonifer* and *A. niger* (65). The study has highlighted the broad spectrum antifungal activity of citral and their synergy with fluconazole against azoleresistant strains of *Aspergillus spp.* and *Trichophyton spp.* (66). Furthermore, the antiviral activity of citral against Herpes simplex virus-1 (HSV-1) and its antiparasitic effects were also reported (67; 68).

Anti-inflammatory effects

The anti-inflammatory effects of citral on mouse macrophage-like RAW 264.7 cells have been reported. It inhibited lipopolysaccharide (LPS)-induced nitric oxide (NO) production through the suppression of inducible nitric oxide synthase (iNOS) expression and NF-$\kappa$B activity (69). Citral was demonstrated to inhibit macrophages to produce IL-1$\beta$ and IL-6 both *in vitro* and *in vivo* (70). It suppressed both LPS-induced cyclooxygenase 2 (COX-2) mRNA and protein expression in a dose-dependent manner

on human macrophage-like U937 cells (71). The study has reported that citral exerted its anti-inflammatory effect through an inhibition of NF-$\kappa$B leading to the suppression of IL-1$\beta$, IL-6 and IL-10 productions in macrophage cells (72). Moreover, the study of citral on inflammatory pain has been examined in animal models. It was demonstrated that citral possessed central and peripheral antinociceptive effects in rodents (73). Combining of non-steroidal anti-inflammatory drug, naproxen with citral produced the synergistic effect on their anti-inflammatory activity in rats, and contributed to the reduction of gastric damage which is side effect of naproxen (74).

Anticancer effects

Citral has been found to possess anticancer effect against several cancer cell lines. In several hematopoietic cancer cells, treatment with citral induced 58-90% cell death with the inhibitory concentration 50 percent (IC$_{50}$) of 47 µg/ml. Treatment of human U937 and HL60 and mouse RL12 and BS-24-1 leukemic cell lines for 4-24 hours with citral at 45 µg/ml, resulted in activation of caspase-3 activity and induced apoptosis. Citral induced DNA ladder in BS-24-1cells after 70 minutes exposure. Additionally, treatment of leukemic cells with citral metabolism products, geranic acid or geraniol, or the citral derivatives, citronellal and citronellol, did not activate procaspase-3 or induce DNA ladder, indicating that the $\alpha,\beta$-unsaturated aldehyde group of citral is crucial for procaspase-3 activation (9). Moreover, citral inhibited MCF-7 cell growth with the IC$_{50}$ value of $18 \times 10^{-5}$ M at 48 hours incubation. It arrested the cell cycle in G2/M phase and induced apoptosis. It also suppressed COX-2 activity, resulted in the decrease in prostaglandin E2 synthesis after 48 hours (10).

A recent study from our laboratory demonstrated an anticancer effect of citral on human B-lymphoma cells or Ramos cells. Citral at the concentrations of 75 and 150 μM could induce Ramos cells death mainly by apoptosis in a short time (3 hours), but had no effect on the cell distribution in the cell cycle. It activated caspase activity in concentration-and time-dependent manners, leading to the decrease in BCL-2 gene expression. The cytotoxic effect of citral on human peripheral blood mononuclear cells (PBMCs) was much less than on Ramos cells after 6 hours of treatment. It had higher cytotoxic to the normal cells at the longer time of exposure, as 12 hours (12). Recently, Xia H and colleagues has found the cytotoxic effect of citral (0-20 μg/ml) on acute promyelocytic leukemia cell line (NB4 cells) in a concentration- and time dependent manner with the $IC_{50}$ value of 3.995 μg/ml at 24 hours incubation. After 24 hours, the inhibition rate decreased. It induced apoptosis on these cancer cells. This event was attributed to activation of caspase-3, down-regulation of BCL-2 and NF-ĸB expression, and up-regulation of BAX expression (11). Furthermore, chemopreventive potential of citral was also demonstrated in hamster buccal pouch carcinogenesis induced by the carcinogen, 7, 12- dimethylbenz (a) anthracene (DMBA). It was found that oral administration of citral at 100 mg/kg by weight completely prevented tumor formation and progression in DMBA treated hamster (75).

# CHAPTER III

# MATERIALS AND METHODS

## 3.1 Materials

### 3.1.1 Test compounds

Citral was purchased from Sigma-Aldrich (USA). Doxorubicin (2 mg/ml) and vincristine injection (1 mg/ml) were purchased from Pfizer (USA). Etoposide injection (20 mg/ml) was purchased from Ebewe Pharma (Austria).

### 3.1.2 Cell culture

- **Human peripheral blood mononuclear cells (human PBMCs)**

Human PBMCs were used in this study as the normal white blood cells. The study was performed under three basic principles of Belmont's report, the principles of respect for persons, beneficence and justice. PBMCs were isolated from healthy male blood donors, age between 20 to 35 years old, at the National Blood Bank, Thai Red Cross Society, with the informed consent. This study was approved by the Human Research Ethics Committee from the Faculty of Medicine, Chulalongkorn University, Thailand with COA No. 642/2012.

- **Human B-Lymphoma cells (Ramos cells)**

Human B-lymphoma cells or Ramos cells are Birkitt's lymphoma cells purchased from the American Type Cell Culture (ATCC) (Rockville, MD). The cells were initially cultured at the density of $5x10^5$ cells/ml, and then sub-cultured when the cells reached $2x10^6$ cells/ml. Cells in the exponential growth phase with over 95% viability were used in all experiments.

Ramos cells and human PBMCs were maintained in completed RPMI 1640 medium supplemented with 10% (v/v) fetal bovine serum, 0.5% L-glutamine, 100 µg/ml streptomycin and 100 units/ml penicillin at 37°C in a humidified atmosphere of 5% $CO_2$. Viable cells were determined by staining 0.4% trypan blue dye solution at the ratio 1:1. In this study, Ramos cells and PBMCs were used at the density of $1 \times 10^6$ cells/ml.

### 3.1.3 Equipment and Instruments

The following equipment and instruments were used in this study; autoclave (Hirayama, Japan), fluorescence flow cytometer (BD biosciences USA), biohazard lamina-flow hood, incubator (Science, Germany), analytical balance (GMPH, Satorius, Germany and UMT2, Mettler Toledo, Switzerland), incubator (Thermo, USA), light microscope (Nikon, Japan), vortex mixer (Scientific Industries, USA), refrigerator 4°C and -20°C (Sanyo, Japan), freezer -70°C (Thermo Scientific, USA), pipette (Falcon, USA), pH meter (Mettler tuledo, Switzerland), autopipette (Gilson, France), centrifuge (Hettich, USA and Eppendrof, Germany), Microplate reader (Labsystems Multiskan, USA), Scepter™ Handheld Automated Cell Counter (Millipore, USA), StepOnePlus™ Real time PCR system (Applied Biosystems, USA), MicroAmp Fast 8-tube strip (0.1 ml) (Applied Biosystems, USA), MicroAmp optical 8-cap strip (Applied Biosystems, USA), 96-well microplates (Corning, USA), 24-well microplates (Corning, USA), 6-well culture plates (Corning, USA), and T25 tissue culture flasks (Corning, USA).

**3.1.4 Reagents**

The following reagents and reagent kits were used in this study; RPMI-1640 (Gibco, USA), fetal bovine serum (Gibco, USA), L-glutamine (Gibco, USA), Histopaque®-1077 (Sigma, USA), penicillin/streptomycin (Gibco, USA), 0.4% trypan blue dye (Sigma, USA), resazurin (Sigma, USA), annexin V apoptosis detection kit (Invitrogen, USA), 4',6-diamidino-2-phenylindole (DAPI) (Invitrogen, USA), TRIzol® Reagent (Invitrogen, USA), dietyl pyrocarbonate (DEPC) (Molekula, UK), absolute ethanol (Merck, Germany), Isopropyl alcohol, chloroform, ImProm-II™ Reverse Transcription System (Promega, USA), TaqMan® Gene Expression System (Applied Biosystems, USA).

**3.1.5 Conceptual framework**
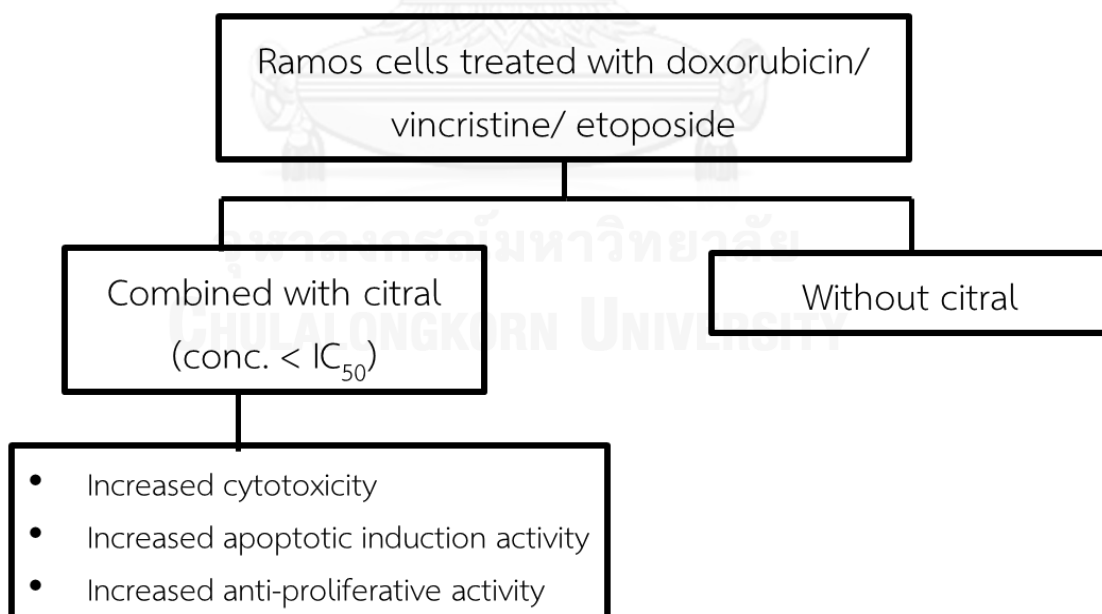
## 3.2 Methods

### 3.2.1 Preparation of tested compounds

Citral was prepared as stock solution by dissolving in 70% ethanol. The working solutions of citral were adjusted by diluting the stock solution with sterile double distilled water (ddH$_2$O) to various final concentrations with the constant 0.5% ethanol. Doxorubicin, vincristine, and etoposide solution injection were freshly prepared by diluting in sterile ddH$_2$O to the required concentrations. 0.5% Ethanol was used as the solvent or negative control in the experiments.

### 3.2.2 Isolation of human peripheral blood mononuclear cells (PBMCs)

Human PBMCs were isolated by Ficoll (Histopaque®-1077) density gradient centrifugation as the followings;

1.  Collect whole blood in ethylenediaminetetraacetic acid (EDTA) tube.

2.  Centrifuge at 3,200 rpm for 10 minutes at room temperature.

3.  Carefully remove top layer solution without disturbing the interface.

4.  Collect buffy coat on the top of the pellet into the 15 ml sterile polypropylene tube, dilute with 5 ml RPMI 1640 medium, and slowly overlay on 5 ml Ficoll solution in a 15 ml tube.

5.  Slowly overlay the diluted blood on 5 ml Ficoll solution in a 15 ml tube.

6.  Centrifuge the tubes at 3,200 rpm for 30 minutes at room temperature.

7.  Collect cells from the interface into a new 15 ml tube, and wash twice with 12.5 ml RPMI 1640 medium by centrifugation at 1,200 rpm for 10 minutes at room temperature.

8.  Discard the supernatant and resuspend the pellet with 5 ml the completed RPMI medium (RPMI 1640 medium with 10% fetal bovine serum, 0.5% L-glutamine, 100 µg/ml streptomycin, and 100 units/ml penicillin).

9.  Determine viable cells by staining with 0.4% trypan blue dye solution at the ratio 1:1 and count the number of the cells on a hemocytometer.

10. Adjust the cells with the completed RPMI 1640 medium to $1 \times 10^6$ cells/ml and incubated overnight at 37°C with 5% $CO_2$ before using. The PBMCs with cell viability more than 90% were used in this study.

### 3.2.3 Resazurin cytotoxicity assay

The cytotoxicity study was performed using resazurin staining assay to detect viable cells. Viable cells have the ability to reduce resazurin (dark-blue, maximum absorption wavelength 605 nm) into resorufin (pink, maximum absorption wavelength 573 nm).

<u>Cytotoxicity of citral, doxorubicin, vincrisitne, and etoposide on Ramos cells</u>

1.  Treat $1 \times 10^6$ cells/ml Ramos cells in the completed RPMI 1640 medium with various concentrations of citral, doxorubicin, vincristine, or etoposise in 96-well plate for 20 hours at 37°C in a humidified atmosphere of 5% $CO_2$.

2.  Add 5 µl of 1 mg/ml resazurin solution in each well, further incubate the treated cells for 4 hours.

3.  Determine the production of resorufin product in viable cells by measuring absorbance at the wavelengths 570 and 600 nm by microplate reader.

4.  Calculate the percentage of cytotoxicity of each compound from the following formula;

$$\% \text{ Cytotoxocity} = \frac{\Delta OD_{\text{(untreated control)}} - \Delta OD_{\text{(sample)}}}{\Delta OD_{\text{(untreated control)}}} \times 100$$

Where $\Delta OD$ = Absorbance 570 nm - Absorbance 600 nm

The $IC_{50}$ values of citral and these anticancer drugs were investigated by using probit analysis with SPSS version 21.0. This assay was performed in triplicate with three independent experiments (n=3).

**Cytotoxic effect of citral-drugs combinations**

The concentrations of citral which had cytotoxicity against Ramos cells less than 50% were selected to further assess its potentiating effect on the cytotoxicity of doxorubicin, vincristine or etoposide. This method was done in triplication with three to five independent experiments (n=3-5) as the followings;

1.  Treat $1 \times 10^6$ cells/ml Ramos cells and PBMCs in 96 wells plate with citral, drugs or the combination of citral and each drug.

2.  Incubate the treated Ramos cells and PBMCs for 20 hours and 10 hours at $37^{\circ}$C, respectively.

3.  Add 5 µl of 1 mg/ml resazurin solution in each well, further incubate the treated Ramos cells and PBMCs for 4 and 14 hours, respectively.

4.  Determine resorufin product in viable cells by measuring absorbance at the wavelengths 570 and 600 nm by microplate reader.

5.  Calculate the percentage of cytotoxicity against Ramos cells and PBMCs of doxorubicin, vincristine and etoposide, either used alone or combined with citral as performed above.

### 3.2.4 Combination index analysis

The $IC_{50}$ values of citral and each drug, alone or in combination, on Ramos cells were calculated by probit analysis using SPSS version 21.0. These $IC_{50}$ values were used to determine the types of citral-drug interaction using the combination index (CI) method of Chou and Talalay (76). This method has been widely used for assessing the interaction of drugs at indicated effect by determining CI value from the following equation;

$$CI = \frac{(C_x)_a}{(IC_x)_a} + \frac{(C_x)_b}{(IC_x)_b}$$

Where $(C_x)_a$ and $(C_x)_b$ are the concentrations of compound a and b used in combination to achieve 50% cytotoxicity. $(IC_x)_a$ and $(IC_x)_b$ are the concentrations of each compound when used alone to produce the same effect. The CI values are interpreted as follows; CI>1.3 antagonism; CI 1.1–1.3 moderate antagonism; CI 0.9–1.1 additive effect; CI 0.8–0.9 slight synergism; CI 0.6–0.8 moderate synergism; CI 0.4–0.6 synergism; CI 0.2–0.4 strong synergism; CI<0.1 very strong synergism (77).

### 3.2.5 Induction of apoptosis

This method is used to determine the effect of citral on apoptotic induction activities of doxorubicin, vincristine, and etoposide on Ramos cells. Apoptotic cells were measured by detecting the exposure of phosphatidylserine (PS) on the outer plasma membrane of apoptotic cells using annexin V-FITC and 4', 6-diamidino-2-phenylindole (DAPI) staining. The assay was achieved with three independent experiments (n=3) as shown in the following procedures;

1. Treat $1 \times 10^6$ cells/ml Ramos cells in the completed RPMI 1640 medium with each agent alone (citral, doxorubicin, vincristine, or etoposide) or each drug combined with citral (citral-doxorubicin, citral-vincristine, or citral-etoposide) in 24-well plate for 18 hours at 37°C.

2. Collect the cells in each well to a micro-centrifuge tube and centrifuge at 12,000 rpm 25°C for 1 minute.

3. Remove the supernatant, wash the cells twice with 500 μl cold phosphate buffer saline solution (PBS), and separate the cells by centrifugation at 12,000 rpm, 25°C for 1 minute.

4. Discard the supernatant, resuspend the cell pellet in 100 μl of the assay buffer and transferred into a flow cytometer tube.

5. Add 1 μl of 0.5 μg/ml DAPI and 1 μl of 200 μg/ml annexin V-FITC in each tube.

6. Incubate the tubes in the dark condition at room temperature for 15 minutes.

7. Consequently, add 400 μl of the assay buffer into each tube and immediately analyze the cells (10,000 cells/sample) by fluorescence flow cytometer.

8.  Assess types of cell death as follow; annexin V-FITC$^-$/DAPI$^-$ cells as viable cells, annexin V-FITC$^+$/DAPI$^-$ cells as early apoptotic cells, annexin V-FITC$^+$/DAPI$^+$ cells as late apoptotic cells, and annexin V-FITC$^-$/DAPI$^+$ cells as necrotic cells.

9.  Compare the apoptotic induction activity of each drug (doxorubicin, vincristine, or etoposide) with the citral-doxorubicin, citral-vincristine, or citral-etoposide combinations.

### 3.2.6 BCL-2 family genes expression

The molecular effect of citral on apoptosis induction activities of doxorubicin, vincristine, and etoposide was investigated by determining the changes in the mRNA expression of pro- and anti-apoptotic BCL-2 family induced by the anticancer agents. These proteins involve in the mitochondrial pathway of apoptosis, including pro-apoptotic BCL-2 (BAX and BAK) and anti-apoptotic BCL-2 (BCL-2 and BCL-XL) proteins. Quantitative RT-PCR (qRT-PCR) reactions were carried out for all genes of interest using TaqMan$^®$ Gene Expression System. The expression of genes of interest was compared to a housekeeping gene, GAPDH. The assay was performed with four independent experiments (n=4) as in the following procedures.

<u>Preparation of total RNA</u>

1.  Treat 1×10$^6$ cells/ml Ramos cells in the completed RPMI 1640 medium with each agent alone (citral, doxorubicin, vincristine, or etoposide) or each drug combined with citral (citral-doxorubicin, citral-vincristine, or citral-etoposide) in 6-well plate for 18 hours at 37°C.

2.  Collect the cells into centrifuge tube 15 ml and separate the cells by centrifugation at 1,200 rpm 25°C for 10 minutes.

3.  Remove the supernatant, lyse and homogenize in 1 ml of TRIzol® reagent by passing the cell up and down through a pipette, transfer and incubate the lysate to a microcentrifuge tube at room temperature for 15 minutes.

4.  Add 0.2 ml of chloroform, vigorously shake the tube by hand for 15 seconds, and incubate at room temperature for 15 minutes.

5.  Centrifuge the tube at 12,000 rpm 4°C for 15 minutes and transfer the aqueous phase to a fresh tube.

6.  Precipitate RNA by adding 0.5 ml isopropyl alcohol, incubate at -20°C for 1 hour and centrifuge at 12,000 rpm for 4°C for 10 minutes.

7.  Discard the supernatant, wash the RNA pellet twice with 1 ml of 75% ethanol, mix by vortexing, and separate the pellet by centrifugation at 7,500 rpm 4°C for 5 minutes.

8.  Discard the supernatant and air-dry the RNA pellet (for 5-10 minutes).

9.  Resuspend the RNA pellet in RNase-free water (0.1% DEPC-treated) and incubate at 55-60°C for 10 minutes.

10. Determine the RNA concentration and DNA contamination by measuring absorbance of RNA and DNA at 260 nm and 280 nm. The ratio of absorbance$_{260/280}$ should be more than 1.8.

## Conversion of total RNA to cDNA

One μg of total RNA was reverse transcribed to cDNA synthesis using reagents of ImProm-II™ Reverse Transcription System with oligo(dT)$_{15}$ primer following the manufacturer protocol.

1.  Mix 1 μg of total RNA with 1 μl of oligo(dT)$_{15}$ primer, and Nuclease-Free Water for a final volume of 5 μl per reaction in 0.2 ml PCR tube.

2.  Heat the tubes at 70°C for 5 minutes and immediately chill on ice for at least 5 minutes.

3.  Prepare transcription mixture solution in a sterile 1.5 ml microcentrifuge tube on ice, containing the following components;

    | | | | |
    |---|---|---|---|
    | 1) | Nuclease-Free Water (to a final volumn of 15 μl) | 7.3 | μl |
    | 2) | ImProm-II™ 5X Reaction Buffer | 4.0 | μl |
    | 3) | 25 mM MgCl$_2$ (final concentration 1.5 mM) | 1.2 | μl |
    | 4) | dNTP Mix (final concentration 0.5 mM each dNTP) | 1.0 | μl |
    | 5) | Recombinant RNasin® Ribonuclease Inhibitor (20 u) | 0.5 | μl |
    | 6) | ImProm-II™ Reverse Transcriptase | 1.0 | μl |
    | | Final volume (per reaction/tube) | 15.0 | μl |

4.  Add 15 μl of mixture solution in to each tube.

5.  Generate cDNA in thermocycle machine using the following conditions; 25°C for 5 minutes, then 42°C for 1:30 hour, and 70°C for 15 minutes.

6.  Store the cDNA samples at -20°C to use as the template for determining gene expression.

**Quantitative RT-PCR**

QRT-PCR reactions were carried out for BCL-2 (Hs00608023_m1), BCL-XL (Hs00236329_m1), BAK (Hs00832876_g1) and BAX (Hs00180269_m1) genes in each sample using TaqMan® Gene Expression System. Specific primers and probes for genes of interest were contained in TaqMan® Gene Expression Assays. The expression levels of the genes were compared to a housekeeping gene, GAPDH, for loading control.

1. Prepare 10 µl singleplex reactions for each sample in 1.5-ml microcentrifuge tube, containing the following components;

    1) 20X TaqMan® Gene Expression Assays     0.5   µl

    2) 2X TaqMan® Gene Expression Master Mix     5.0   µl

    3) cDNA template (50 ng)     1.0   µl

    4) RNase-free water     3.5   µl

2. Cap the tube, mix the reaction component, and centrifuge the tube.

3. Load the microcentrifuge tube into StepOnePlus™Real time PCR

4. Run experiment using the following conditions; pre-incubation at 95°C for 10 minutes, then cycling for 45 cycles of 95°C for 15 seconds, and 60°C for 1 minute.

5. Quantify the gene expression levels by StepOnePlus™Real time PCR system version 2.3 (Applied Biosystems, USA) using comparative threshold cycle ($\Delta\Delta_{CT}$) method to provide relative quantification (RQ) as a following formula;

$$RQ = 2^{-\Delta\Delta c_T}$$

Where $C_T$ = cycle threshold

### 3.2.7 Anti-proliferative study

Effect of citral on anti-proliferative effects of doxorubicin, vincristine, and etoposide was determined using automated cell counter. The assay was performed with three independent experiments (n=3) as in the following;

1. Treat $1\times10^6$ cells/ml Ramos cells in the completed RPMI 1640 medium with each agent alone (citral, doxorubicin, vincristine, or etoposide) or each drug combined with citral (citral-doxorubicin, citral-vincristine, or citral-etoposide) in 24-well plate for 3 hours at 37°C.

2. Remove the supernatant, wash the cells twice with 2 ml of RPMI 1640 medium, and separate the cells by centrifugation at 1,200 rpm 25°C for 10 minutes.

3. Discard the supernatant and resuspend the cells pellet in 1ml of freshly completed RPMI 1640 medium.

4. Transfer the cells suspension into each well of 24-well plates and further incubate the cells at 37°C for 48 hours.

5. Collect the cells in each well to a micro-centrifuge tube and centrifuge at 1,200 rpm 25°C for 10 minutes.

6. Resuspend the cell pellets in cold PBS for a proper concentration of cells.

7. Count the number of cells in each well using Scepter™ Handheld Automated Cell Counter with 40 µm sensors.

8. Calculate the percentages of cell proliferation using the following formula;

$$\% \text{ Proliferation} = \frac{\text{Total cell count }_{(sample)}}{\text{Total cell count }_{(untreated\ control)}} \times 100$$

9. Compare the anti-proliferative effect of each drug (doxorubicin, vincristine, or etoposide) to the citral-doxorubicin, citral-vincristine, or citral-etoposide combinations.

### 3.2.8 Statistical analysis

All data obtained from this study were presented as mean with standard error of mean (mean ± SEM). Statistical evaluation was determined by one-way analysis of variance (ANOVA) followed by Tukey's *post hoc* test. SPSS program version 21.0 was used to perform all statistical analysis. Any p-values less than 0.05 were considered statistically significant.

# CHAPTER IV

# RESULTS

## 4.1 Effect of citral on cytotoxic activities of doxorubicin, vincristine, and etoposide

To investigate the potentiating activity of citral on cytotoxicities of anticancer drugs, the cytotoxic effect of citral on Ramos cells was initially determined using resazurin dye reduction assay. Ramos cells were treated with 0-160 μM citral for 24 hours. 0.5% Ethanol was used as the solvent control in this study. The result demonstrated that citral had cytotoxic effect on Ramos cells with $IC_{50}$ value of 75.9 μM (Figure 13). Citral at lower concentrations than its $IC_{50}$ value, 10-40 μM, was used to combine with 1-3 μM doxorubicin, $10^{0}$-$10^{-6}$ μM vincristine, or 5-25 μM etoposide to treat Ramos cells for 24 hours. The cytotoxic effects of doxorubicin vincristine, and etoposide significantly increased when compared to each drug alone. The $IC_{50}$ values of these drugs when treated alone and combined with citral were used to quantitatively evaluate the types of citral-drug interactions by using CI analysis. The CI values are interpreted as follows; CI>1.3 antagonism; CI 1.1–1.3 moderate antagonism; CI 0.9–1.1 additive effect; CI 0.8–0.9 slight synergism; CI 0.6–0.8 moderate synergism; CI 0.4–0.6 synergism; CI 0.2–0.4 strong synergism; CI<0.1 very strong synergism.

Citral significantly increased the cytotoxicity of doxorubicin. The $IC_{50}$ value of doxorubicin was reduced from 2.48 to 2.19, 1.94, and 1.23 μM when combined with 10, 20, and 40 μM of citral, respectively (Figure 14). The CI values of the combination of doxorubicin and citral were 1.01-1.04 as presented in Table 3. This suggests that citral additively enhances the cytotoxic effect of doxorubicin on Ramos cells.

Citral synergistically increased the cytotoxicity of vincristine only at the concentrations lower than its $IC_{50}$ value (at $10^{-6}$-$10^{-4}$ µM) as presented in Figure 15. It did not change the cytotoxicity of vincristine at $10^{-3}$ – 1 µM.

Citral also significantly increased the cytotoxicity of etoposide. The $IC_{50}$ value of etoposide was reduced from 13.97 to 11.67, 8.81, and 5.62 µM when combined with 10, 20, and 40 µM of citral, respectively (Figure 16). The CI values of the combination of etoposide and citral were 0.89-0.97 as presented in Table 3. This indicates the additive effect of citral on etoposide cytotoxicity against Ramos cells.
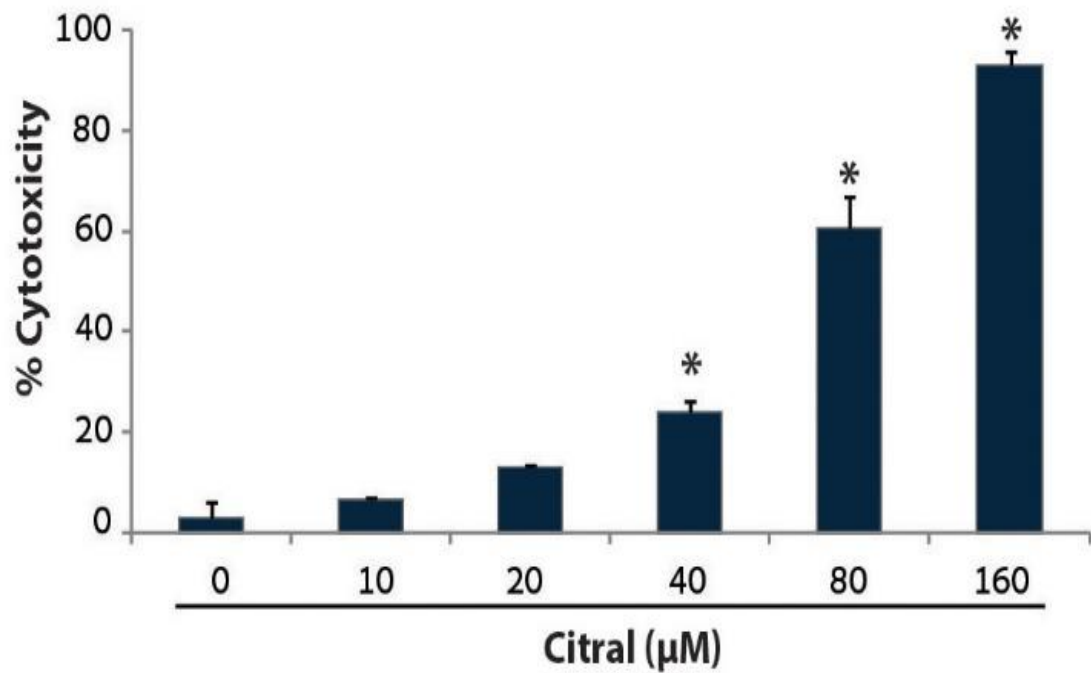
**Figure 13:** The cytotoxic effect of citral on Ramos cells. The cells were treated with citral at 0-160 μM for 24 hours. The cytotoxicity was determined by resazurin reduction assay. The data represent the means $\pm$ SEM of three independent experiments.

* $p < 0.05$ denotes statistically significant difference from 0.5% ethanol.
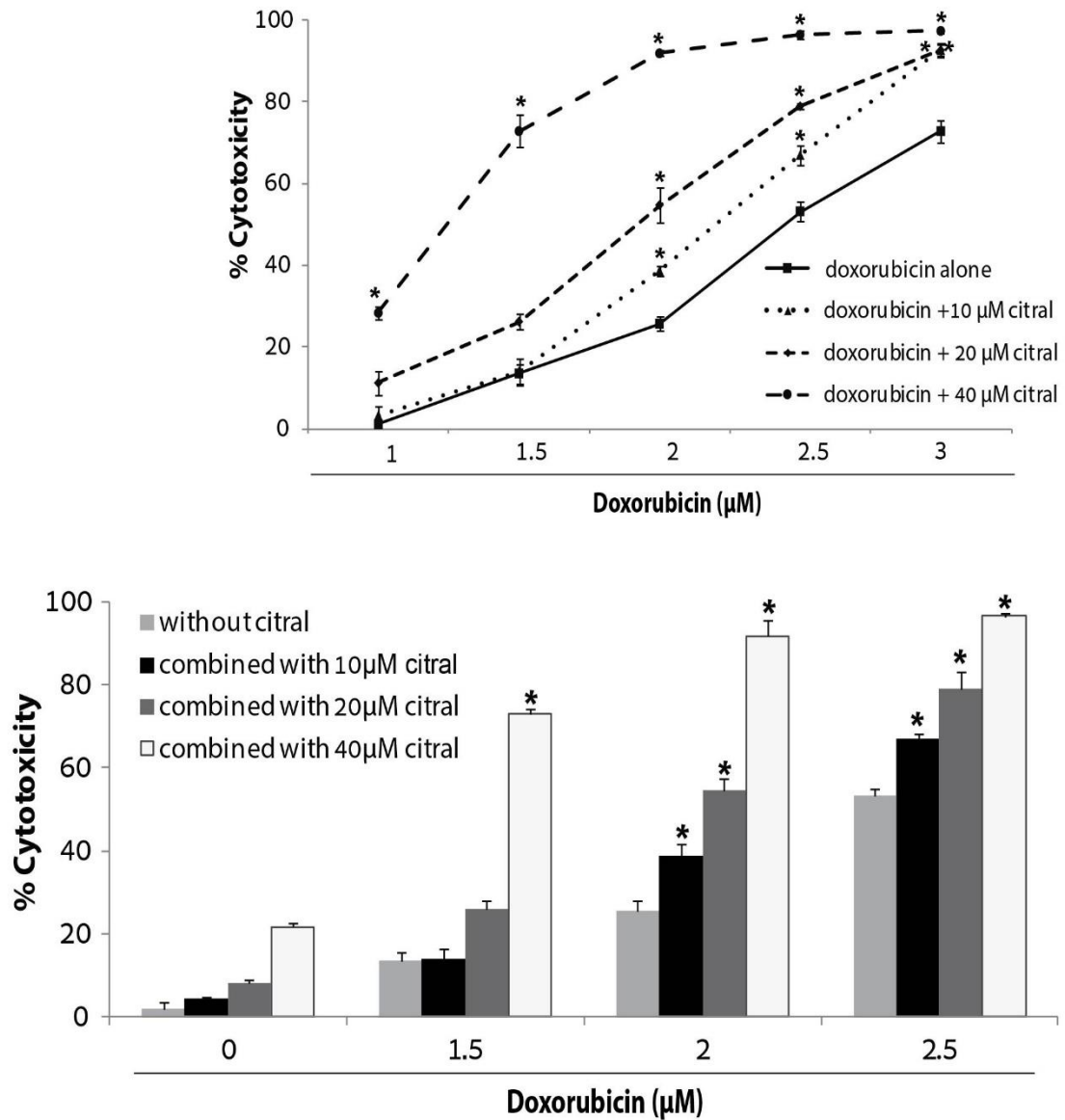
**Figure 14:** The effect of citral on cytotoxic activity of doxorubicin on Ramos cells. The cells were treated with doxorubicin in the absence and presence of 10-40 μM citral for 24 hours. The cytotoxicity was determined by resazurin reduction assay. The data represent the means ± SEM of three independent experiments.

* $p < 0.05$ denotes statistically significant difference from doxorubicin alone.
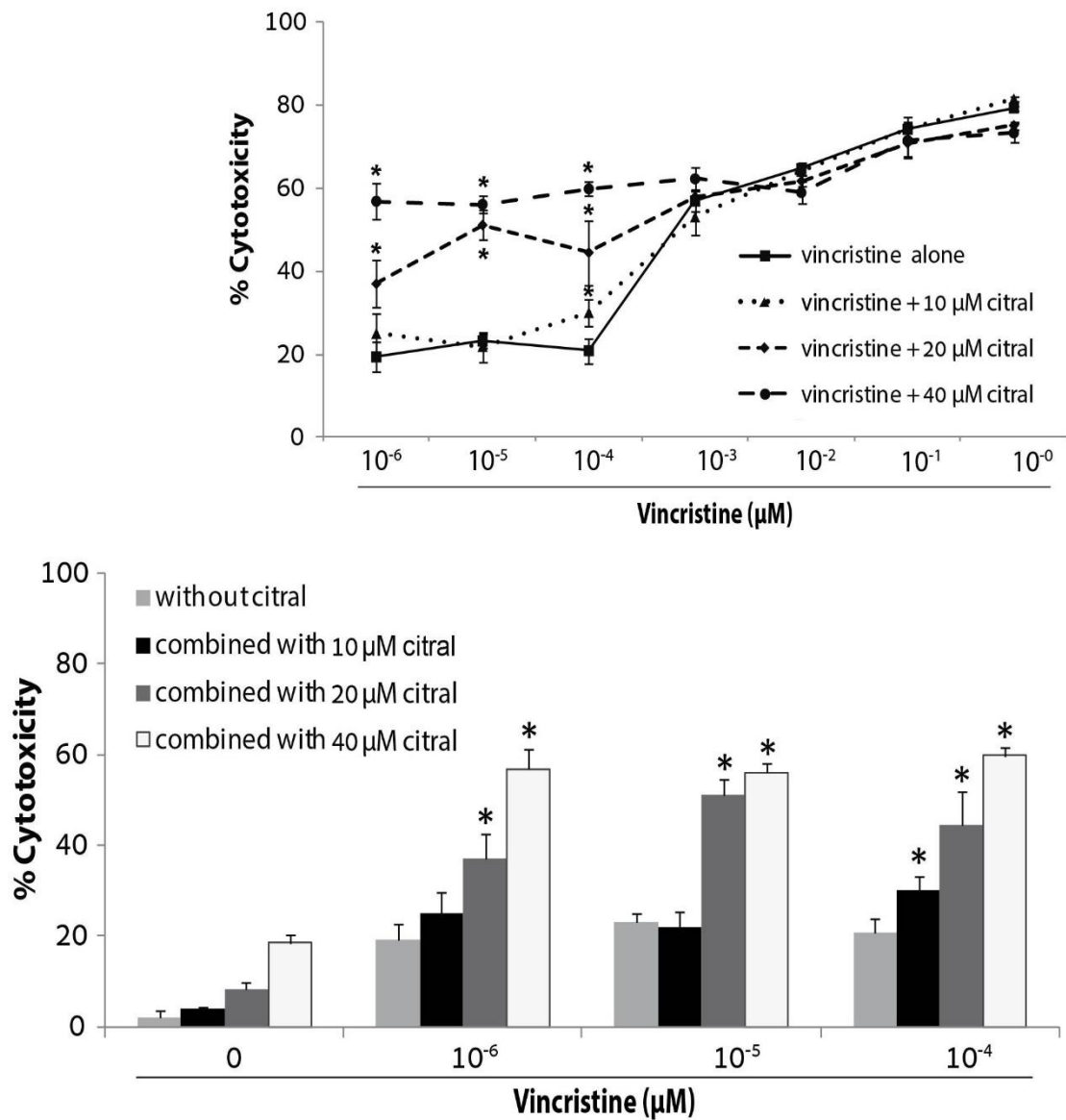
**Figure 15:** The effect of citral on cytotoxic activity of vincristine on Ramos cells. The cells were treated with vincristine in the absence and presence of 10-40 µM citral for 24 hours. The cytotoxicity was determined by resazurin reduction assay. The data represent the means ± SEM of three independent experiments.

* $p < 0.05$ denotes statistically significant difference from vincristine alone.
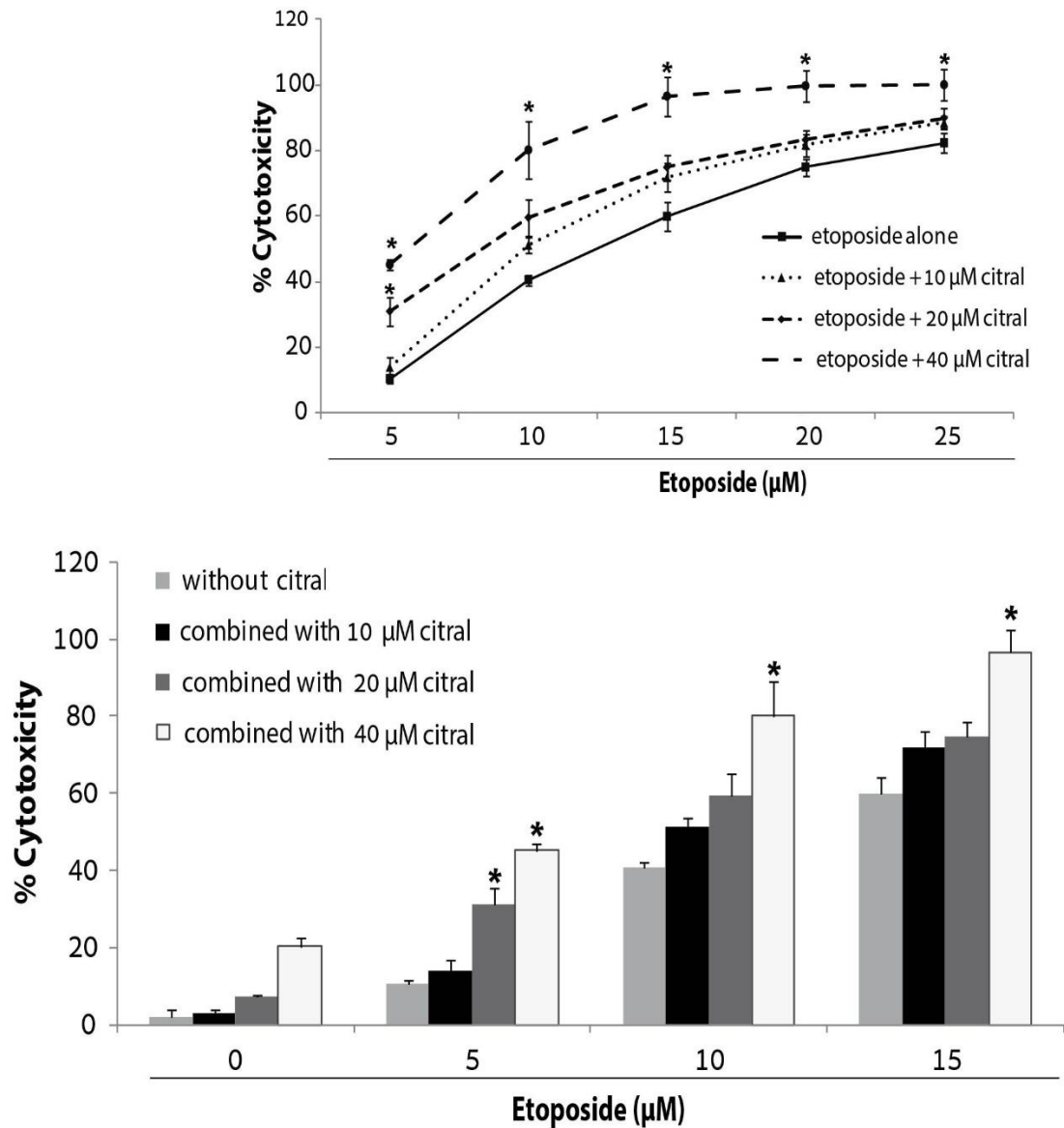
**Figure 16:** The effect of citral on cytotoxic activity of etoposide on Ramos cells. The cells were treated with etoposide in the absence and presence of 10-40 μM citral for 24 hours. The cytotoxicity was determined by resazurin reduction assay. The data represent the means ± SEM of three independent experiments.

* $p < 0.05$ denotes statistically significant difference from etoposide alone.

**Table 3:** The cytotoxic $IC_{50}$ and combination index (CI) values of doxorubicin, and etoposide assessed after 24 hours incubation. The $IC_{50}$ of cytotoxicity against Ramos cells of each drug when used alone or combined with citral was used to calculate CI value of the combination treatments.

| Drugs alone | Drugs combined with citral | | |
|---|---|---|---|
| | 10 µM Citral | 20 µM Citral | 40 µM Citral |
| Doxorubicin $IC_{50}$ = 2.48 µM | $IC_{50}$ =2.19 µM [CI = 1.01] | $IC_{50}$ = 1.94 µM [CI = 1.04] | $IC_{50}$ = 1.23 µM [CI = 1.02] |
| Etoposide $IC_{50}$ = 13.97 µM | $IC_{50}$ = 11.67µM [CI = 0.97] | $IC_{50}$ = 8.81 µM [CI = 0.89] | $IC_{50}$ = 5.62 µM [CI = 0.93] |

The $IC_{50}$ values were obtained from three independent experiments, analyzed by probit analysis with SPSS version 21.0.

Effect of citral on cytotoxicity of anticancer drugs against normal human PBMCs was also evaluated. The result demonstrated that doxorubicin, vincristine, and etoposide had very little or did not exhibit cytotoxicity against the normal cells. Citral also did not potentiate the cytotoxicity of these anticancer drugs on the cells as shown in Figure 17-19. These results demonstrated the selectivity of citral to increase killing effects of doxorubicin, vincristine, and etoposide on cancer cells without the harmful actions to the normal cells.
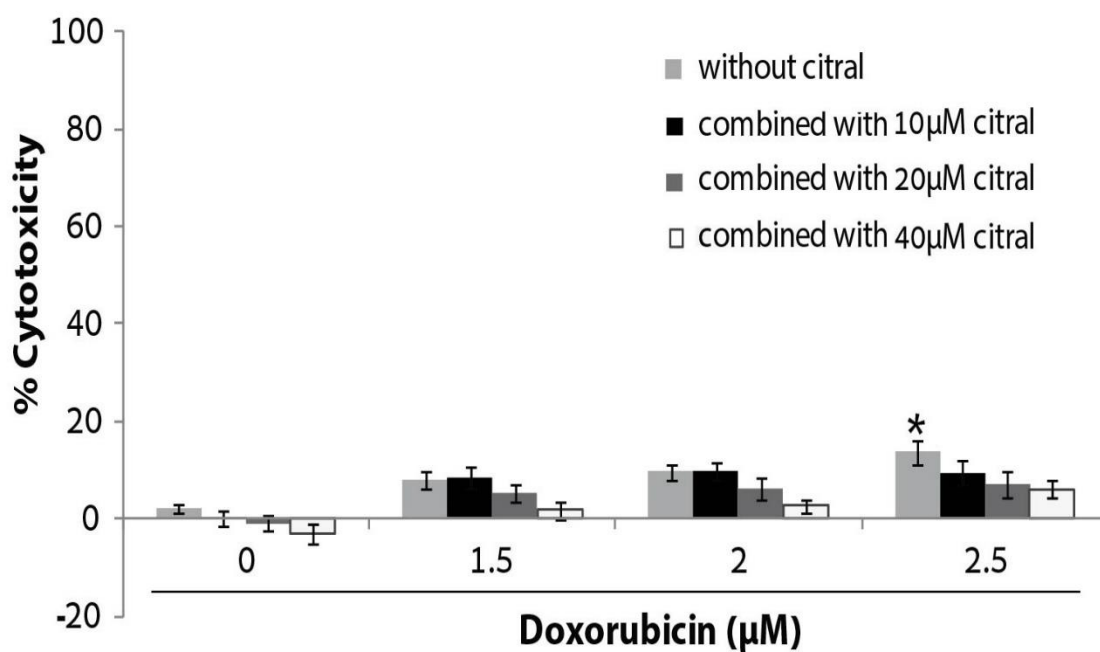
**Figure 17:** The effect of citral on cytotoxic activity of doxorubicin against normal human PBMCs. The cells were treated with doxorubicin in the absence and presence of 10-40 µM citral for 24 hours. The cytotoxicity was determined by resazurin reduction assay. The data are expressed as means ± SEM of five independent experiments.

* $p < 0.05$ denotes statistically significant difference from 0.5% ethanol.
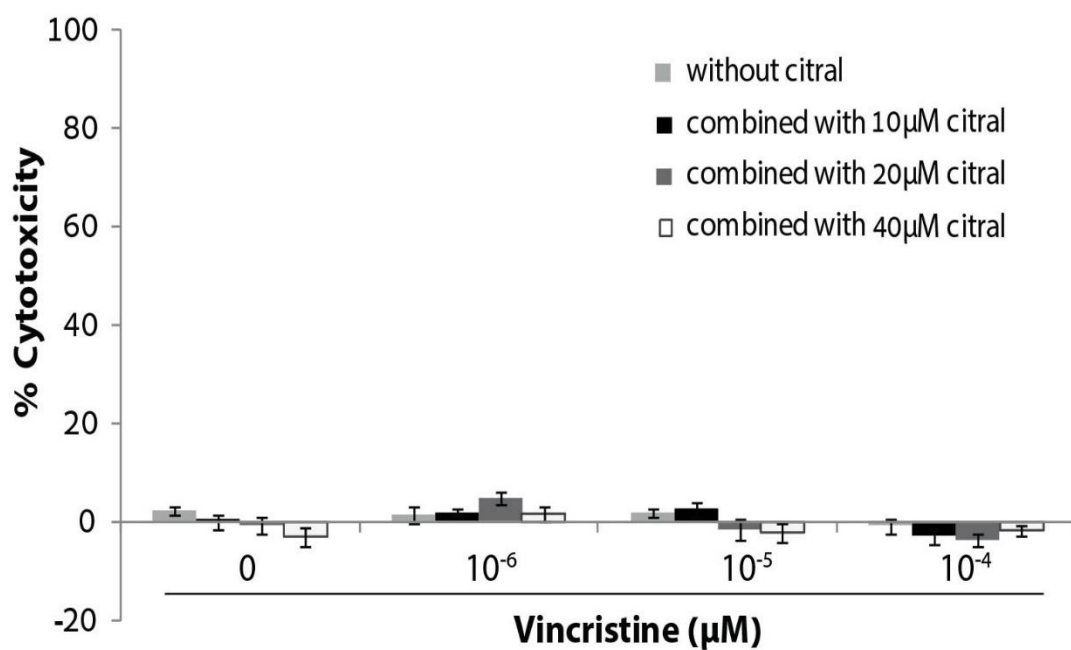
**Figure 18:** The effect of citral on cytotoxic activity of vincristine against normal human PBMCs. The cells were treated with vincristine in the absence and presence of 10-40 µM citral for 24 hours. The cytotoxicity was determined by resazurin reduction assay. The data are expressed as means ± SEM of five independent experiments.
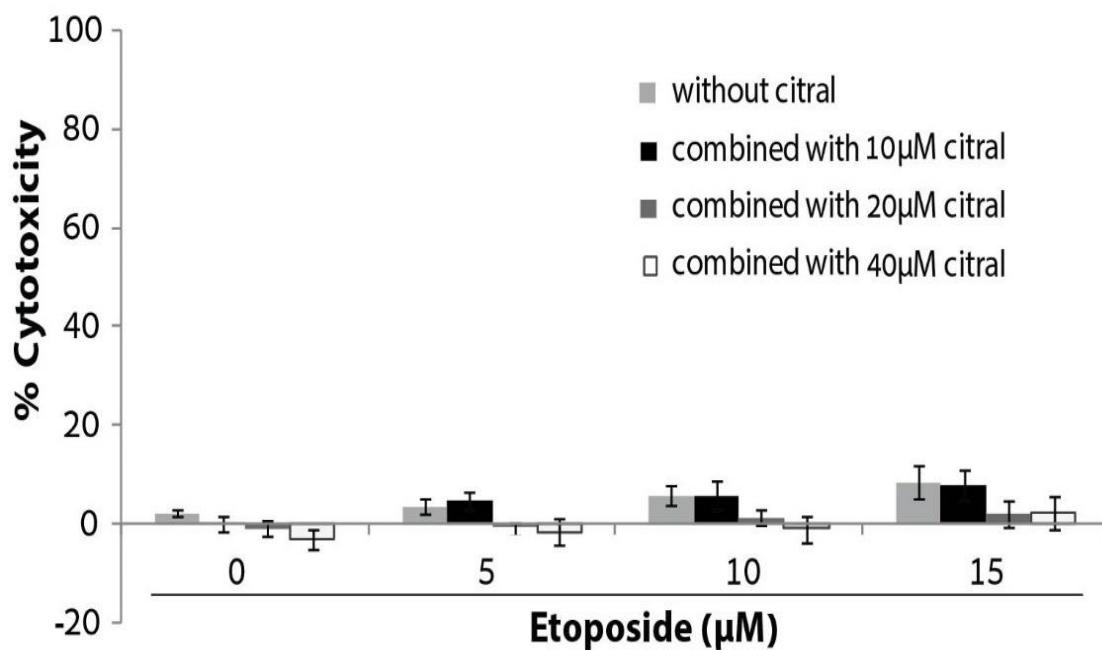
**Figure 19:** The effect of citral on cytotoxic activity of etoposide against normal human PBMCs. The cells were treated with etoposide in the absence and presence of 10-40 µM citral for 24 hours. The cytotoxicity was determined by resazurin reduction assay. The data are expressed as means ± SEM of five independent experiments.

**4.2 Effect of citral on apoptosis induction activities of doxorubicin, vincristine, and etoposide**

Apoptosis is an important mechanism of cell death involved in antitumor activities of many anticancer drugs. Apoptotic cells can be identified as annexin V-FITC$^+$ cells after staining with annexin V-FITC/DAPI and detecting with fluorescence flow cytometer. Ramos cells were treated with doxorubicin (1.5-2.5 μM), vincristine (10$^{-6}$-10$^{-4}$ μM), or etoposide (5-15 μM) in the absence and presence of citral (0-40 μM) for 18 hours. The types of Ramos cell death were assessed as follows; annexin V-FITC$^+$ cells were apoptotic cells, DAPI$^+$ cells were necrotic cells, annexin V-FITC$^+$/DAPI$^+$ cells were late apoptotic cells, and annexin V-FITC$^-$/DAPI$^-$ cells were viable cells (Figure 20).

As shown in Figure 21-23 and Table 4-6, 40 μM citral induced 19.67±2.26% Ramos cell apoptosis. Citral at 20 and 40 μM significantly enhanced apoptotic activity of doxorubicin on Ramos cells when compared to the doxorubicin- or citral-treated cells. Citral at 40 μM increased the apoptotic induction activity of 1.5 and 2 μM doxorubicin to 4.79 and 3.30-folds, respectively, when compared to the effect of doxorubicin alone (Figure 21A and Table 4). At the highest concentration of doxorubicin used in this study, 40 μM citral plus 2.5 μM doxorubicin increased the most total cell death but the cell death pattern was shifted from early apoptosis to late apoptosis (Figure 21B and Table 4).

Citral at 20 and 40 μM significantly increased apoptotic effect of vincristine on Ramos cells when compared to the vincristine- or citral-treated cells. Citral at 40 μM increased the apoptotic activity of 10$^{-6}$, 10$^{-5}$ and 10$^{-4}$ μM vincristine to 6.17, 2.62, and 2.09-folds, respectively, when compared to the effect of vincristine alone (Figure 22 and Table 5).

Citral at 40 μM also significantly increased apoptotic effect of 5 and 10 μM etoposide to 3.67, and 1.95-fold, respectively, when compared the effect of etoposide alone (Figure 23A and Table 6). Citral at 40 μM in combination with 15 μM etoposide increased the most total cell death but the cell death pattern was shifted from early apoptosis to late apoptosis (Figure 23B and Table 6).

Doxorubicin, vincristine, and etoposide at 1.5, $10^{-6}$, and 5 μM, respectively, were further used to investigate the potentiating effect of citral on the expression of BCL-2 family proteins in Ramos cells.
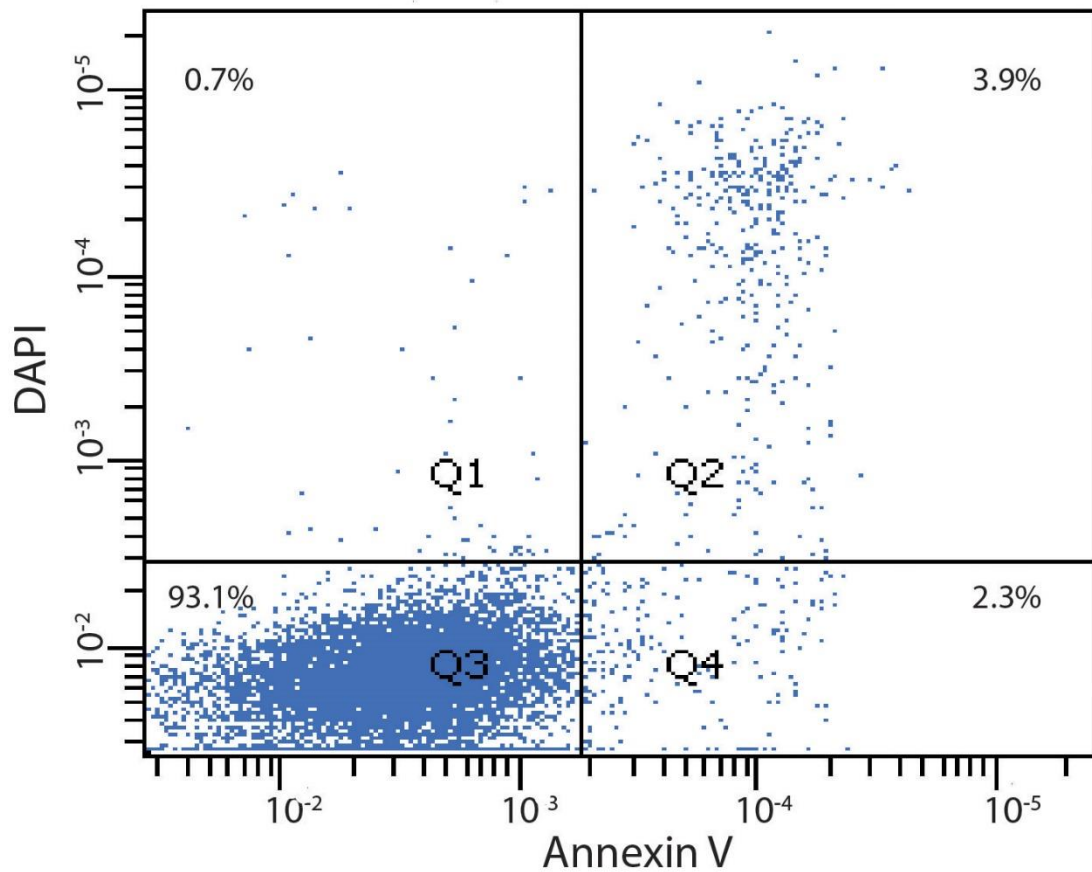
**Figure 20:** A representative dot plot histogram from annexin V-FITC/DAPI staining assay using fluorescent flow cytometer of 0.5% ethanol-treated Ramos cells for 18 hours. Cells in each quadrant (Q1-Q4) were interpreted as in the following; Q1: necrotic cells (annexin V⁻/DAPI⁺), Q2: late apoptotic cells (annexin V⁺/DAPI⁺), Q3: viable cells (annexin V⁻/DAPI⁻), and Q4: apoptotic cells (annexin V⁺/DAPI⁻).
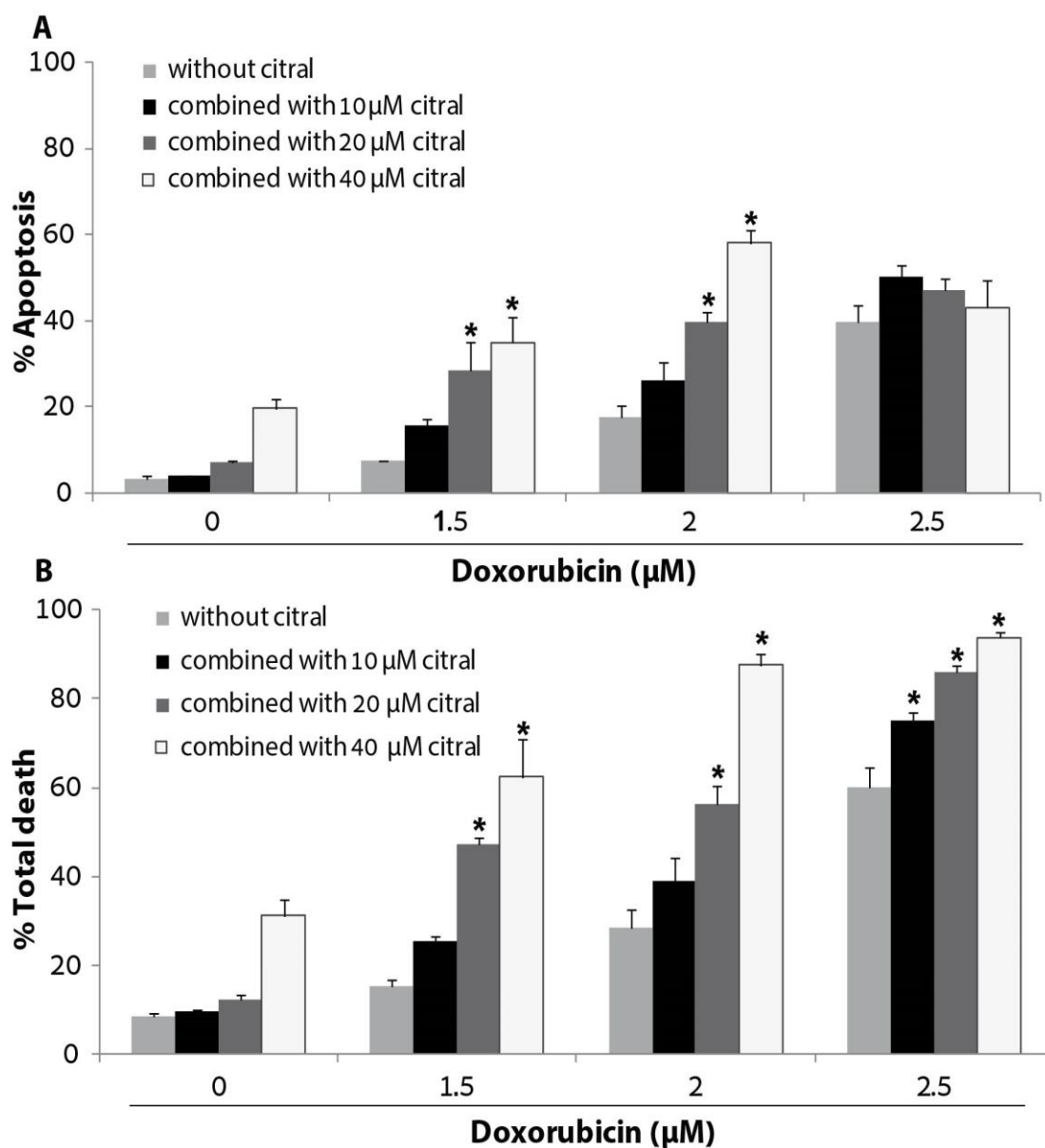
**Figure 21:** The effect of citral on apoptotic induction activity of doxorubicin in Ramos cells. The cells were treated with doxorubicin in the absence and presence of citral for 18 hours. The treated cells were stained with annexin V-FITC/DAPI and analyzed by flow cytometry. The percentage of cells labeled with annexin $V^+$/DAPI$^-$ (early apoptotic cells) (Fig. 21A), and total cell death was plotted (Fig. 21B). The data are expressed as means $\pm$ SEM of three independents experiments.

$* p < 0.05$ denotes statistically significant difference from doxorubicin alone.

**Table 4**: Ramos cell death patterns induced by doxorubicin (DOX) or doxorubicin in combination with citral (CT) for 18 hours. The data are expressed as mean ± SEM of three independent experiments (n=3).

| Treatments | % Viable cells | % Total death | % Death cells | | |
|---|---|---|---|---|---|
| | | | Annexin V positive | DAPI positive | Double positive |
| 0.5% Ethanol | 91.43±0.9 | 8.57±0.9 | 3.10±0.8 | 0.57±0.1 | 4.93±0.6 |
| CT 10 µM | 90.20±0.4 | 9.80±0.4 | 3.93±0.2 | 0.70±0.1 | 5.13±0.4 |
| CT 20 µM | 87.63±1.3 | 12.37±1.3 | 6.93±0.5 | 0.87±0.2 | 4.57±1.2 |
| CT 40 µM | 68.83±3.7* | 31.17±3.7* | 19.67±2.3 | 3.03±1.7 | 8.47±1.2 |
| DOX 1.5 µM | 84.47±1.3 | 15.53±1.3 | 7.30±0.4 | 0.87±0.3 | 8.37±1.2 |
| DOX 1.5 µM+CT 10 µM | 74.40±1.0 | 25.60±1.0 | 15.80±1.4 | 0.80±0.4 | 9.03±0.6 |
| DOX 1.5 µM+CT 20 µM | 52.87±1.7*# | 47.13±1.7*# | 28.47±6.5*# | 4.80±4.3 | 14.67±3.9 |
| DOX 1.5 µM+CT 40 µM | 37.60±8.5*# | 62.40±8.5*# | 34.93±6.1*# | 8.77±5.2 | 18.67±6.0* |
| DOX 2 µM | 71.4±3.9* | 28.60±3.9* | 17.57±0.8 | 0.97±0.2 | 10.07±1.2 |
| DOX 2 µM+CT 10 µM | 61.13±5.4* | 38.87±5.4* | 26.17±0.2* | 0.50±0.1 | 12.20±1.1 |
| DOX  2 µM+CT 20 µM | 43.57±3.9*# | 56.43±3.8*# | 39.70±2.5*# | 2.13±0.2 | 14.57±2.5 |
| DOX  2 µM+CT 40 µM | 12.53±2.7*# | 87.47±2.7*# | 57.93±0.1*# | 4.17±1.6 | 25.40±4.3*# |
| DOX  2.5 µM | 39.90±4.3* | 60.10±4.3* | 39.53±0.1 | 2.90±1.0 | 17.60±1.8 |
| DOX  2.5 µM+CT 10 µM | 24.90±1.7*# | 75.10±1.7*# | 50.33±0.7* | 3.67±0.8 | 21.17±0.9* |
| DOX  2.5 µM+CT 20 µM | 14.03±1.6*# | 85.97±1.6*# | 46.87±0.9* | 11.03±2.5 | 32.03±2.8*# |
| DOX  2.5 µM+CT 40 µM | 6.30±1.3*# | 93.70±1.3*# | 43.10±6.5* | 10.13±3.9 | 40.50±3.7*# |

* $p < 0.05$ denotes statistically significant difference from  0.5% ethanol.

# $p < 0.05$ denotes statistically significant difference from doxorubicin alone compared to each concentration.

**Figure 22:** The effect of citral on apoptotic induction activity of vincristine in Ramos cells. The cells were treated with vincristine in the absence and presence of citral for 18 hours. The treated cells were stained with annexin V-FITC/DAPI and analyzed by flow cytometry. The percentage of cells labeled with annexin $V^+$/DAPI$^-$ (early apoptotic cells) (Fig. 22A), and total cell death was plotted (Fig. 22B). The data are expressed as means ± SEM of three independents experiments.

* $p < 0.05$ denotes statistically significant difference from vincristine alone.

**Table 5:** Ramos cell death patterns induced by vincristine (VIN) or vincristine in combination with citral (CT) for 18 hours. The data are expressed as mean ± SEM of three independent experiments (n=3).

| Treatment | % Viable cells | % Total death | % Death cells | | |
|---|---|---|---|---|---|
| | | | Annexin V positive | DAPI positive | Double positive |
| 0.5% Ethanol | 90.77±1.4 | 9.23±1.4 | 3.97±0.7 | 1.13±0.1 | 4.17±0.8 |
| CT 10 µM | 87.73±0.2 | 12.27±0.2 | 5.67±0.2 | 0.90±0.0 | 5.77±0.4 |
| CT 20 µM | 84.30±1.1 | 15.70±1.1 | 8.47±0.4 | 1.37±0.4 | 5.90±0.6 |
| CT 40 µM | 64.40±1.5* | 35.60±1.5* | 20.73±1.1* | 3.00±1.1 | 11.80±1.8 |
| VIN $10^{-6}$ µM | 88.03±1.9 | 11.97±1.2 | 5.80±1.0 | 1.10±0.3 | 5.07±0.4 |
| VIN $10^{-6}$ µM+CT 10 µM | 76.73±1.9 | 23.27±1.9 | 14.60±1.5 | 1.30±0.3 | 7.37±0.6 |
| VIN $10^{-6}$ µM+CT 20 µM | 65.20±1.5*# | 34.80±1.5*# | 21.77±2.1*# | 2.83±0.6 | 10.23±0.6 |
| VIN $10^{-6}$ µM+CT 40 µM | 44.07±2.5*# | 55.93±2.5*# | 35.80±1.0*# | 4.87±0.9*# | 15.27±3.4*# |
| VIN $10^{-5}$ µM | 79.93±4.6 | 20.07±4.6 | 12.03±3.0 | 1.80±0.6 | 6.23±1.3 |
| VIN $10^{-5}$ µM+CT 10 µM | 66.83±5.3* | 33.17±5.3* | 20.53±1.8* | 1.77±0.5 | 10.87±3.5 |
| VIN $10^{-5}$ µM+CT 20 µM | 58.57±1.2*# | 41.43±1.2*# | 21.83±2.1* | 3.67±0.3 | 15.93±0.6*# |
| VIN $10^{-5}$ µM+CT 40 µM | 46.27±2.2*# | 53.73±2.2*# | 31.50±3.0*# | 6.33±0.4*# | 15.90±0.4*# |
| VIN $10^{-4}$ µM | 76.40±6.0 | 23.60±6.0 | 14.73±4.0 | 1.77±0.7 | 7.07±1.5 |
| VIN $10^{-4}$ µM+CT 10 µM | 64.50±1.7* | 35.50±1.7* | 20.17±0.8* | 3.53±0.7 | 11.77±1.5 |
| VIN $10^{-4}$ µM+CT 20 µM | 59.97±2.6*# | 40.03±2.6*# | 23.87±3.8* | 3.07±0.8 | 13.10±1.1* |
| VIN $10^{-4}$ µM+CT 40 µM | 49.37±5.1*# | 50.63±5.1*# | 30.83±4.3*# | 5.73±0.8*# | 14.07±1.5* |

* $p < 0.05$ denotes statistically significant difference from 0.5% ethanol.

# $p < 0.05$ denotes statistically significant difference from vincristine alone compared to each concentration.
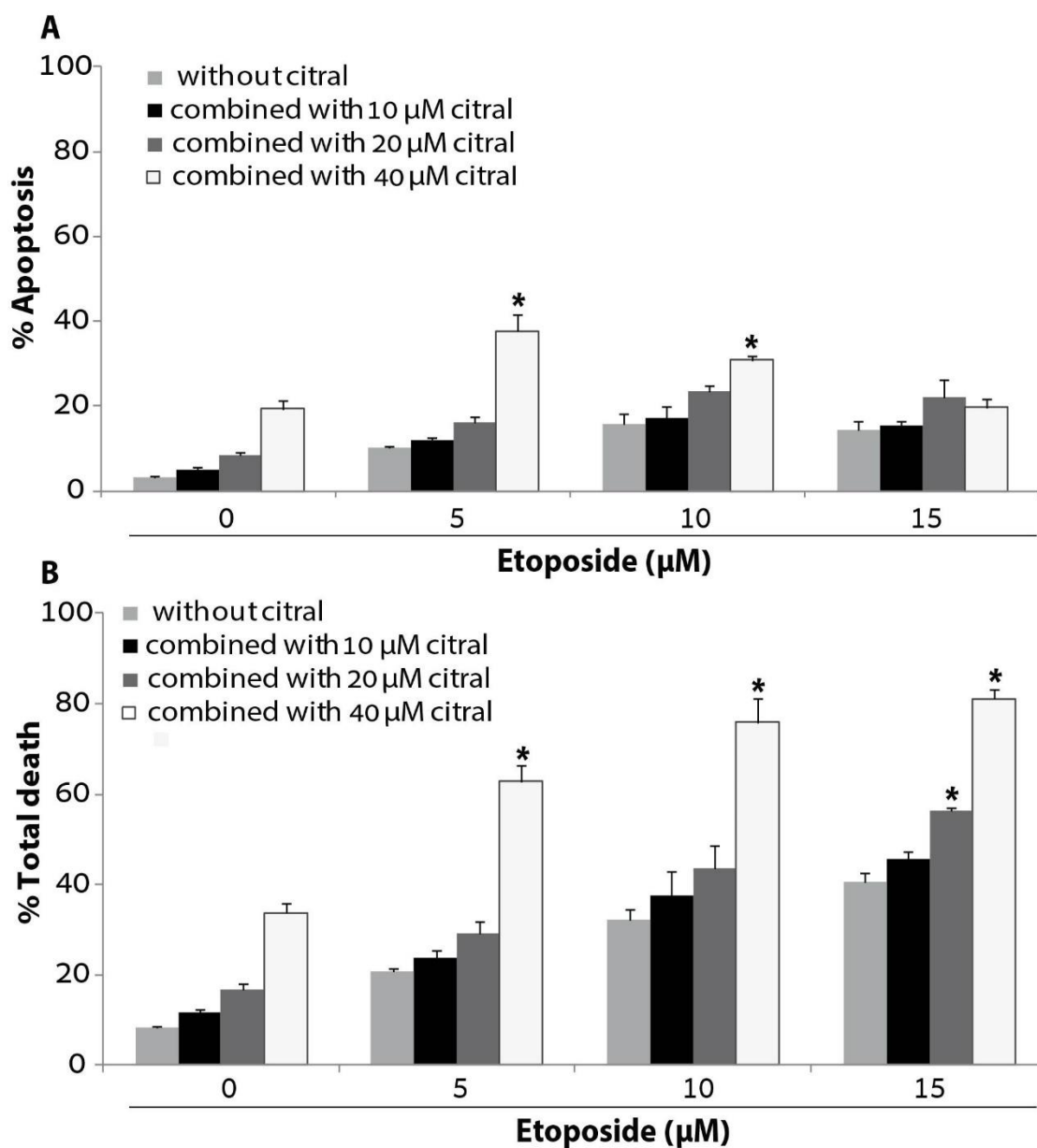
**Figure 23:** The effect of citral on apoptotic induction activity of etoposide in Ramos cells. The cells were treated with etoposide in the absence and presence of citral for 18 hours. The treated cells were stained with annexin V-FITC/DAPI and analyzed by flow cytometry. The percentage of cells labeled with annexin $V^+$/DAPI$^-$ (early apoptotic cells) (Figure 23A), and total cell death was plotted (Figure 23B). The data are expressed as means $\pm$ SEM of three independents experiments.
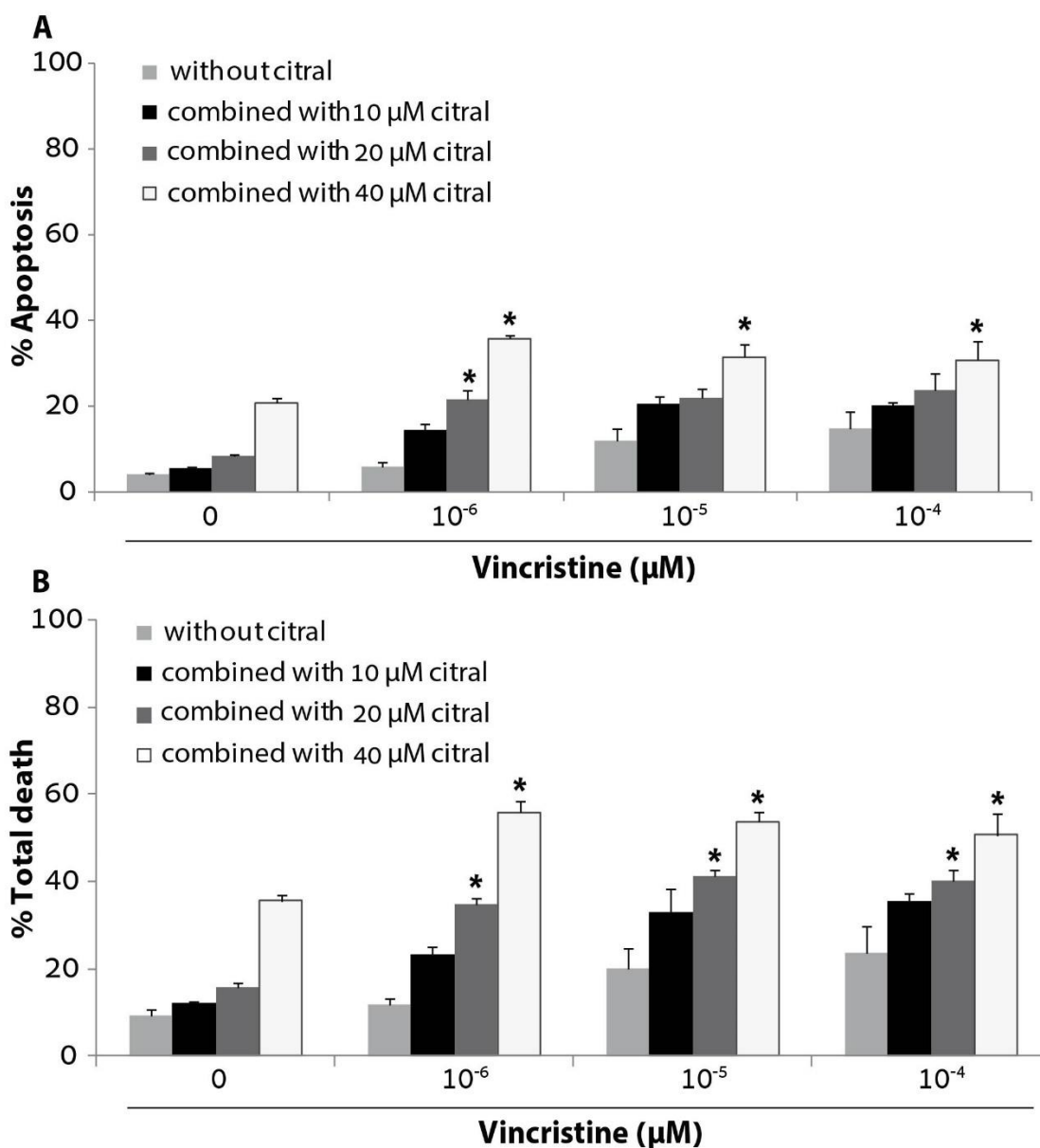
* $p < 0.05$ denotes statistically significant difference from etoposide alone.

**Table 6:** Ramos cell death patterns induced by etoposide (ETO) or etoposide in combination with citral (CT) for 18 hours. The data are expressed as mean ± SEM of three independent experiments (n=3).

| Treatment | % Viable cells | % Total death | % Death cells | | |
|---|---|---|---|---|---|
| | | | Annexin V positive | DAPI positive | Double positive |
| 0.5% Ethanol | 91.53±0.2 | 8.47±0.2 | 3.33±0.3 | 0.93±0.2 | 4.17±0.4 |
| CT 10 μM | 90.10±0.7 | 11.73±0.7 | 4.93±0.6 | 0.83±0.1 | 6.00±0.4 |
| CT 20 μM | 83.13±1.2 | 16.87±1.2 | 8.33±0.7 | 1.20±0.4 | 7.37±0.7 |
| CT 40 μM | 66.23±2.0* | 33.77±2.0* | 19.40±1.8* | 6.63±1.0 | 7.70±1.2 |
| ETO 5 μM | 79.17±0.6 | 20.83±0.6 | 10.30±0.1 | 1.47±0.3 | 9.07±0.3 |
| ETO 5 μM+CT 10 μM | 76.27±1.8* | 23.73±1.8* | 11.87±0.9 | 1.47±0.3 | 10.37±1.3 |
| ETO 5 μM+CT 20 μM | 70.77±2.6* | 29.23±2.6* | 16.17±1.2* | 2.97±0.9 | 10.10±1.8 |
| ETO 5 μM+CT 40 μM | 37.27±3.7*# | 62.73±3.7*# | 37.73±3.7*# | 7.10±2.9 | 17.87±1.9* |
| ETO 10 μM | 67.73±2.1* | 32.27±2.1* | 15.80±2.5* | 1.97±0.2 | 14.50±1.9 |
| ETO 10 μM+CT 10 μM | 62.43±5.3* | 37.57±5.3* | 17.07±2.8* | 4.67±1.2 | 15.83±2.9 |
| ETO 10 μM+CT 20 μM | 56.40±4.9* | 43.60±4.9* | 23.40±1.5* | 4.40±1.0 | 15.83±2.7 |
| ETO 10 μM+CT 40 μM | 24.20±5.3*# | 75.80±5.3*# | 30.80±0.9*# | 22.00±4.1*# | 23.03±4.3* |
| ETO 15 μM | 59.33±1.9* | 40.67±1.9* | 14.47±1.8* | 7.60±1.0 | 18.60±1.1* |
| ETO 15 μM+CT 10 μM | 54.47±1.8* | 45.53±1.8* | 15.37±1.0* | 9.67±2.8 | 20.47±4.4* |
| ETO 15 μM+CT 20 μM | 43.53±0.7*# | 56.47±0.7*# | 21.97±4.3* | 8.70±1.3 | 25.77±4.5* |
| ETO 15 μM+CT 40 μM | 18.87±2.0*# | 81.13±2.0*# | 19.70±2.0* | 30.10±3.9*# | 31.30±3.5*# |

* $p < 0.05$ denotes statistically significant difference from  0.5% ethanol.

# $p < 0.05$ denotes statistically significant difference from etoposide alone compared to each concentration.

Most of chemotherapeutic anticancer drugs induced cancer cell apoptosis via the intrinsic pathway of caspase activation. Modulation of pro-apoptotic and anti-apoptotic BCL-2 family protein expression is the main regulatory mechanism of caspase activation in this pathway. Ramos cells were treated with anticancer drugs in the absence and the presence of citral for 18 hours. The mRNA expression of pro-apoptotic (BAX and BAK) and anti-apoptotic (BCL-2 and BCL-XL) proteins of the treated cells was analyzed by qRT-PCR. The results were presented as RQ numbers which indicate the fold changes in the expression level of interested genes, normalized to endogenous gene control, GAPDH. The solvent control, 0.5% ethanol, had RQ value of 1 for all genes.

Ramos cells expressed much higher amount of BCL-XL, BAX and BAK than BCL-2 (Figure 24). Citral at 40 µM significantly increased the expression of pro-apoptotic protein BAK (Figure 25-27). The ratio of pro-apoptotic proteins to anti-apoptotic proteins (BAX plus BAK: BCL-2 plus BCL-XL) of the citral-treated cells flavored apoptotic stage to survival stage. Citral at 40 µM significantly decreased the expression of anti-apoptotic BCL-XL in 1.5 µM doxorubicin-treated Ramos cells when compared to either doxorubicin- or citral- treated cells. The potentiating effect of citral on doxorubicin induced apoptosis in Ramos cells may possibly come from the decrease of BCL-XL expression (Figure 25). Citral at this concentration increased the mRNA expression of both pro-apoptotic BAK and anti-apoptotic BCL-2 in vincristine-treated Ramos cells (Figure 26). It also increased the mRNA expression of BAK in 5 µM etoposide-treated cells (Figure 27).
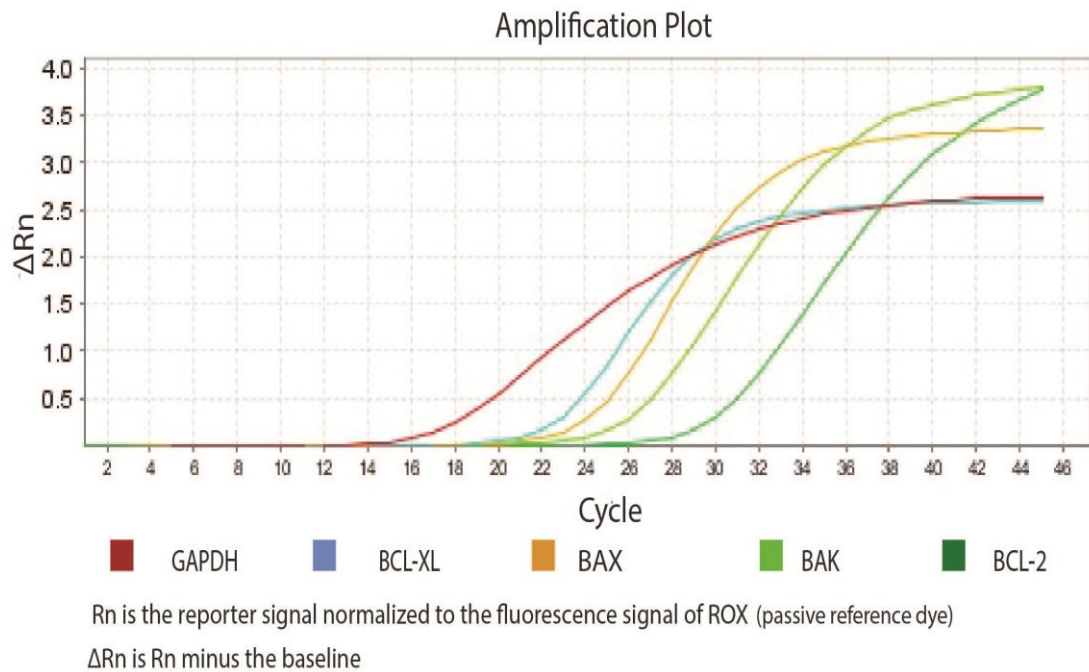
**Figure 24:** Graphical representation by real-time PCR represented the mRNA expression profiles of GAPDH, BCL-XL, BAX, BAK, and BCL-2 in Ramos cells treated with 0.5% ethanol (negative control) at 18 hours incubation.
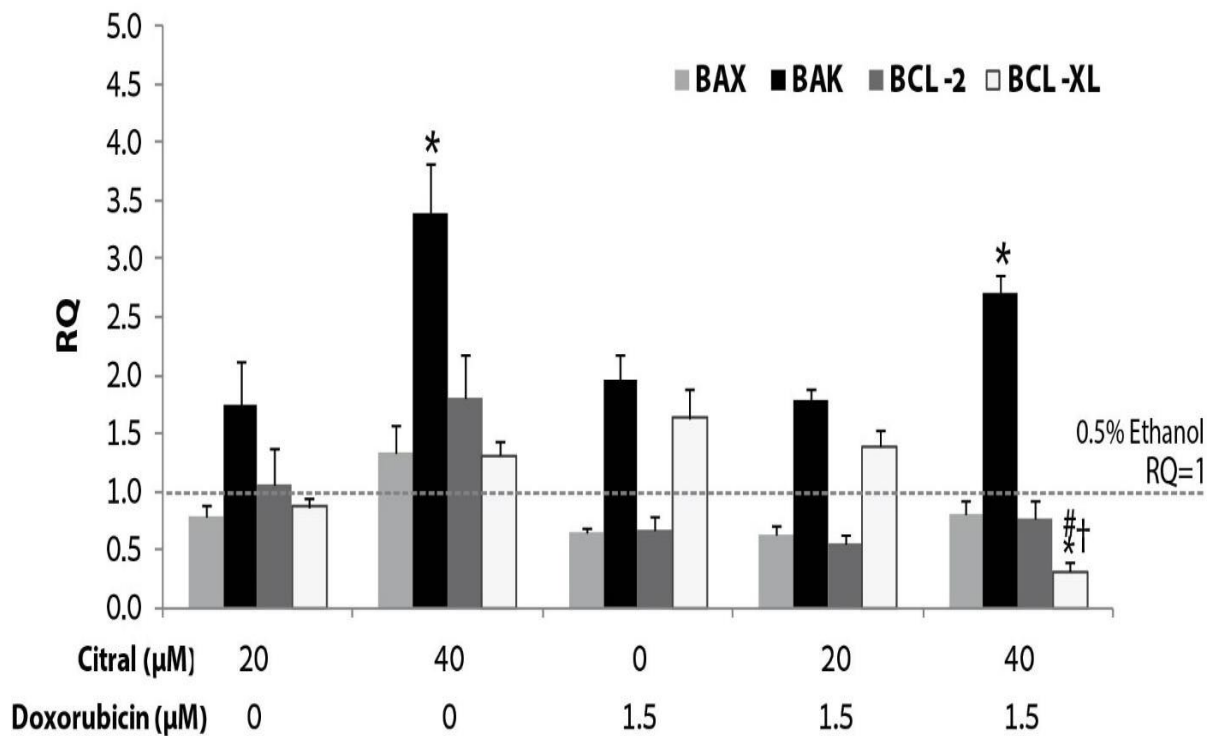
**Figure 25:** The effect of citral on the expression of BAX, BAK, BCL-XL, and BCL-2 in 1.5 μM doxorubicin -treated Ramos cells for 18 hours. The mRNA expression of these BCL-2 family proteins was determined by qRT-PCR. GAPDH was used as an endogenous gene control for normalization. The expression levels of these interested genes from 0.5% ethanol treated Ramos cells were regarded to have RQ=1. The data are expressed as means ± SEM of four independent experiments.

\* $p < 0.05$ denotes statistically significant difference from 0.5% ethanol.

\# $p < 0.05$ denotes statistically significant difference from doxorubicin alone.

† $p < 0.05$ denotes statistically significant difference from 40 μM citral alone.
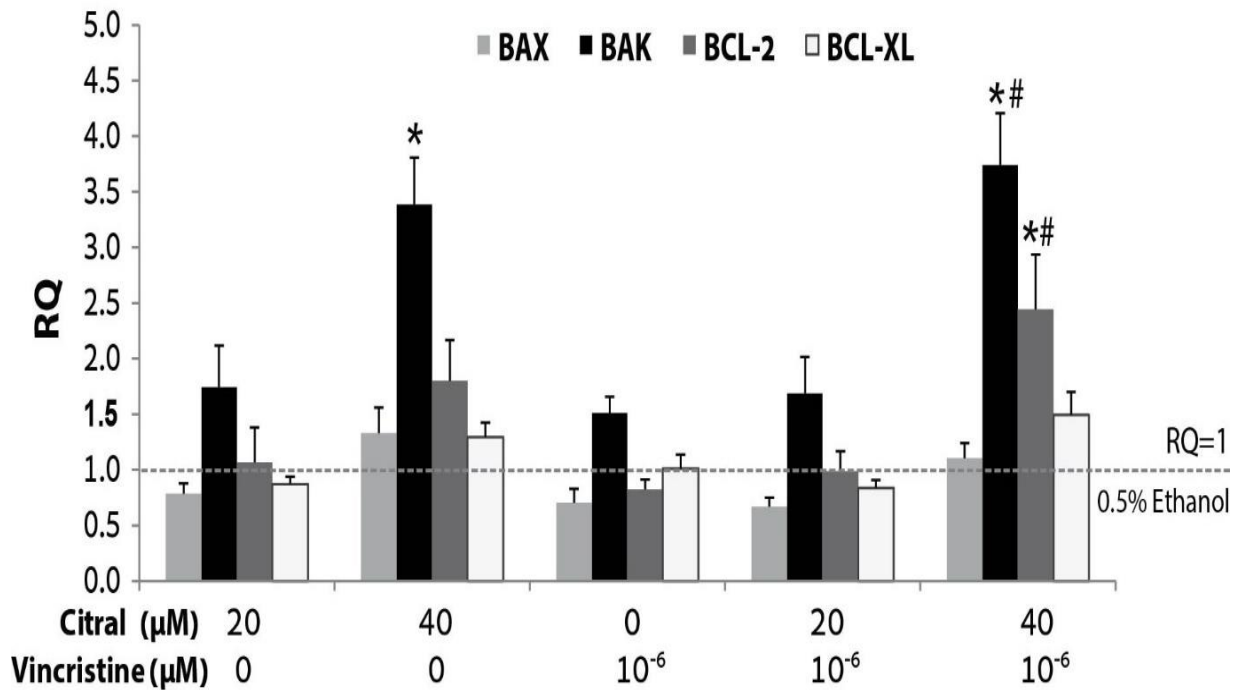
**Figure 26:** The effect of citral on the expression of BAX, BAK, BCL-XL, and BCL-2 in $10^{-6}$ μM vincristine -treated Ramos cells for 18 hours. The mRNA expression of these BCL-2 family proteins was determined qRT-PCR. GAPDH was used as an endogenous gene control for normalization. The expression levels of these interested genes from 0.5% ethanol treated Ramos cells were regarded to have RQ=1. The data are expressed as means ± SEM of four independent experiments.

* $p < 0.05$ denotes statistically significant difference from 0.5% ethanol.

# $p < 0.05$ denotes statistically significant difference from vincristine alone.
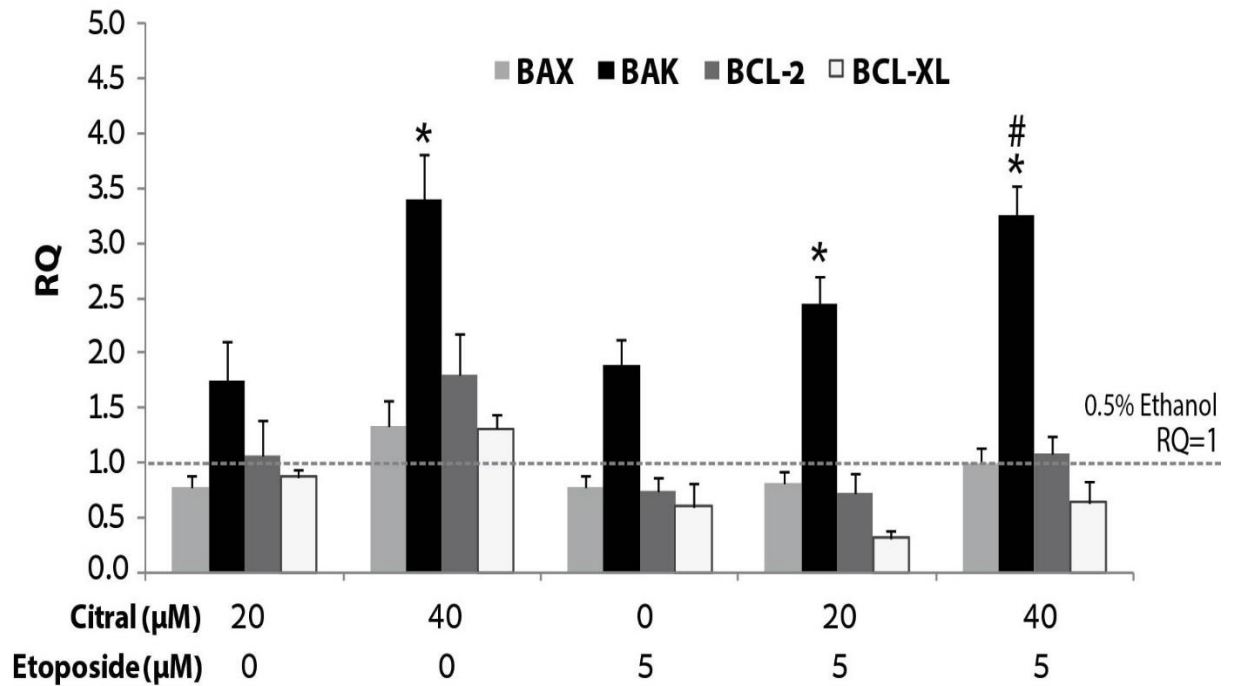
**Figure 27:** The effect of citral on the expression of BAX, BAK, BCL-XL, and BCL-2 in 5 μM etoposide -treated Ramos cells for 18 hours. The mRNA expression of these BCL-2 family proteins was determined by qRT-PCR. GAPDH was used as an endogenous gene control for normalization. The expression levels of these interested genes from 0.5% ethanol treated Ramos cells were regarded to have RQ=1. The data are expressed as means ± SEM of four independent experiments.

* $p < 0.05$ denotes statistically significant difference from 0.5% ethanol.

# $p < 0.05$ denotes statistically significant difference from etoposide alone.

**4.3 Effect of citral on anti-proliferative activities of doxorubicin, vincristine, and etoposide**

This study also elucidated the effect of citral at 10, 20, and 40 µM on anti-proliferative activities of 1.5 µM doxorubicin, 5 µM etoposide, and $10^{-6}$ µM vincristine, respectively. After treating Ramos cells with tested compounds for 3 hours, the treated cells were washed, further incubated in fresh medium without the tested compounds for 48 hours, and counted by Scepter™ Handheld Automated Cell Counter. As presented in Figure 28-30, treatment of 40 µM citral alone significantly decreased Ramos cell proliferation. Doxorubicin and etoposide at 1.5 and 5 µM, respectively, significantly inhibited Ramos cell proliferation whereas vincristine at $10^{-6}$ µM did not have anti-proliferative activity. Citral did not affect the anti-proliferative activities of doxorubicin (Figure 28), and etoposide (Figure 30). It slightly inhibited Ramos cell proliferation in the vincristine-treated cells (Figure 29).
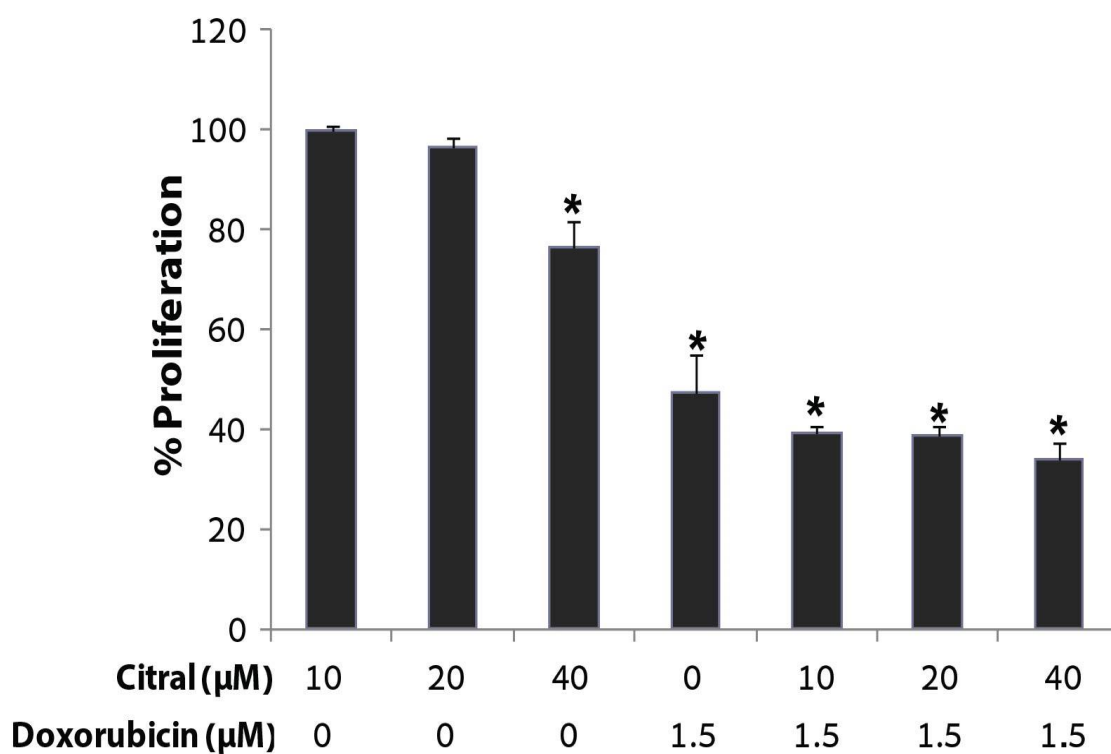
**Figure 28:** The effect of citral on the anti-proliferative effect of 1.5 µM doxorubicin-treated Ramos cells. The inhibition of cell proliferation was compared to 0.5% ethanol treated Ramos cells. The data are expressed as means ± SEM of three independent experiments.

* $p < 0.05$ denotes statistically significant difference from 0.5% ethanol.
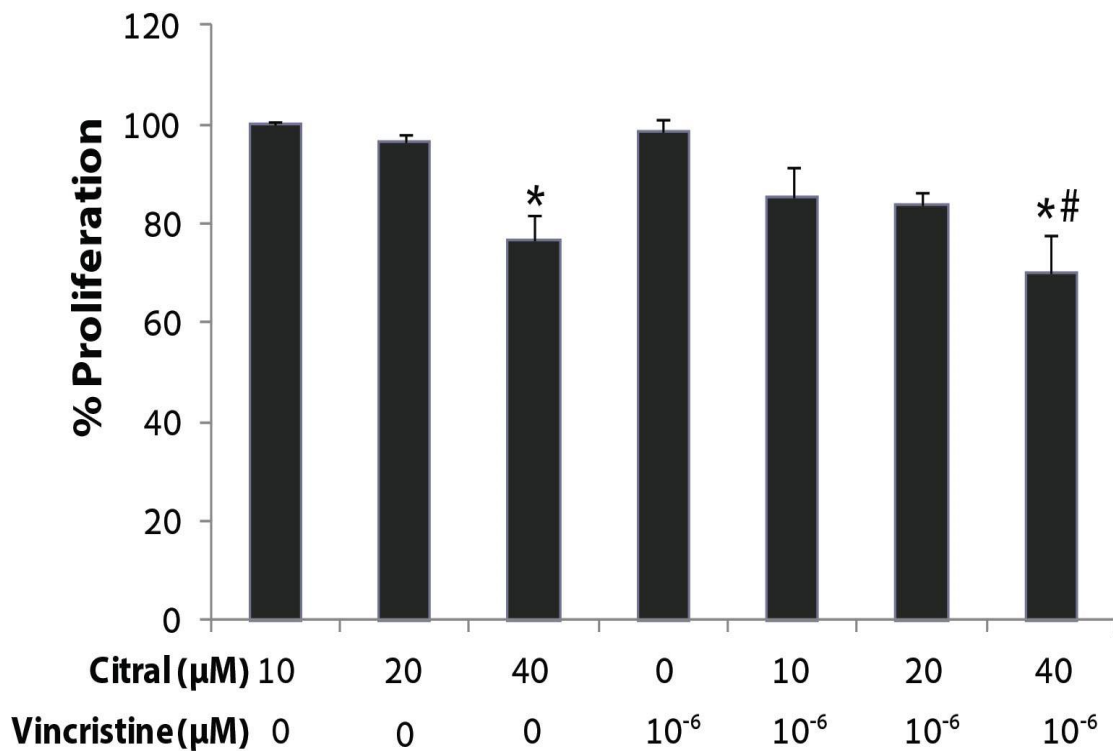
**Figure 29:** The effect of citral on the anti-proliferative effect of $10^{-6}$ µM vincristine-treated Ramos cells. The inhibition of cell proliferation was compared to 0.5% ethanol treated Ramos cells. The data are expressed as means ± SEM of three independent experiments.

* $p < 0.05$ denotes statistically significant difference from 0.5% ethanol.

# $p < 0.05$ denotes statistically significant difference from vincristine alone.
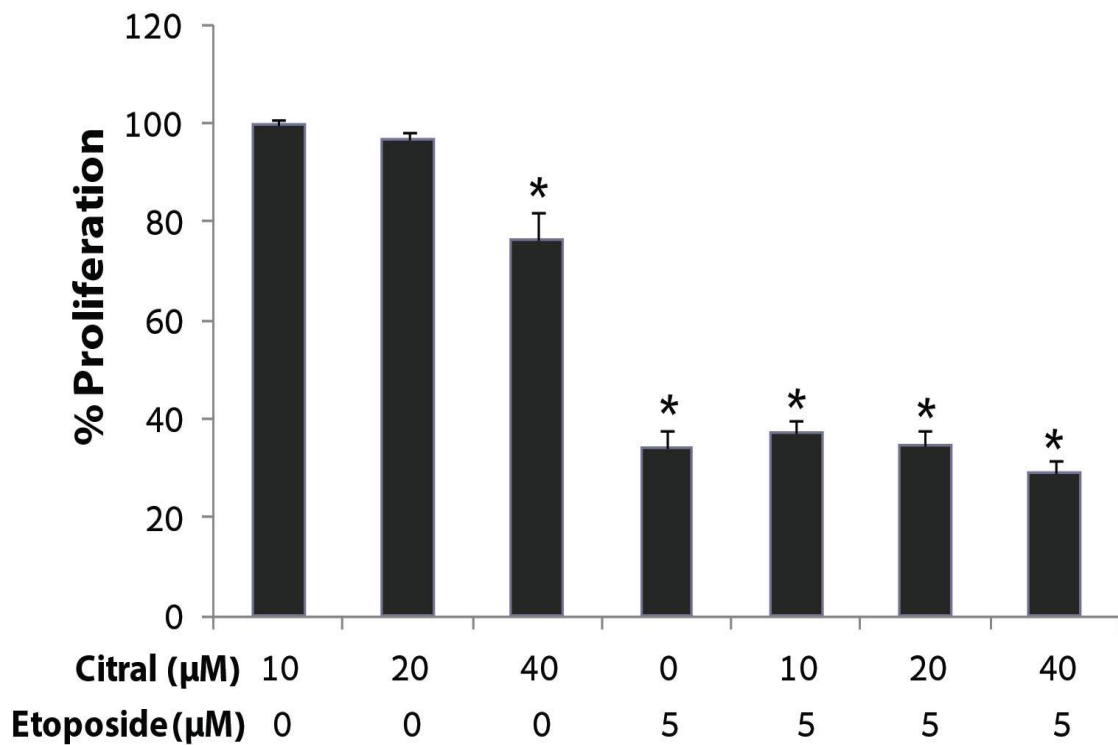
**Figure 30:** The effect of citral on the anti-proliferative effect of 5 μM etoposide -treated Ramos cells. The inhibition of cell proliferation was compared to 0.5% ethanol treated Ramos cells. The data are expressed as means ± SEM of three independent experiments.

* $p < 0.05$ denotes statistically significant difference from 0.5% ethanol.

# CHAPTER V

# DISCUSSION AND CONCLUSION

Treatment for NHL patients has been improved dramatically. Benefits of a targeted cancer drug rituximab, a monoclonal antibody against CD20, with a gold standard CHOP regimen have highlighted the success of combination anticancer therapy (13; 15). Although such combination has shown to be an effective strategy, its use is restricted due to high cost of target-based antibody. Moreover, unpredictable resistance to rituximab in the patients becomes another burden of such chemotherapy. Recently, several compounds from natural source have been explored for their anticancer activity. The combination of these compounds with standard anticancer therapy may not only reduce the dose of concurrent chemotherapy to achieve an effective anticancer activity but also improve upon the adverse events of potent therapeutic agents such as doxorubicin, vincristine, and etoposide which are the chemotherapeutic agents regularly used in NHL patients. Combining of potentiating agent and chemotherapy may reduce the dose of cytotoxic agent and therefore drug-associated toxicity in cancer patients without compromising anticancer activity. Citral was used in this study to explore its possibility to potentiate anticancer activity of clinically used chemotherapeutic agents.

Citral, at 10-40 μM concentrations which were lower than its $IC_{50}$, additively enhanced cytotoxicities of doxorubicin, and etoposide against Ramos cells (Table 3; Figure 14 and 16). Although this edible oil only potentiated cytotoxicity of vincristine at the low concentrations of the chemotherapeutic drug, it did not show antagonist effect when combined with the higher concentrations of this drug (Figure 15).

Citral, as high as 150 μM, did not have any harmful effect on normal PBMCs (12). This study also demonstrated no harmful effect of citral at 10-40 μM on normal human PBMCs, and it did not potentiate effect of all anticancer drugs used in this study on these human normal cells (Figure 17-19). Taken together, these results indicated that citral has no harmful effect on normal cells but selectively potentiate cytotoxicities of doxorubicin, vincristine, and etoposide against cancer cells.

Apoptosis is the most important cellular mechanism to induce cancer cell death. Activation of apoptosis signaling following treatment with cytotoxic drugs has been shown to lead to activation of the mitochondrial (intrinsic) pathway of apoptosis. To investigate the mechanism(s) underlying potentiating effect, this study determined effects of citral on the anticancer drugs-mediated apoptosis. An early indicator of apoptosis is the rapid translocation and accumulation of the membrane phospholipid PS from the cytoplasmic interface of membrane to the extracellular surface (78). This loss of membrane asymmetry can be detected using annexin V. The percentage of annexin V-positive cells was quantified as apoptotic cells in this study. The results showed that citral increased the total cell death induced by doxorubicin, vincristine, and etoposide (Figure 21-23). Citral significantly increased the apoptotic induction activity of these anticancer drugs (Figure 21A-23A). However, at the highest concentrations of doxorubicin and etoposide used in this study, citral could increase the total cell death by increasing the percentage of late apoptotic and necrotic cells (Figure 21B and Figure 23B). It is possible that the higher concentrations of anticancer drugs, the early apoptotic cells *in vitro*, which were not removed by phagocytes *as in vivo* (79), changed to late apoptotic cells quicker than the effect of citral with the lower concentrations of these drugs.

Modulation of pro-apoptotic and anti-apoptotic BCL-2 family protein expression is the main regulatory mechanism of caspase activation in the intrinsic or mitochondrial-dependent apoptosis pathway. This study investigated the effect of citral on doxorubicin, vincristine, and etoposide-induced apoptosis by evaluating the expression of proteins in BCL-2 family. Proteins in this family can either suppress or promote the changes in mitochondrial membrane permeability. BAK and BAX are pro-apoptotic BCL-2 members that are expressed abundantly during apoptosis to promote cell death. BCL-2 and BCL-XL are anti-apoptotic proteins that preserve the membrane integrity of the mitochondria to prevent the release of several apoptotic promoting factors from these organelles. Many mitochondrial apoptogenic factors such as cytochrome c and SMAC/DIABLO trigger caspase activation when they are released into the cytosol (41). Both pro-apoptotic BAK and BAX and anti-apoptotic BCL-2 and BCL-XL expressions were determined by qRT-PCR. Citral alone at 40 µM dramatically upregulated the expression of pro-apoptotic BAK in Ramos cells. BAK is usually on the outer membrane of mitochondria and inhibited by binding to anti-apoptotic proteins such as BCL-XL (80). In the presence of apoptotic stimuli, it changes conformation and undergoes oligomerization to form pore on the mitochondria membrane. BAK plays the key role in cytochrome c release from the mitochondrial inter-membrane space into the cytosol, initiating caspase activation. The function of BAK to initiate apoptosis is faster than pro-apoptotic BAX which has to locate from cytosol to mitochondria for oligomerization (81). The increase in BAK expression in this study (Figure 25-27) was correlated with apoptotic induction activity of citral that mediated by caspase activation in many cancer cell lines (9; 10) as well as human B-lymphoma cells (12) from previous studies.

Doxorubicin at 1.5 µM, $10^{-6}$ µM vincristine, and 5 µM etoposide, which demonstrated potentiating effect of citral on apoptotic induction activities of these drugs, were used to study the expression of proteins in BCL-2 family. Each of these drugs did not significantly change in the expressions of both pro- and anti-apoptotic proteins. Citral at 40 µM significantly attenuated the expression of anti-apoptotic BCL-XL in doxorubicin treated Ramos cells. It also increased the expression of BAK in Ramos cells similar to those treated with 40 µM citral alone. It has been found that anti-apoptotic BCL-XL inhibits BAX and BAK functions by directly forming heterodimer with these pro-apoptotic proteins (44; 80; 82). The decrease in BCL-XL expression led to the formation of BAX oligomers which triggers the caspase activation and apoptosis (82). Several studies have suggested that BCL-XL is the main anti-apoptotic protein to protect B-cells from apoptosis. Over-expression of BCL-XL in immature mouse B-cells, WEH1-231, and several lymphoma cell lines, Ramos, RC-K8 and BJAB, protected these cells from many stimuli-induced apoptosis (83; 84). Its cellular levels could also predict the sensitivity of many B-lymphoma cells and hepatoblastoma HepG2 cells to anticancer agents and apoptotic stimuli better than the cellular levels of BCL-2 (85; 86). Previous study revealed that rituximab synergistically increased the apoptotic induction activity of paclitaxel on NHL B cell lines by suppressing BCL-XL expression (87). Furthermore, BCL-XL inhibitor gossypol synergistically potentiated cytotoxicity of chemotherapeutic drugs, etoposide, doxorubicin, and paclitaxel on Ramos cells (6). Taken together, our results demonstrated that citral could potentiate doxorubicin activity by up-regulating BAK expression and down-regulating BCL-XL expression. Mechanisms underlying these effects of citral should be further evaluated.

Recent study in leukemic NB4 cells illustrated that citral could induce cells to undergo apoptosis by inhibiting of NF-$\kappa$B activity (11). Transcription factor NF-$\kappa$B plays a critical role in anti-apoptosis, cell proliferation, and tumorigenesis. It is activated by multiple activators including growth factors, cytokines, stress and pharmacological agents, such as doxorubicin. The constitutive activation of NF-$\kappa$B has been found in B-cell lymphoma contributing to chemotherapy failure in the patients by preventing cancer cells from undergoing apoptosis (88). Naturally potentiating agent genestine exerted its beneficial effect on the cytotoxicity of CHOP on NHL cell lines through the suppression of NF-$\kappa$B induced by the chemotherapeutic agents (7). In fact, suppression of NF-$\kappa$B activity has become an interesting approach to render cancer cells more susceptible to chemotherapy (88; 89). It is reported that NF-$\kappa$B directly regulates the anti-apoptotic BCL-XL genes, but not BCL-2 (90). Given these into consideration, it is very possible that NF-$\kappa$B partly attribute to the potentiating effect of citral on doxorubicin-mediated apoptosis. Additional studies to determine the effect of citral on the NF-$\kappa$B expression are warranted.

There was an ambiguous to suggest the molecular effect of citral on apoptosis induction of vincristine and etoposide in Ramos cells in this study. Citral significantly increased the expression of BAK in vincristine- and etoposide- treated Ramos cells similar to the effect of citral alone on these cells. The activity of BCL-2 family proteins is controlled at transcriptional, translational and post-translational levels. The interaction between the proteins in this family is also essential for controlling their activity. It has been reported that the anti-apoptotic function of BCL-XL was inhibited by phosphorylation (91). The elucidation on proteins levels and phosphorylation of BCL-2 family members may clearly clarify the effect of citral on the expression of

proteins in BCL-2 family in these anticancer drug treated cells. Citral upregulated BCL-2 mRNA expression in vincristine- treated Ramos cells (Figure 26). However, BCL-2 has less critical anti-apoptotic role than BCL-XL in several B-cells as well as Ramos cells (83; 84; 86). The increase of BCL-2 expression may not be able to overcome the effect from the increase in BAK expression in Ramos cells treated with citral and vincristine. Effects of citral on molecular mechanism(s) of each anticancer drug-mediated apoptosis require in-depth studies in the future.

In summary, this study demonstrated the possibly beneficial effects of citral on the killing effects of doxorubicin, vincristine and etoposide against human cancer B cells without a harm on normal blood cells. Citral potentiated drug-induced cytotoxicity and apoptosis in Ramos cells. Therefore, combination of citral with anticancer drugs may represent an alternative strategy to increase anticancer activity, reduce the dose of these drugs against cancer cells as well as enhance the safety profile of such potent anti-cancer agents in NHL patients. This preliminary work may give direction to use citral with anticancer drugs. However, the potentiating effect of citral still needs several further investigations.

# REFERENCES

1. Jemal A, Bray F, Center MM, Ferlay J, Ward E, Forman D. 2011. Global cancer statistics. *CA: A Cancer Journal for Clinicians* 61:69-90

2. Pfreundschuh M, Trümper L, Kloess M, Schmits R, Feller AC, et al. 2004. Two-weekly or 3-weekly CHOP chemotherapy with or without etoposide for the treatment of elderly patients with aggressive lymphomas: results of the NHL-B2 trial of the DSHNHL. *Blood* 104:634-41

3. Pfreundschuh M, Trümper L, Kloess M, Schmits R, Feller AC, et al. 2004. Two-weekly or 3-weekly CHOP chemotherapy with or without etoposide for the treatment of young patients with good-prognosis (normal LDH) aggressive lymphomas: results of the NHL-B1 trial of the DSHNHL. *Blood* 104:626-33

4. Garg AK, Buchholz TA, Aggarwal BB. 2005. Chemosensitization and radiosensitization of tumors by plant polyphenols. *Antioxidants & Redox Signaling* 7:1630-47

5. Jazirehi AR, Bonavida B. 2004. Resveratrol modifies the expression of apoptotic regulatory proteins and sensitizes non-Hodgkin's lymphoma and multiple myeloma cell lines to paclitaxel-induced apoptosis. *Molecular Cancer Therapeutics* 3:71-84

6. Li Z-M, Jiang W-Q, Zhu Z-Y, Zhu X-F, Zhou J-M, et al. 2008. Synergistic cytotoxicity of BCL-XL inhibitor, gossypol and chemotherapeutic agents in non-Hodgkin's lymphoma cells. *Cancer Biology & Therapy* 7:51-60

7. Mohammad RM, Al-Katib A, Aboukameel A, Doerge DR, Sarkar F, Kucuk O. 2003. Genistein sensitizes diffuse large cell lymphoma to CHOP (cyclophosphamide, doxorubicin, vincristine, prednisone) chemotherapy. *Molecular Cancer Therapeutics* 2:1361-8

8. Edris AE. 2007. Pharmaceutical and therapeutic potentials of essential oils and their individual volatile constituents: a review. *Phytotherapy Research* 21:308-23

9. Dudai N, Weinstein Y, Krup M, Rabinski T, Ofir R. 2005. Citral is a new inducer of caspase-3 in tumor cell lines. *Planta Medica* 71:484-8

10. Chaouki W, Leger DY, Liagre B, Beneytout JL, Hmamouchi M. 2009. Citral inhibits cell proliferation and induces apoptosis and cell cycle arrest in MCF‑7 cells. *Fundamental & Clinical Pharmacology* 23:549-56

11. Xia H, Liang W, Song Q, Chen X, Chen X, Hong J. 2013. The *in vitro* study of apoptosis in NB4 cell induced by citral. *Cytotechnology* 65:49-57

12. Bunkrai C. 2009. *Induction of cell cycle arrest and apoptosis in human B-lymphoma cells by citral*. Chulalongkorn University. 81 pp.

13. Zhong Y. 2006. Non-Hodgkin lymphoma: what primary care professionals need to know. *The Journal for Nurse Practitioners* 2:309-38

14. Turner JJ. 2005. WHO non-Hodgkin's lymphoma classification by criterion-based report review followed by targeted pathology review: an effective strategy for epidemiology studies. *Cancer Epidemiology Biomarkers & Prevention* 14:2213-9

15. Hennessy BT, Hanrahan EO, Daly PA. 2004. Non-Hodgkin lymphoma: an update. *The Lancet Oncology* 5:341-53

16. Zinzani PL. 2005. Lymphoma: diagnosis, staging, natural history, and treatment strategies. *Seminars in Oncology* 32:4-10

17. Michallet A-S, Coiffier B. 2009. Recent developments in the treatment of aggressive non-Hodgkin lymphoma. *Blood Reviews* 23:11-23

18. Müller AM, Ihorst G, Mertelsmann R, Engelhardt M. 2005. Epidemiology of non-Hodgkin's lymphoma (NHL): trends, geographic distribution, and etiology. *Annals of Hematology* 84:1-12

19. Evans LS, Hancock BW. 2003. Non-Hodgkin lymphoma. *The Lancet* 362:139-46

20. Bilodeau BA, Fessele KL. 1998. Non-Hodgkin's lymphoma. *Seminars in Oncology Nursing* 14:273-83

21. Chu E, Sartorelli AC. 2009. Cancer chemotherapy. In *Basic and clinical pharmacology*, ed. BG Katzung, SB Masters, AJ Trevor:935-62. New York McGraw-Hill. Number of 935-62 pp.

22. Chabner BA. 2011. General principles of cancer chemotherapy. In *Goodman & Gilman's the pharmacological basis of therapeutics*, ed. LL Brunton, BA Chabner, BC Knollmann:1315-404. New York McGraw-Hill. Number of 1315-404 pp.

23. Kiyomiya K-i, Matsuo S, Kurebe M. 2001. Mechanism of specific nuclear transport of adriamycin: the mode of nuclear translocation of adriamycin-proteasome complex. *Cancer Research* 61:2467-71

24. Lee K, Qian DZ, Rey S, Wei H, Liu JO, Semenza GL. 2009. Anthracycline chemotherapy inhibits HIF-1 transcriptional activity and tumor-induced mobilization of circulating angiogenic cells. *Proceedings of the National Academy of Sciences* 106:2353-8

25. Greenstein S, Ghias K, Krett NL, Rosen ST. 2002. Mechanisms of glucocorticoid-mediated apoptosis in hematological malignancies. *Clinical Cancer Research* 8:1681-94

26. Coiffier B, Lepage E, Brière J, Herbrecht R, Tilly H, et al. 2002. CHOP chemotherapy plus rituximab compared with CHOP alone in elderly patients with diffuse large-B-cell lymphoma. *New England Journal of Medicine* 346:235-42

27. Feugier P, Van Hoof A, Sebban C, Solal-Celigny P, Bouabdallah R, et al. 2005. Long-term results of the R-CHOP study in the treatment of elderly patients with diffuse large B-cell lymphoma: a study by the Groupe d'Etude des Lymphomes de l'Adulte. *Journal of Clinical Oncology* 23:4117-26

28. Mounier N, Briere J, Gisselbrecht C, Emile J-F, Lederlin P, et al. 2003. Rituximab plus CHOP (R-CHOP) overcomes BCL-2—associated resistance to chemotherapy in elderly patients with diffuse large B-cell lymphoma (DLBCL). *Blood* 101:4279-84

29. Limat S, Demesmay K, Voillat L, Bernard Y, Deconinck E, et al. 2003. Early cardiotoxicity of the CHOP regimen in aggressive non-Hodgkin's lymphoma. *Annals of Oncology* 14:277-81

30. Soni H, Pandya G, Patel P, Acharya A, Jain M, Mehta AA. 2011. Beneficial effects of carbon monoxide-releasing molecule-2 (CORM-2) on acute doxorubicin cardiotoxicity in mice: role of oxidative stress and apoptosis. *Toxicology and Applied Pharmacology* 253:70-80

31. Debatin K-M. 2004. Apoptosis pathways in cancer and cancer therapy. *Cancer Immunology, Immunotherapy* 53:153-9

32. Weinberg RA. 2013. *The biology of cancer*. pp 331-390. New York: Garland Science. 960 pp.

33. Taylor RC, Cullen SP, Martin SJ. 2008. Apoptosis: controlled demolition at the cellular level. *Nature Reviews Molecular Cell Biology* 9:231-41

34. Ghavami S, Hashemi M, Ande SR, Yeganeh B, Xiao W, et al. 2009. Apoptosis and cancer: mutations within caspase genes. *Journal of Medical Genetics* 46:497-510

35. Riedl SJ, Shi Y. 2004. Molecular mechanisms of caspase regulation during apoptosis. *Nature Reviews Molecular Cell Biology* 5:897-907

36. Wang X. 2001. The expanding role of mitochondria in apoptosis. *Genes & Development* 15:2922-33

37. Zou H, Li Y, Liu X, Wang X. 1999. An APAF-1-cytochrome c multimeric complex is a functional apoptosome that activates procaspase-9. *Journal of Biological Chemistry* 274:11549-56

38. Srinivasula SM, Hegde R, Saleh A, Datta P, Shiozaki E, et al. 2001. A conserved XIAP-interaction motif in caspase-9 and SMAC/DIABLO regulates caspase activity and apoptosis. *Nature* 410:112-6

39. Chipuk JE, Green DR. 2008. How do BCL-2 proteins induce mitochondrial outer membrane permeabilization? *Trends in Cell Biology* 18:157-64

40. Martinou J-C, Green DR. 2001. Breaking the mitochondrial barrier. *Nature Reviews Molecular Cell Biology* 2:63-7

41. Chipuk J, Bouchier-Hayes L, Green D. 2006. Mitochondrial outer membrane permeabilization during apoptosis: the innocent bystander scenario. *Cell Death & Differentiation* 13:1396-402

42. Youle RJ, Strasser A. 2008. The BCL-2 protein family: opposing activities that mediate cell death. *Nature Reviews Molecular Cell Biology* 9:47-59

43. Dewson G, Kluck RM. 2009. Mechanisms by which BAK and BAX permeabilise mitochondria during apoptosis. *Journal of Cell Science* 122:2801-8

44. Martinou J-C, Youle RJ. 2011. Mitochondria in apoptosis: BCL-2 family members and mitochondrial dynamics. *Developmental Cell* 21:92-101

45. Dey S, Spring PM, Arnold S, Valentino J, Chendil D, et al. 2003. Low-dose fractionated radiation potentiates the effects of paclitaxel in wild-type and mutant p53 head and neck tumor cell lines. *Clinical Cancer Research* 9:1557-65

46. Sarkar FH, Li Y. 2006. Using chemopreventive agents to enhance the efficacy of cancer therapy. *Cancer Research* 66:3347-50

47. Igney FH, Krammer PH. 2002. Death and anti-death: tumour resistance to apoptosis. *Nature Reviews Cancer* 2:277-88

48. Stolz C, Hess G, Hähnel PS, Grabellus F, Hoffarth S, et al. 2008. Targeting BCL-2 family proteins modulates the sensitivity of B-cell lymphoma to rituximab-induced apoptosis. *Blood* 112:3312-21

49. Shabbits JA, Hu Y, Mayer LD. 2003. Tumor chemosensitization strategies based on apoptosis manipulations. *Molecular Cancer Therapeutics* 2:805-13

50. Alas S, Emmanouilides C, Bonavida B. 2001. Inhibition of interleukin 10 by rituximab results in down-regulation of BCL-2 and sensitization of B-cell non-Hodgkin's lymphoma to apoptosis. *Clinical Cancer Research* 7:709-23

51. Habermann TM, Weller EA, Morrison VA, Gascoyne RD, Cassileth PA, et al. 2006. Rituximab-CHOP versus CHOP alone or with maintenance rituximab in older patients with diffuse large B-cell lymphoma. *Journal of Clinical Oncology* 24:3121-7

52. Mohammad RM, Wang S, Aboukameel A, Chen B, Wu X, et al. 2005. Preclinical studies of a nonpeptidic small-molecule inhibitor of BCL-2 and BCL-XL [(−)-gossypol] against diffuse large cell lymphoma. *Molecular Cancer Therapeutics* 4:13-21

53. Pihlasalo J, Klika KD, Murzin DY, Nieminen V. 2007. Conformational equilibria of citral. *Journal of Molecular Structure: THEOCHEM* 814:33-41

54. Silva CdBd, Guterres SS, Weisheimer V, Schapoval EE. 2008. Antifungal activity of the lemongrass oil and citral against *Candida spp. Brazilian Journal of Infectious Diseases* 12:63-6

55. Ress NB, Hailey JR, Maronpot RR, Bucher JR, Travlos GS, et al. 2003. Toxicology and carcinogenesis studies of microencapsulated citral in rats and mice. *Toxicological Sciences* 71:198-206

56. Phillips JC, Kingsnorth J, Gangolli SD, Gaunt IF. 1976. Studies on the absorption, distribution and excretion of citral in the rat and mouse. *Food and Cosmetics Toxicology* 14:537-40

57. Jackson GM, Hall DE, Walker R. 1987. Comparison of the short-term hepatic effects of orally administered citral in Long Evans hooded and Wistar albino rats. *Food and Chemical Toxicology* 25:505-13

58. Roffey SJ, Walker R, Gibson GG. 1990. Hepatic peroxisomal and microsomal enzyme induction by citral and linalool in rats. *Food and Chemical Toxicology* 28:403-8

59. Vinitketkumnuen U, Puatanachokchai R, Kongtawelert P, Lertprasertsuke N, Matsushima T. 1994. Antimutagenicity of lemon grass (*Cymbopogon citratus* Stapf) to various known mutagens in salmonella mutation assay. *Mutation Research Genetic Toxicology* 341:71-5

60. Hayes A, Markovic B. 2002. Toxicity of Australian essential oil *Backhousia citriodora* (Lemon myrtle). Part 1. An antimicrobial activity and *in vitro* cytotoxicity. *Food and Chemical Toxicology* 40:535-43

61. Sandri IG, Zacaria J, Fracaro F, Delamare APL, Echeverrigaray S. 2007. Antimicrobial activity of the essential oils of Brazilian species of the genus *Cunila* against foodborne pathogens and spoiling bacteria. *Food Chemistry* 103:823-8

62. Naik MI, Fomda BA, Jaykumar E, Bhat JA. 2010. Antibacterial activity of lemongrass (*Cymbopogon citratus*) oil against some selected pathogenic bacterias. *Asian Pacific Journal of Tropical Medicine* 3:535-8

63. Saddiq AA, Khayyat SA. 2010. Chemical and antimicrobial studies of monoterpene: Citral. *Pesticide Biochemistry and Physiology* 98:89-93

64. Lima IO, de Medeiros Nóbrega F, de Oliveira WA, de Oliveira Lima E, Albuquerque Menezes E, et al. 2012. Anti-*Candida albicans* effectiveness of citral and investigation of mode of action. *Pharmaceutical Biology* 50:1536-41

65. Tzortzakis NG, Economakis CD. 2007. Antifungal activity of lemongrass (*Cympopogon citratus*) essential oil against key postharvest pathogens. *Innovative Food Science & Emerging Technologies* 8:253-8

66. Khan MSA, Ahmad I. 2011. Antifungal activity of essential oils and their synergy with fluconazole against drug-resistant strains of *Aspergillus fumigatus* and *Trichophyton rubrum*. *Applied Microbiology and Biotechnology* 90:1083-94

67. Hierro I, Valero A, Navarro MC. 2006. *In vivo* larvicidal activity of monoterpenic derivatives from aromatic plants against L3 larvae of *Anisakis simplex* s.l. *Phytomedicine* 13:527-31

68. Minami M, Kita M, Nakaya T, Yamamoto T, Kuriyama H, Imanishi J. 2003. The inhibitory effect of essential oils on herpes simplex virus type-1 replication *in vitro*. *Microbiology and Immunology* 47:681

69. Lee HJ, Jeong HS, Kim DJ, Noh YH, Yuk DY, Hong JT. 2008. Inhibitory effect of citral on NO production by suppression of iNOS expression and NF-$\kappa$B activation in RAW264.7 cells. *Archives of Pharmacal Research* 31:342-9

70. Sforcin JM, Amaral JT, Fernandes BA, Sousa JP, Bastos JK. 2009. Lemongrass effects on IL-1$\beta$ and IL-6 production by macrophages. *Natural product research* 23:1151-9

71. Katsukawa M, Nakata R, Takizawa Y, Hori K, Takahashi S, Inoue H. 2010. Citral, a component of lemongrass oil, activates PPAR$\alpha$ and $\gamma$ and suppresses COX-2 expression. *Biochimica et Biophysica Acta (BBA)-Molecular and Cell Biology of Lipids* 1801:1214-20

72. Bachiega TF, Sforcin JM. 2011. Lemongrass and citral effect on cytokines production by murine macrophages. *Journal of Ethnopharmacology* 137:909-13

73. Quintans-Júnior LJ, Guimarães AG, Santana MTd, Araújo BE, Moreira FV, et al. 2011. Citral reduces nociceptive and inflammatory response in rodents. *Revista Brasileira de Farmacognosia* 21:497-502

74. Ponce Monter HA. 2010. Synergistic effect of the interaction between naproxen and citral on inflammation in rats. *Phytomedicine* 18:74-9

75. Rajasekaran D, Manoharan S, Baskaran N, Vasudevan K. 2011. Evaluation of chemopreventive efficacy of citral in 7, 12- dimethylbenz (a) anthracene (DMBA) induced hamster buccal pouch carcinogenesis. *International Journal of Research in Phytochemistry and Pharmacology* 1:136-43

76. Chou T-C. 2010. Drug combination studies and their synergy quantification using the Chou-Talalay method. *Cancer Research* 70:440-6

77. Chougule MB, Patel A, Sachdeva P, Jackson T, Singh M. 2011. Enhanced anticancer activity of gemcitabine in combination with noscapine via antiangiogenic and apoptotic pathway against non-small cell lung cancer. *Plos One* 6:e27394

78. Elmore S. 2007. Apoptosis: a review of programmed cell death. *Toxicologic Pathology* 35:495-516

79. Nagata S, Hanayama R, Kawane K. 2010. Autoimmunity and the clearance of dead cells. *Cell* 140:619-30

80. Willis SN, Chen L, Dewson G, Wei A, Naik E, et al. 2005. Proapoptotic BAK is sequestered by MCL-1 and BCL-XL, but not BCL-2, until displaced by BH3-only proteins. *Genes & Development* 19:1294-305

81. Yao Y, Marassi FM. 2009. BAX and BAK caught in the act. *Molecular Cell* 36:353-4

82. Billen LP, Kokoski CL, Lovell JF, Leber B, Andrews DW. 2008. BCL-XL inhibits membrane permeabilization by competing with BAX. *Plos Biology* 6:e147

83. Fang W, Rivard JJ, Ganser JA, LeBien TW, Nath KA, et al. 1995. BCL-XL rescues WEHI 231 B lymphocytes from oxidant-mediated death following diverse apoptotic stimuli. *The Journal of Immunology* 155:66-75

84. Gottschalk AR, Boise LH, Thompson CB, Quintans J. 1994. Identification of immunosuppressant-induced apoptosis in a murine B-cell line and its prevention by BCL-X but not BCL-2. *Proceedings of the National Academy of Sciences* 91:7350-4

85. Luo D, Cheng SC-S, Xie H, Xie Y. 2000. Effects of BCL-2 and BCL-XL protein levels on chemoresistance of hepatoblastoma HepG2 cell line. *Biochemistry and Cell Biology* 78:119-26

86. Yeo AT, Porco Jr JA, Gilmore TD. 2012. BCL-X, but not BCL-2, can protect human B-lymphoma cell lines from parthenolide-induced apoptosis. *Cancer Letters* 318:53-60

87. Jazirehi AR, Gan XH, Vos SD, Emmanouilides C, Bonavida B. 2003. Rituximab (anti-CD20) selectively modifies BCL-XL and apoptosis protease activating factor-1 (APAF-1) expression and sensitizes human non-Hodgkin's lymphoma B cell lines to paclitaxel-induced apoptosis. *Molecular Cancer Therapeutics* 2:1183-93

88. Sethi G, Sung B, Aggarwal BB. 2008. Nuclear factor-**K**B activation: from bench to bedside. *Experimental Biology and Medicine* 233:21-31

89. Bednarski BK, Baldwin Jr AS, Kim HJ. 2009. Addressing reported pro-apoptotic functions of NF-**K**B: targeted inhibition of canonical NF-**K**B enhances the apoptotic effects of doxorubicin. *Plos One* 4:e6992

90. Chen C, Edelstein LC, Gélinas C. 2000. The Rel/NF-**K**B family directly activates expression of the apoptosis inhibitor BCL-XL. *Molecular and Cellular Biology* 20:2687-95

91. Basu A, Haldar S. 2003. Identification of a novel BCL-XL phosphorylation site regulating the sensitivity of taxol-or 2-methoxyestradiol-induced apoptosis. *FEBS Letters* 538:41-7

APPENDIX

# APPENDIX A

## Buffers and Reagents

1. RPMI 1640 stock solution 1 liter

| | | |
|---|---|---|
| RPMI powder | 10.4 | g |
| $NaHCO_3$ | 1.5 | g |
| Glucose | 4.5 | g |
| Sodium pyruvate | 0.11 | g |
| HEPES (1M) | 10 | ml |
| Penicillin/streptomycin | 10 | ml |
| $ddH_2O$ | 900 | ml |

Adjust pH to 7.2 with 1M HCl.

Add $ddH_2O$ to 1 liter and sterilized by filtering through a 0.22 μm sterile membrane filter.

2. Complete RPMI 1640 medium 200 ml

| | | |
|---|---|---|
| RPMI stock | 180 | ml |
| Fetal Bovine Serum | 20 | ml |

3. 10x Phosphate Buffered Saline (PBS) 1 liter

| | | |
|---|---|---|
| NaCl | 80.65 | g |
| KCl | 2 | g |
| $KH_2PO_4$ | 2 | g |
| $Na_2HPO_4$ | 11.5 | g |
| $ddH_2O$ | 900 | ml |

Adjust pH to 7.4 with 1M HCl.

Add $ddH_2O$ to 1 liter and sterilized by autoclaving.

4. 10x Assay Buffered 100 ml

| | | |
|---|---|---|
| HEPES (1M) | 10 | ml |
| $CaCl_2$ (0.1M) | 28 | ml |
| NaCl (5M) | 25 | ml |
| $ddH_2O$ | 37 | ml |

5. Tris-HCl 1M pH 8.0 100 ml

| | | |
|---|---|---|
| Tris-base | 12.114 | g |
| $ddH_2O$ | 80 | ml |

Adjust pH to 8.0 with concentrated HCl solution.

Add $ddH_2O$ to 100 ml and sterilized by autoclaving.

6. DEPC 0.1% v/v 500 ml

| | | |
|---|---|---|
| $ddH_2O$ | 500 | ml |
| DEPC | 500 | μl |

Adjust to 500 ml by $ddH_2O$ and sterilized by autoclaving.

# APPENDIX B

## Results

**Table 7:** Descriptive data by SPSS of the percentage of cytotoxicity of citral (CT), doxorubicin (DOX), and the combinations against Ramos cells at 24 hours incubation of three independent experiments (n=3).

| Treatments | N | Mean | Std. Deviation | Std. Error | 95% Confidence Interval for Mean | | Minimum | Maximum |
|---|---|---|---|---|---|---|---|---|
| | | | | | Lower Bound | Upper Bound | | |
| 0.5%Ethanol | 3 | 2.1400 | 2.75158 | 1.58863 | -4.6953 | 8.9753 | -.90 | 4.46 |
| 10µM CT | 3 | 3.9233 | .81144 | .46848 | 1.9076 | 5.9391 | 3.34 | 4.85 |
| 20µM CT | 3 | 8.2267 | 2.91138 | 1.68089 | .9944 | 15.4589 | 5.72 | 11.42 |
| 40µM CT | 3 | 18.4133 | 3.03009 | 1.74942 | 10.8862 | 25.9405 | 15.88 | 21.77 |
| 1µM DOX | 3 | 1.0733 | .85002 | .49076 | -1.0382 | 3.1849 | .22 | 1.92 |
| 1.5µM DOX | 3 | 13.5167 | 4.18002 | 2.41333 | 3.1329 | 23.9004 | 8.69 | 15.93 |
| 2µM DOX | 3 | 25.7233 | 2.90748 | 1.67863 | 18.5008 | 32.9459 | 22.63 | 28.40 |
| 2.5µM DOX | 3 | 53.2000 | 3.92000 | 2.26321 | 43.4622 | 62.9378 | 50.08 | 57.60 |
| 3µM DOX | 3 | 72.8367 | 4.60029 | 2.65598 | 61.4089 | 84.2644 | 69.06 | 77.96 |
| 1µM DOX | 3 | 3.2533 | 3.64245 | 2.10297 | -5.7950 | 12.3017 | -.68 | 6.51 |
| 1.5µM DOX+10µM CT | 3 | 10.4600 | .66506 | .38397 | 8.8079 | 12.1121 | 9.79 | 11.12 |
| 2µM DOX+10µM CT | 3 | 38.6833 | 1.90799 | 1.10158 | 33.9436 | 43.4230 | 36.84 | 40.65 |
| 2.5µM DOX+10µM CT | 3 | 67.0233 | 4.26897 | 2.46469 | 56.4186 | 77.6281 | 62.31 | 70.63 |
| 3µM DOX+10µM CT | 3 | 92.7033 | 2.72034 | 1.57059 | 85.9456 | 99.4610 | 89.89 | 95.32 |
| 1µM DOX+20µM CT | 3 | 11.2167 | 4.81806 | 2.78171 | -.7521 | 23.1854 | 8.15 | 16.77 |
| 1.5µM DOX+20µM CT | 3 | 23.7100 | 4.49508 | 2.59523 | 12.5436 | 34.8764 | 20.03 | 28.72 |
| 2µM DOX+20µM CT | 3 | 54.7633 | 7.51481 | 4.33868 | 36.0955 | 73.4312 | 47.48 | 62.49 |
| 2.5µM DOX+20µM CT | 3 | 78.9333 | 1.38911 | .80200 | 75.4826 | 82.3841 | 77.82 | 80.49 |
| 3µM DOX+20µM CT | 3 | 92.6367 | 2.17939 | 1.25827 | 87.2228 | 98.0506 | 90.35 | 94.69 |
| 1µM DOX+40µM CT | 3 | 28.3600 | 2.78372 | 1.60718 | 21.4449 | 35.2751 | 25.15 | 30.11 |
| 1.5µM DOX+40µM CT | 3 | 72.8467 | 6.72997 | 3.88555 | 56.1285 | 89.5648 | 65.39 | 78.47 |
| 2µM DOX+40µM CT | 3 | 91.8800 | 1.14333 | .66010 | 89.0398 | 94.7202 | 90.60 | 92.80 |
| 2.5µM DOX+40µM CT | 3 | 96.4567 | 1.67444 | .96674 | 92.2971 | 100.6162 | 94.67 | 97.99 |
| 3µM DOX+40µM CT | 3 | 97.3733 | .79513 | .45907 | 95.3981 | 99.3485 | 96.57 | 98.16 |
| Total | 72 | 44.1397 | 35.23691 | 4.15271 | 35.8595 | 52.4200 | -.90 | 98.16 |

**Table 8:** Descriptive data by SPSS of the percentage of cytotoxicity of citral (CT), vincristine (VIN), and the combinations against Ramos cells at 24 hours incubation of three independent experiments (n=3).

| Treatments | N | Mean | Std. Deviation | Std. Error | 95% Confidence Interval for Mean | | Minimum | Maximum |
|---|---|---|---|---|---|---|---|---|
| | | | | | Lower Bound | Upper Bound | | |
| 0.5%Ethanol | 3 | 2.1400 | 2.75158 | 1.58863 | -4.6953 | 8.9753 | -.90 | 4.46 |
| 10µM CT | 3 | 3.9233 | .81144 | .46848 | 1.9076 | 5.9391 | 3.34 | 4.85 |
| 20µM CT | 3 | 8.2267 | 2.91138 | 1.68089 | .9944 | 15.4589 | 5.72 | 11.42 |
| 40µM CT | 3 | 18.4133 | 3.03009 | 1.74942 | 10.8862 | 25.9405 | 15.88 | 21.77 |
| $10^{-6}$µM VIN | 3 | 19.3367 | 6.11216 | 3.52886 | 4.1532 | 34.5201 | 14.65 | 26.25 |
| $10^{-5}$µM VIN | 3 | 23.1633 | 3.07053 | 1.77277 | 15.5357 | 30.7909 | 19.77 | 25.75 |
| $10^{-4}$µM VIN | 3 | 20.8233 | 5.37695 | 3.10439 | 7.4662 | 34.1804 | 15.12 | 25.80 |
| $10^{-3}$µM VIN | 3 | 56.8800 | 3.99674 | 2.30752 | 46.9516 | 66.8084 | 53.41 | 61.25 |
| $10^{-2}$µM VIN | 3 | 64.6233 | 2.62938 | 1.51807 | 58.0916 | 71.1551 | 61.63 | 66.56 |
| $10^{-6}$µM VIN+10µM CT | 3 | 24.9733 | 8.44125 | 4.87356 | 4.0041 | 45.9426 | 17.15 | 33.92 |
| $10^{-5}$µM VIN+10µM CT | 3 | 21.8500 | 6.18071 | 3.56844 | 6.4963 | 37.2037 | 15.47 | 27.81 |
| $10^{-4}$µM VIN+10µM CT | 3 | 57.5100 | 5.78591 | 3.34049 | 43.1370 | 71.8830 | 53.42 | 64.13 |
| $10^{-3}$µM VIN+10µM CT | 3 | 52.9867 | 7.57236 | 4.37190 | 34.1759 | 71.7975 | 47.63 | 61.65 |
| $10^{-2}$µM VIN+10µM CT | 3 | 63.9900 | 1.61242 | .93093 | 59.9845 | 67.9955 | 62.17 | 65.24 |
| $10^{-6}$µM VIN+20µM CT | 3 | 36.9133 | 9.95296 | 5.74634 | 12.1888 | 61.6379 | 26.47 | 46.29 |
| $10^{-5}$µM VIN+20µM CT | 3 | 51.0433 | 6.14814 | 3.54963 | 35.7705 | 66.3162 | 44.50 | 56.70 |
| $10^{-4}$µM VIN+20µM CT | 3 | 57.4633 | 4.30722 | 2.48677 | 46.7636 | 68.1631 | 54.41 | 62.39 |
| $10^{-3}$µM VIN+20µM CT | 3 | 57.8400 | 3.11597 | 1.79901 | 50.0995 | 65.5805 | 54.68 | 60.91 |
| $10^{-2}$µM VIN+20µM CT | 3 | 61.6400 | 2.26007 | 1.30485 | 56.0257 | 67.2543 | 59.06 | 63.27 |
| $10^{-6}$µM VIN+40µM CT | 3 | 56.7767 | 7.49491 | 4.32719 | 38.1583 | 75.3951 | 49.13 | 64.11 |
| $10^{-5}$µM VIN+40µM CT | 3 | 56.0333 | 3.73129 | 2.15426 | 46.7643 | 65.3024 | 53.28 | 60.28 |
| $10^{-4}$µM VIN+40µM CT | 3 | 58.6667 | .57735 | .33333 | 57.2324 | 60.1009 | 58.00 | 59.00 |
| $10^{-3}$µM VIN+40µM CT | 3 | 62.1700 | 5.12583 | 2.95940 | 49.4367 | 74.9033 | 58.72 | 68.06 |
| $10^{-2}$µM VIN+40µM CT | 3 | 58.8633 | 4.55030 | 2.62712 | 47.5598 | 70.1669 | 55.18 | 63.95 |
| Total | 72 | 41.5104 | 21.65518 | 2.55209 | 36.4217 | 46.5991 | -.90 | 68.06 |

**Table 9:** Descriptive data by SPSS of the percentage of cytotoxicity of citral (CT), etoposide (ETO), and the combinations against Ramos cells at 24 hours incubation of three independent experiments (n=3).

| Treatments | N | Mean | Std. Deviation | Std. Error | 95% Confidence Interval for Mean | | Minimum | Maximum |
|---|---|---|---|---|---|---|---|---|
| | | | | | Lower Bound | Upper Bound | | |
| 0.5%Ethanol | 3 | 2.1400 | 2.75158 | 1.58863 | -4.6953 | 8.9753 | -.90 | 4.46 |
| 10μM CT | 3 | 3.9233 | .81144 | .46848 | 1.9076 | 5.9391 | 3.34 | 4.85 |
| 20μM CT | 3 | 8.2267 | 2.91138 | 1.68089 | .9944 | 15.4589 | 5.72 | 11.42 |
| 40μM CT | 3 | 18.4133 | 3.03009 | 1.74942 | 10.8862 | 25.9405 | 15.88 | 21.77 |
| 5μM ETO | 3 | 10.4000 | 2.17771 | 1.25730 | 4.9903 | 15.8097 | 8.40 | 12.72 |
| 10μM ETO | 3 | 40.5467 | 2.82546 | 1.63128 | 33.5278 | 47.5655 | 37.38 | 42.81 |
| 15μM ETO | 3 | 59.8933 | 7.70089 | 4.44611 | 40.7633 | 79.0234 | 51.33 | 66.25 |
| 20μM ETO | 3 | 74.9033 | 4.45710 | 2.57331 | 63.8313 | 85.9754 | 69.95 | 78.59 |
| 25μM ETO | 3 | 82.3067 | 5.06830 | 2.92618 | 69.7163 | 94.8970 | 77.85 | 87.82 |
| 5μM ETO+10μM CT | 3 | 13.9000 | 5.18385 | 2.99290 | 1.0226 | 26.7774 | 8.99 | 19.32 |
| 10μM ETO+10μM CT | 3 | 51.1267 | 4.17777 | 2.41203 | 40.7485 | 61.5048 | 47.88 | 55.84 |
| 15μM ETO+10μM CT | 3 | 71.6767 | 7.46354 | 4.30908 | 53.1362 | 90.2171 | 66.12 | 80.16 |
| 20μM ETO+10μM CT | 3 | 81.5933 | 5.70754 | 3.29525 | 67.4150 | 95.7717 | 75.59 | 86.95 |
| 25μM ETO+10μM CT | 3 | 88.3967 | 3.55607 | 2.05310 | 79.5629 | 97.2304 | 84.47 | 91.40 |
| 5μM ETO+20μM CT | 3 | 30.9500 | 7.64671 | 4.41483 | 11.9545 | 49.9455 | 24.95 | 39.56 |
| 10μM ETO+20μM CT | 3 | 59.5067 | 9.56077 | 5.51991 | 35.7564 | 83.2569 | 49.76 | 68.87 |
| 15μM ETO+20μM CT | 3 | 74.8567 | 6.42656 | 3.71037 | 58.8922 | 90.8211 | 68.35 | 81.20 |
| 20μM ETO+20μM CT | 3 | 83.1933 | 4.82707 | 2.78691 | 71.2022 | 95.1844 | 77.78 | 87.05 |
| 25μM ETO+20μM CT | 3 | 89.8433 | 5.39935 | 3.11731 | 76.4306 | 103.2561 | 83.61 | 93.07 |
| 5μM ETO+40μM CT | 3 | 45.1833 | 2.99453 | 1.72889 | 37.7445 | 52.6222 | 43.22 | 48.63 |
| 10μM ETO+40μM CT | 3 | 80.1367 | 15.24000 | 8.79882 | 42.2784 | 117.9949 | 66.54 | 96.61 |
| 15μM ETO+40μM CT | 3 | 96.5333 | 10.42341 | 6.01796 | 70.6402 | 122.4265 | 86.36 | 107.19 |
| 20μM ETO+40μM CT | 3 | 99.6767 | 8.14696 | 4.70365 | 79.4385 | 119.9148 | 93.67 | 108.95 |
| 25μM ETO+40μM CT | 3 | 100.9167 | 8.51214 | 4.91449 | 79.7713 | 122.0620 | 95.53 | 110.73 |
| Total | 72 | 57.0101 | 33.29842 | 3.92426 | 49.1854 | 64.8349 | -.90 | 110.73 |

**Table 10:** Descriptive data by SPSS of the percentage of cytotoxicity of citral (CT), doxorubicin (DOX), and the combinations on PBMCs at 24 hours incubation of five independent experiments (n=5).

| Treatments | N | Mean | Std. Deviation | Std. Error | 95% Confidence Interval for Mean | | Minimum | Maximum |
|---|---|---|---|---|---|---|---|---|
| | | | | | Lower Bound | Upper Bound | | |
| 0.5%Ethanol | 5 | 2.2140 | 1.66641 | .74524 | .1449 | 4.2831 | .14 | 4.60 |
| 10μM CT | 5 | -.1140 | 3.04755 | 1.36291 | -3.8980 | 3.6700 | -5.32 | 2.06 |
| 20μM CT | 5 | -.5240 | 4.01630 | 1.79614 | -5.5109 | 4.4629 | -7.05 | 3.55 |
| 40μM CT | 5 | -2.5220 | 4.14666 | 1.85444 | -7.6708 | 2.6268 | -7.55 | 3.53 |
| 1.5μM DOX | 5 | 8.0600 | 3.72555 | 1.66612 | 3.4341 | 12.6859 | 3.93 | 13.72 |
| 2μM DOX | 5 | 9.7920 | 3.45396 | 1.54466 | 5.5033 | 14.0807 | 5.95 | 13.22 |
| 2.5μM DOX | 5 | 13.7320 | 5.50811 | 2.46330 | 6.8928 | 20.5712 | 8.05 | 22.66 |
| 1.5μM DOX+10μM CT | 5 | 8.4240 | 4.73822 | 2.11900 | 2.5407 | 14.3073 | 2.58 | 14.53 |
| 2μM DOX+10μM CT | 5 | 9.8640 | 4.28742 | 1.91739 | 4.5405 | 15.1875 | 5.33 | 16.22 |
| 2.5μM DOX+10μM CT | 5 | 9.5580 | 5.19192 | 2.32190 | 3.1114 | 16.0046 | 3.34 | 17.34 |
| 1.5μM DOX+20μM CT | 5 | 5.4820 | 4.08037 | 1.82480 | .4156 | 10.5484 | .04 | 9.98 |
| 2μM DOX+20μM CT | 5 | 6.2520 | 5.07751 | 2.27073 | -.0526 | 12.5566 | -.15 | 12.33 |
| 2.5μM DOX+20μM CT | 5 | 7.2340 | 6.22833 | 2.78540 | -.4995 | 14.9675 | .04 | 16.53 |
| 1.5μM DOX+40μM CT | 5 | 1.8780 | 3.91619 | 1.75137 | -2.9846 | 6.7406 | -2.19 | 7.48 |
| 2μM DOX+40μM CT | 5 | 2.7460 | 3.18687 | 1.42521 | -1.2110 | 6.7030 | -1.31 | 6.24 |
| 2.5μM DOX+40μM CT | 5 | 6.1000 | 3.88661 | 1.73815 | 1.2741 | 10.9259 | .64 | 10.67 |
| Total | 80 | 5.5110 | 5.83156 | .65199 | 4.2133 | 6.8087 | -7.55 | 22.66 |

**Table 11:** Descriptive data by SPSS of the percentage of cytotoxicity of citral (CT), vincristine (VIN), and the combinations on PBMCs at 24 hours incubation of five independent experiments (n=5).

| Treatments | N | Mean | Std. Deviation | Std. Error | 95% Confidence Interval for Mean | | Minimum | Maximum |
|---|---|---|---|---|---|---|---|---|
| | | | | | Lower Bound | Upper Bound | | |
| 0.5%Ethanol | 5 | 2.2140 | 1.66641 | .74524 | .1449 | 4.2831 | .14 | 4.60 |
| 10µM CT | 5 | .1280 | 3.30086 | 1.47619 | -3.9706 | 4.2266 | -5.32 | 3.27 |
| 20µM CT | 5 | -.8160 | 3.87288 | 1.73200 | -5.6248 | 3.9928 | -7.05 | 3.55 |
| 40µM CT | 5 | -3.0020 | 4.04232 | 1.80778 | -8.0212 | 2.0172 | -7.55 | 3.53 |
| $10^{-6}$µM VIN | 5 | 1.4020 | 3.40158 | 1.52123 | -2.8216 | 5.6256 | -2.50 | 4.75 |
| $10^{-5}$µM VIN | 5 | 2.0480 | 1.32362 | .59194 | .4045 | 3.6915 | 1.04 | 3.77 |
| $10^{-4}$µM VIN | 5 | 4.8220 | 2.44643 | 1.09408 | 1.7844 | 7.8596 | 1.74 | 7.55 |
| $10^{-6}$µM VIN+10µM CT | 5 | 1.6920 | 3.26287 | 1.45920 | -2.3594 | 5.7434 | -4.07 | 3.51 |
| $10^{-5}$µM VIN+10µM CT | 5 | 1.8640 | 2.20069 | .98418 | -.8685 | 4.5965 | -1.81 | 4.02 |
| $10^{-4}$µM VIN+10µM CT | 5 | 2.6060 | 3.27525 | 1.46474 | -1.4608 | 6.6728 | -2.56 | 5.24 |
| $10^{-6}$µM VIN+20µM CT | 5 | -1.6940 | 4.63548 | 2.07305 | -7.4497 | 4.0617 | -7.59 | 3.42 |
| $10^{-5}$µM VIN+20µM CT | 5 | -2.1200 | 4.14157 | 1.85217 | -7.2624 | 3.0224 | -7.59 | 2.57 |
| $10^{-4}$µM VIN+20µM CT | 5 | -.9180 | 3.61641 | 1.61731 | -5.4084 | 3.5724 | -5.42 | 2.57 |
| $10^{-6}$µM VIN+40µM CT | 5 | -2.9900 | 3.43283 | 1.53521 | -7.2524 | 1.2724 | -6.91 | 1.22 |
| $10^{-5}$µM VIN+40µM CT | 5 | -3.7920 | 2.78371 | 1.24491 | -7.2484 | -.3356 | -7.51 | .03 |
| $10^{-4}$µM VIN+40µM CT | 5 | -1.6640 | 2.31298 | 1.03440 | -4.5359 | 1.2079 | -3.69 | 1.70 |
| Total | 80 | -.0138 | 3.77482 | .42204 | -.8538 | .8263 | -7.59 | 7.55 |

**Table 12:** Descriptive data by SPSS of the percentage of cytotoxicity of citral (CT), etoposide (ETO), and the combinations on PBMCs at 24 hours incubation of five independent experiments (n=5).

| Treatments | N | Mean | Std. Deviation | Std. Error | 95% Confidence Interval for Mean | | Minimum | Maximum |
|---|---|---|---|---|---|---|---|---|
| | | | | | Lower Bound | Upper Bound | | |
| 0.5%Ethanol | 5 | 2.2140 | 1.66641 | .74524 | .1449 | 4.2831 | .14 | 4.60 |
| 10μM CT | 5 | .1280 | 3.30086 | 1.47619 | -3.9706 | 4.2266 | -5.32 | 3.27 |
| 20μM CT | 5 | -.8160 | 3.87288 | 1.73200 | -5.6248 | 3.9928 | -7.05 | 3.55 |
| 40μM CT | 5 | -3.0020 | 4.04232 | 1.80778 | -8.0212 | 2.0172 | -7.55 | 3.53 |
| 5μM ETO | 5 | 3.6080 | 3.38019 | 1.51167 | -.5891 | 7.8051 | .95 | 9.52 |
| 10μM ETO | 5 | 5.7860 | 4.71904 | 2.11042 | -.0735 | 11.6455 | .04 | 10.94 |
| 15μM ETO | 5 | 8.5440 | 7.05922 | 3.15698 | -.2212 | 17.3092 | .95 | 17.07 |
| 5μM ETO+10μM CT | 5 | 4.8800 | 4.16197 | 1.86129 | -.2878 | 10.0478 | -.95 | 9.38 |
| 10μM ETO+10μM CT | 5 | 5.8700 | 6.56313 | 2.93512 | -2.2792 | 14.0192 | -2.81 | 13.86 |
| 15μM ETO+10μM CT | 5 | 8.0320 | 6.77163 | 3.02836 | -.3761 | 16.4401 | -.38 | 15.36 |
| 5μM ETO+20μM CT | 5 | -.6700 | 2.39430 | 1.07076 | -3.6429 | 2.3029 | -3.21 | 2.47 |
| 10μM ETO+20μM CT | 5 | 1.3600 | 3.69508 | 1.65249 | -3.2281 | 5.9481 | -3.11 | 6.82 |
| 15μM ETO+20μM CT | 5 | 2.1020 | 6.09632 | 2.72636 | -5.4676 | 9.6716 | -4.75 | 9.98 |
| 5μM ETO+40μM CT | 5 | -1.5080 | 6.02833 | 2.69595 | -8.9932 | 5.9772 | -7.24 | 8.21 |
| 10μM ETO+40μM CT | 5 | -.9900 | 5.67409 | 2.53753 | -8.0353 | 6.0553 | -5.42 | 8.32 |
| 15μM ETO+40μM CT | 5 | 2.1400 | 7.41428 | 3.31577 | -7.0660 | 11.3460 | -2.21 | 15.30 |
| Total | 80 | 2.3549 | 5.70687 | .63805 | 1.0849 | 3.6249 | -7.55 | 17.07 |
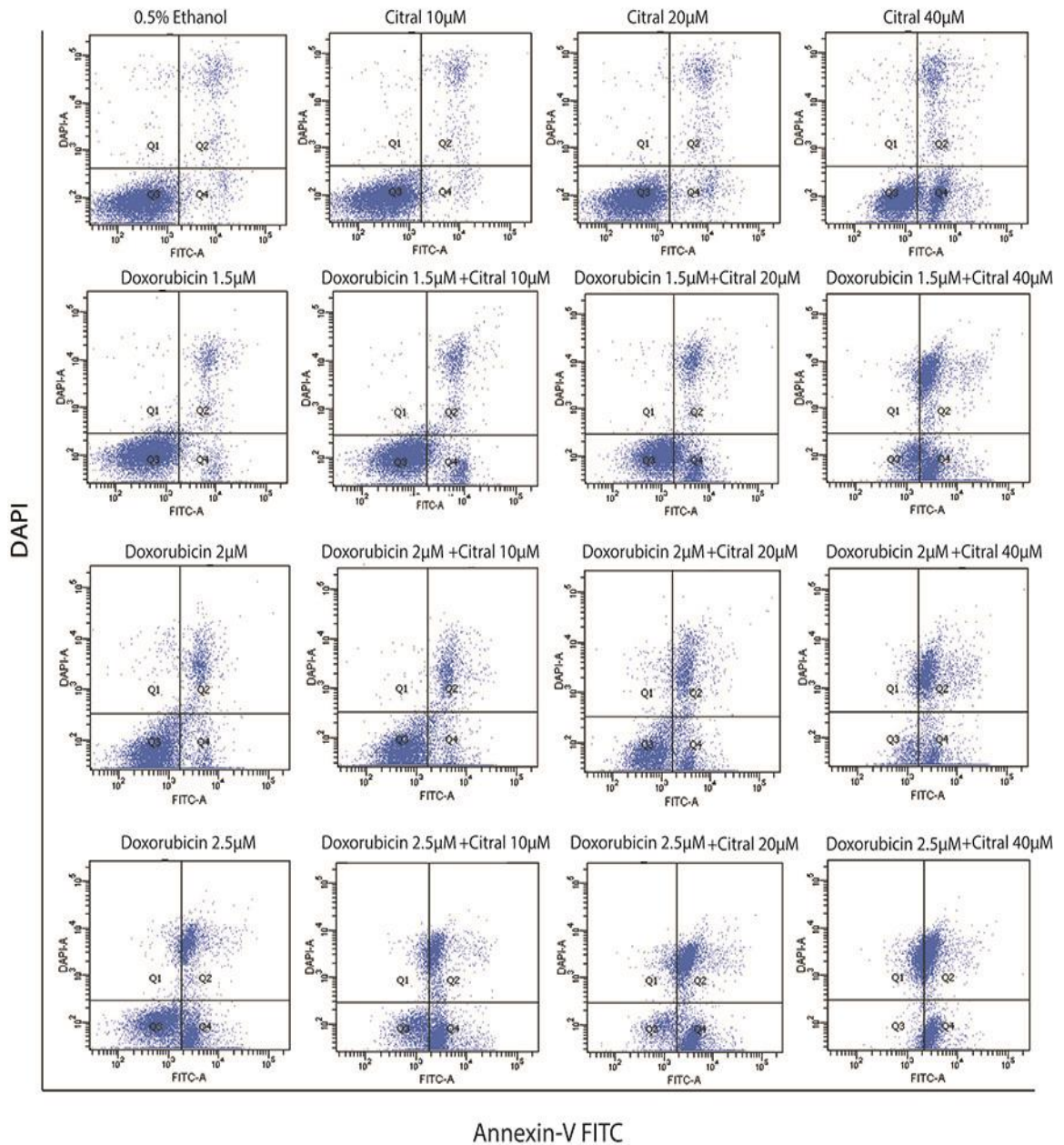
**Figure 31:** A representative dot plot histogram from annexin V-FITC/DAPI staining assay using fluorescent flow cytometer of citral, doxorubicin, and doxorubicin-citral combination treatments in Ramos cells at 18 hours exposure.
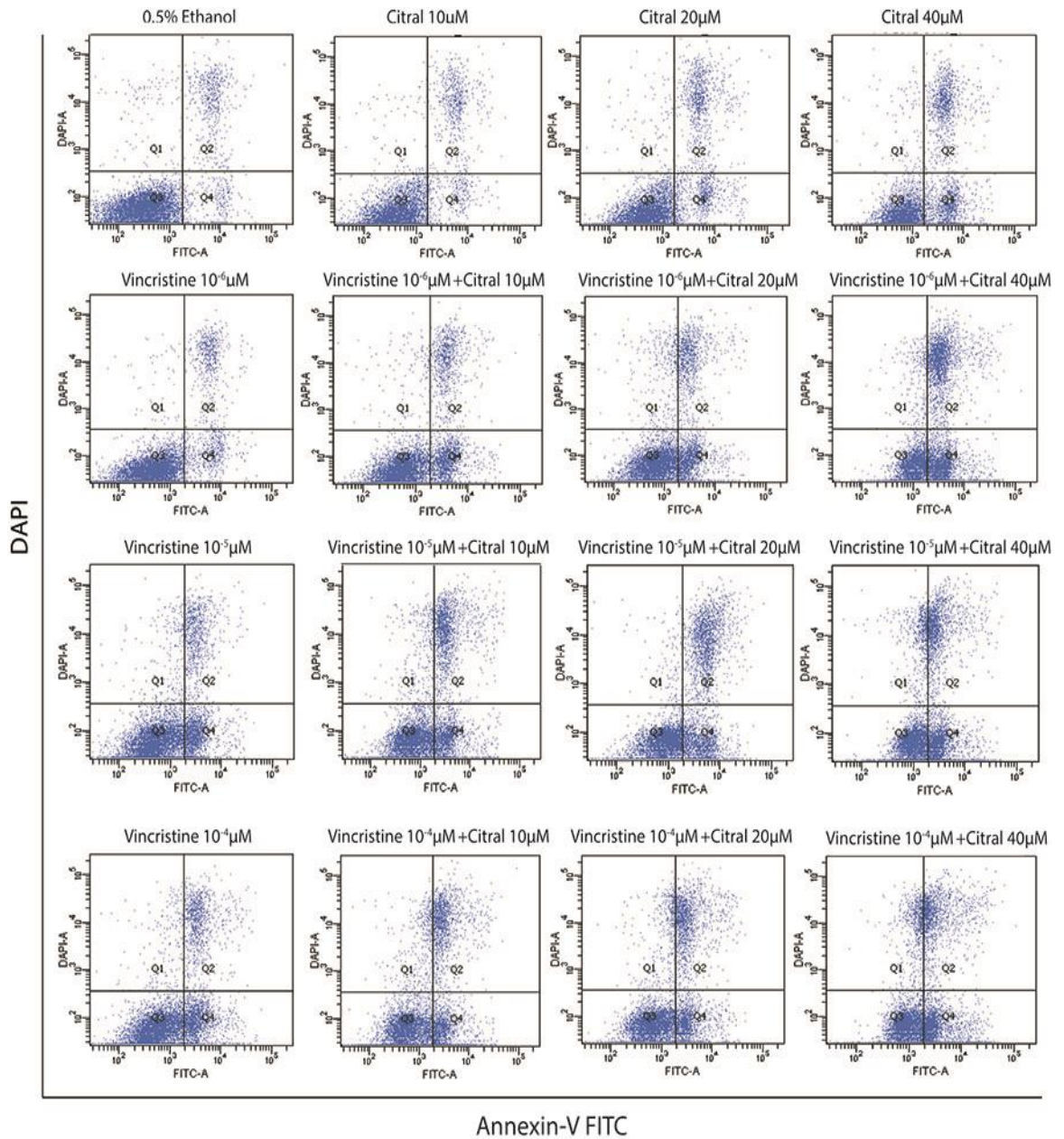
**Figure 32:** A representative dot plot histogram from annexin V-FITC/DAPI staining assay using fluorescent flow cytometer of citral, vincristine, and vincristine-citral combination treatments in Ramos cells at 18 hours exposure.
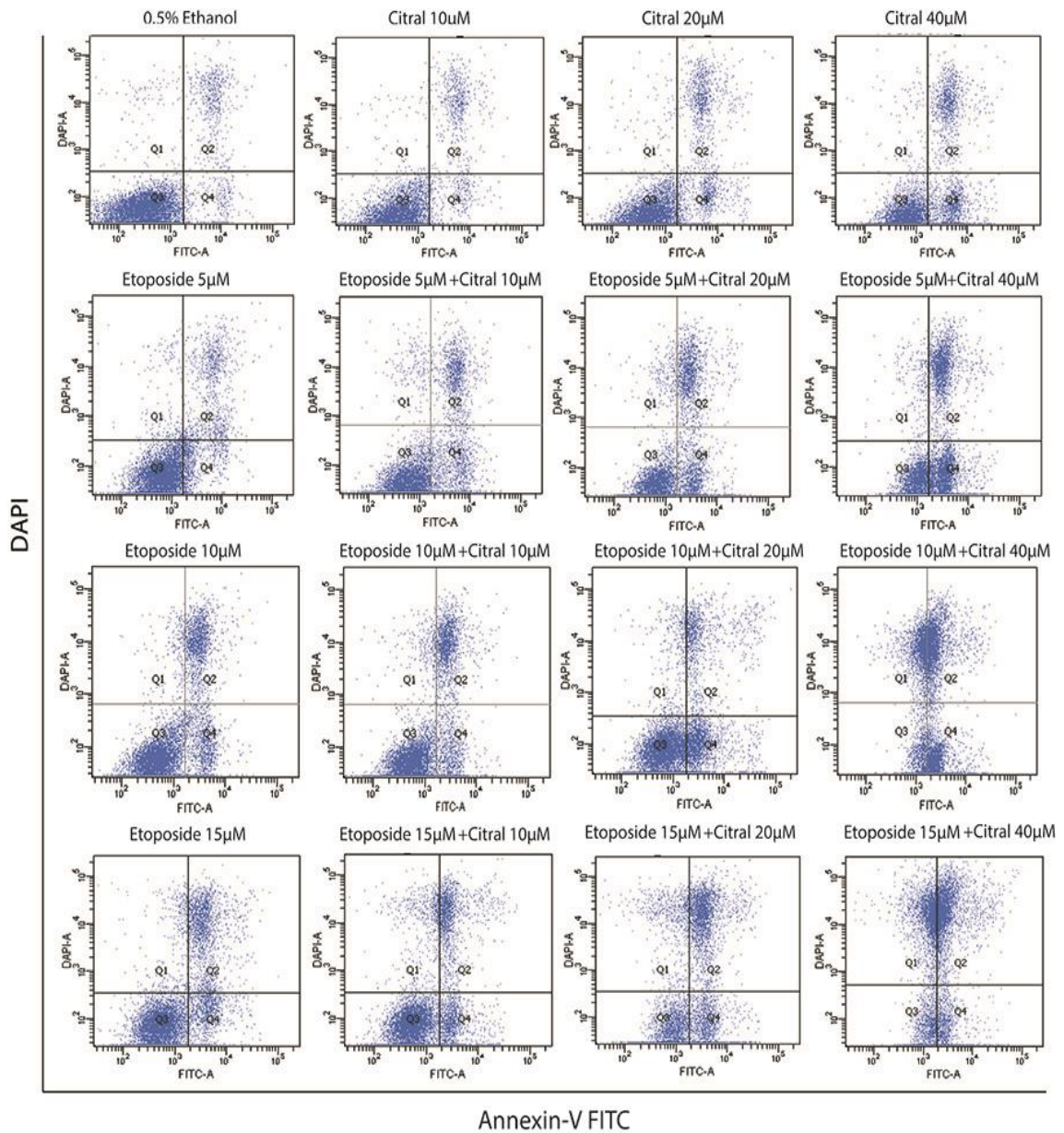
**Figure 33:** A representative dot plot histogram from annexin V-FITC/DAPI staining assay using fluorescent flow cytometer of citral, etoposide, and etoposide-citral combination treatments in Ramos cells at 18 hours exposure.
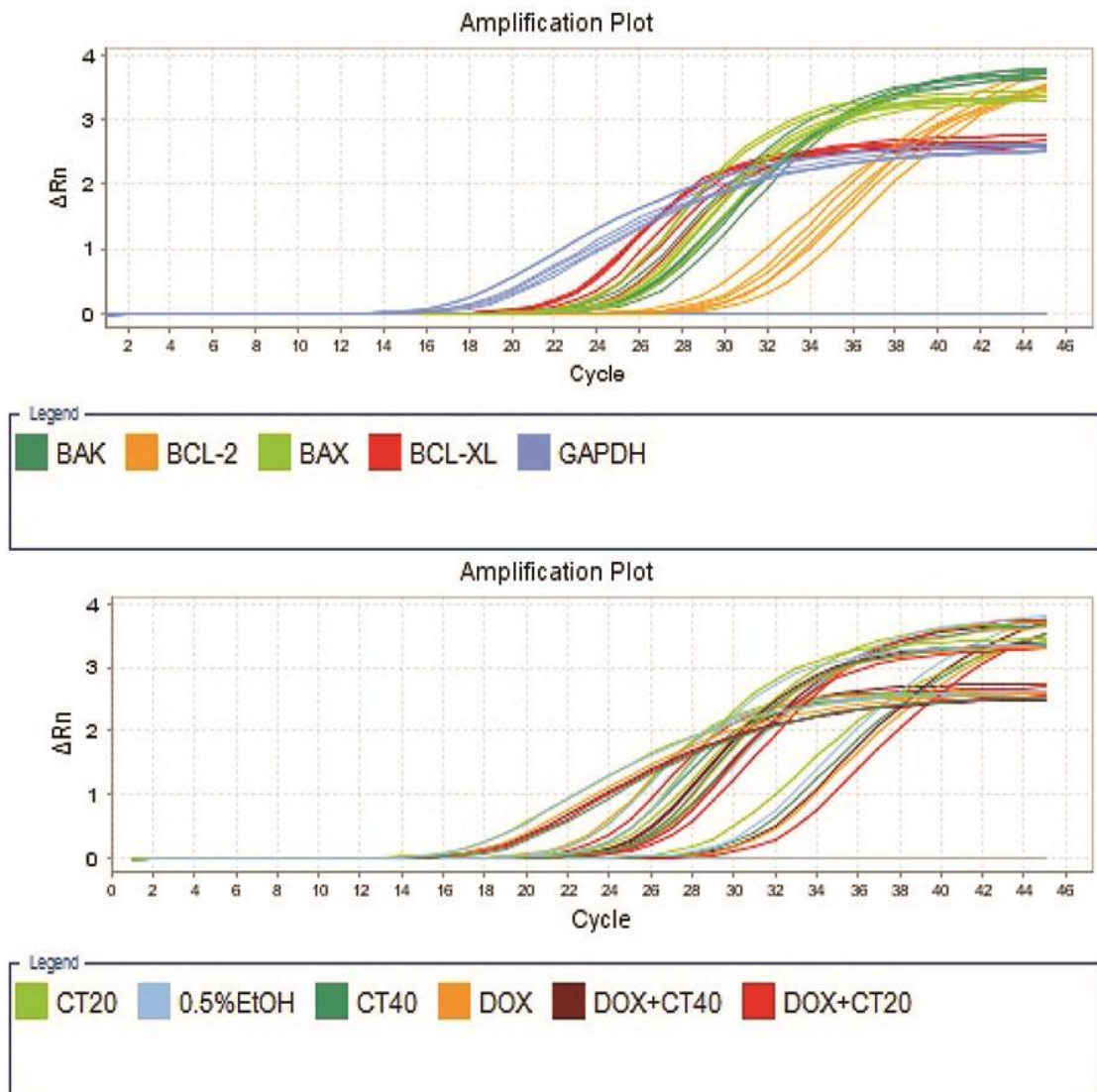
Rn is the reporter signal normalized to the fluorescence signal of ROX (passive reference dye)

ΔRn is Rn minus the baseline

**Figure 34:** Graphical representation by qRT-PCR represented the molecular effect of citral (CT) on the mRNA expression of BCL-2 family proteins induced by doxorubicin (DOX) in Ramos cells at 18 hours exposure.

**Table 13:** Descriptive data by SPSS of BAX, BAK, BCL-2, and BCL-XL expression, at mRNA level, induced by citral (CT), doxorubicin (DOX), and their combinations in Ramos cells at 18 hours exposure of four independent experiments (n=4).

| | treatments | N | Mean | Std. Deviation | Std. Error | 95% Confidence Interval for Mean Lower Bound | Upper Bound | Minimum | Maximum |
|---|---|---|---|---|---|---|---|---|---|
| BAX | 0.5% Ethanol | 4 | 1.0000 | 0.00000 | 0.00000 | 1.0000 | 1.0000 | 1.00 | 1.00 |
| | 20µM CT | 4 | .7837 | .19149 | .09574 | .4790 | 1.0884 | .61 | 1.02 |
| | 40µM CT | 4 | 1.3317 | .45882 | .22941 | .6017 | 2.0618 | .67 | 1.73 |
| | 1.5 µM DOX | 4 | .6401 | .09601 | .04801 | .4873 | .7928 | .56 | .78 |
| | 1.5 µMDOX+20µM CT | 4 | .6276 | .15019 | .07509 | .3886 | .8666 | .44 | .77 |
| | 1.5 µMDOX+40µM CT | 4 | .8134 | .22241 | .11120 | .4595 | 1.1673 | .60 | 1.13 |
| | Total | 24 | .8661 | .32265 | .06586 | .7298 | 1.0023 | .44 | 1.73 |
| BAK | 0.5% Ethanol | 4 | 1.0000 | 0.00000 | 0.00000 | 1.0000 | 1.0000 | 1.00 | 1.00 |
| | 20µM CT | 4 | 1.7372 | .74746 | .37373 | .5479 | 2.9266 | 1.00 | 2.73 |
| | 40µM CT | 4 | 3.3979 | .82926 | .41463 | 2.0784 | 4.7174 | 2.57 | 4.52 |
| | 1.5 µM DOX | 4 | 1.9629 | .40743 | .20372 | 1.3146 | 2.6112 | 1.57 | 2.32 |
| | 1.5 µMDOX+20µM CT | 4 | 1.7845 | .18760 | .09380 | 1.4860 | 2.0830 | 1.55 | 2.00 |
| | 1.5 µMDOX+40µM CT | 4 | 2.7010 | .31580 | .15790 | 2.1985 | 3.2035 | 2.23 | 2.93 |
| | Total | 24 | 2.0973 | .90083 | .18388 | 1.7169 | 2.4776 | 1.00 | 4.52 |
| BCL2 | 0.5% Ethanol | 4 | 1.0000 | 0.00000 | 0.00000 | 1.0000 | 1.0000 | 1.00 | 1.00 |
| | 20µM CT | 4 | 1.0664 | .62197 | .31098 | .0767 | 2.0561 | .68 | 1.99 |
| | 40µM CT | 4 | 1.8047 | .73074 | .36537 | .6419 | 2.9674 | 1.11 | 2.83 |
| | 1.5 µM DOX | 4 | .6656 | .25800 | .12900 | .2551 | 1.0761 | .45 | 1.00 |
| | 1.5 µMDOX+20µM CT | 4 | .5436 | .16050 | .08025 | .2882 | .7990 | .43 | .78 |
| | 1.5 µMDOX+40µM CT | 4 | .7608 | .33889 | .16945 | .2216 | 1.3001 | .46 | 1.25 |
| | Total | 24 | .9735 | .57044 | .11644 | .7326 | 1.2144 | .43 | 2.83 |
| BCLXL | 0.5% Ethanol | 4 | 1.0000 | 0.00000 | 0.00000 | 1.0000 | 1.0000 | 1.00 | 1.00 |
| | 20µM CT | 4 | .8721 | .13225 | .06613 | .6617 | 1.0826 | .71 | 1.03 |
| | 40µM CT | 4 | 1.3068 | .26372 | .13186 | .8871 | 1.7264 | 1.02 | 1.59 |
| | 1.5 µM DOX | 4 | 1.6286 | .52736 | .26368 | .7894 | 2.4678 | 1.16 | 2.38 |
| | 1.5 µMDOX+20µM CT | 4 | 1.3889 | .27923 | .13961 | .9446 | 1.8332 | 1.19 | 1.80 |
| | 1.5 µMDOX+40µM CT | 4 | .3131 | .14498 | .07249 | .0824 | .5438 | .22 | .53 |
| | Total | 24 | 1.0849 | .49930 | .10192 | .8741 | 1.2958 | .22 | 2.38 |
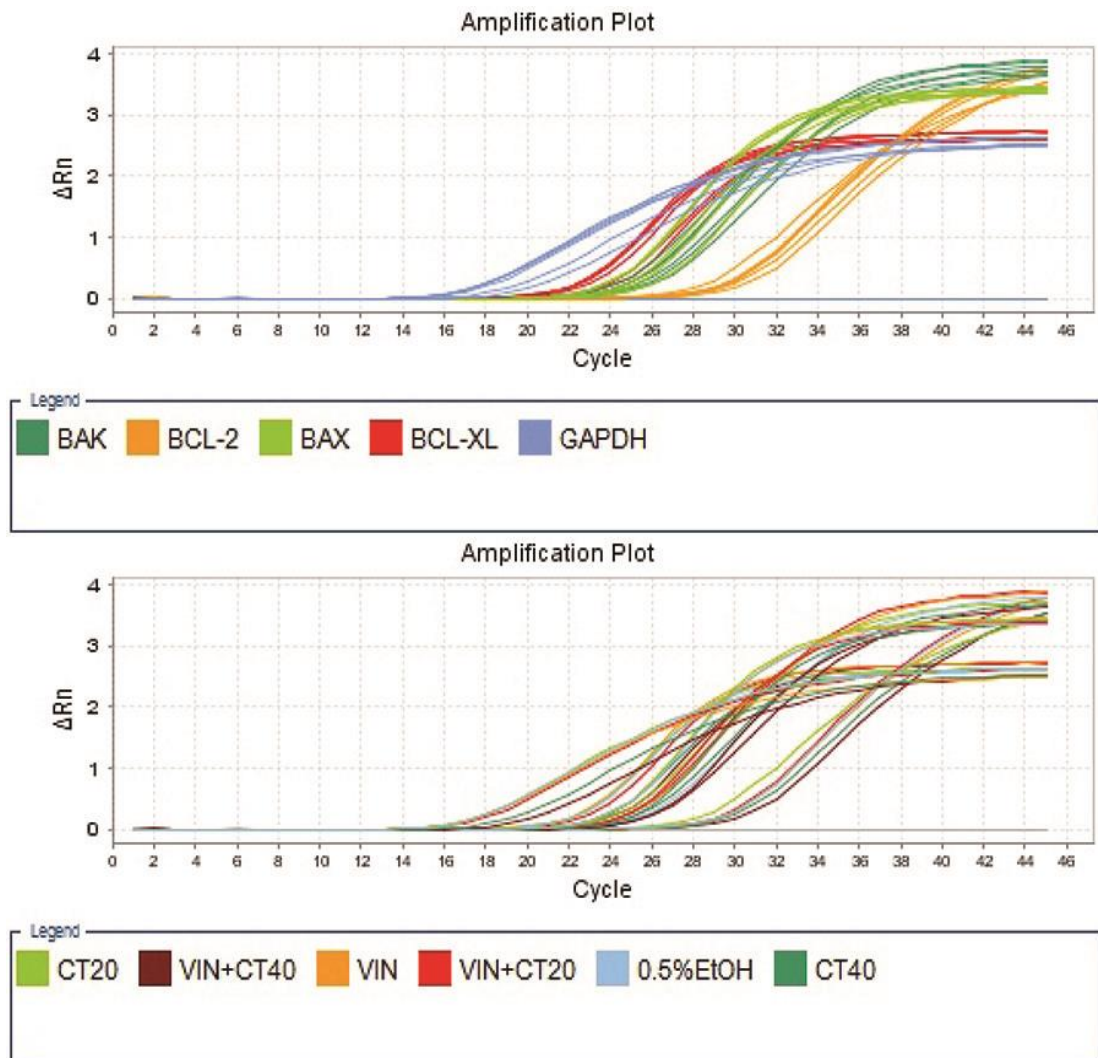
**Figure 35:** Graphical representation by qRT-PCR represented the molecular effect of citral (CT) on the mRNA expression of BCL-2 family proteins induced by vincristine (VIN) in Ramos cells at 18 hours exposure.

**Table 14:** Descriptive data by SPSS of BAX, BAK, BCL-2, and BCL-XL expression, at mRNA level, induced by citral (CT), vincristine (VIN), and their combinations in Ramos cells at 18 hours exposure of four independent experiments (n=4).

| | treatments | N | Mean | Std. Deviation | Std. Error | 95% Confidence Interval for Mean Lower Bound | 95% Confidence Interval for Mean Upper Bound | Minimum | Maximum |
|---|---|---|---|---|---|---|---|---|---|
| BAX | 0.5% Ethanol | 4 | 1.0000 | 0.00000 | 0.00000 | 1.0000 | 1.0000 | 1.00 | 1.00 |
| | 20µM CT | 4 | .7836 | .19261 | .09630 | .4771 | 1.0901 | .61 | 1.02 |
| | 40µM CT | 4 | 1.3311 | .46194 | .23097 | .5961 | 2.0662 | .66 | 1.73 |
| | $10^{-6}$µM VIN | 4 | .7050 | .24714 | .12357 | .3117 | 1.0982 | .54 | 1.07 |
| | $10^{-6}$µMVIN+20µM CT | 4 | .6702 | .16665 | .08333 | .4050 | .9353 | .49 | .86 |
| | $10^{-6}$µMVIN+40µM CT | 4 | 1.1059 | .26756 | .13378 | .6801 | 1.5316 | .80 | 1.45 |
| | Total | 24 | .9326 | .33478 | .06834 | .7913 | 1.0740 | .49 | 1.73 |
| BAK | 0.5% Ethanol | 4 | 1.0000 | 0.00000 | 0.00000 | 1.0000 | 1.0000 | 1.00 | 1.00 |
| | 20µM CT | 4 | 1.7435 | .74700 | .37350 | .5549 | 2.9322 | 1.00 | 2.74 |
| | 40µM CT | 4 | 3.3885 | .83968 | .41984 | 2.0524 | 4.7246 | 2.58 | 4.53 |
| | $10^{-6}$µM VIN | 4 | 1.5104 | .29067 | .14534 | 1.0478 | 1.9729 | 1.23 | 1.88 |
| | $10^{-6}$µMVIN+20µM CT | 4 | 1.6882 | .65587 | .32793 | .6446 | 2.7318 | 1.17 | 2.63 |
| | $10^{-6}$µMVIN+40µM CT | 4 | 3.7407 | .93310 | .46655 | 2.2560 | 5.2255 | 3.02 | 5.11 |
| | Total | 24 | 2.1785 | 1.19097 | .24311 | 1.6756 | 2.6815 | 1.00 | 5.11 |
| BCL2 | 0.5% Ethanol | 4 | 1.0000 | 0.00000 | 0.00000 | 1.0000 | 1.0000 | 1.00 | 1.00 |
| | 20µM CT | 4 | 1.0669 | .62865 | .31432 | .0666 | 2.0672 | .67 | 2.00 |
| | 40µM CT | 4 | 1.7994 | .73526 | .36763 | .6294 | 2.9693 | 1.11 | 2.83 |
| | $10^{-6}$µM VIN | 4 | .8260 | .16901 | .08451 | .5571 | 1.0949 | .63 | 1.04 |
| | $10^{-6}$µMVIN+20µM CT | 4 | .9839 | .36517 | .18259 | .4029 | 1.5650 | .65 | 1.50 |
| | $10^{-6}$µMVIN+40µM CT | 4 | 2.4433 | .98524 | .49262 | .8756 | 4.0111 | 1.25 | 3.65 |
| | Total | 24 | 1.3533 | .78682 | .16061 | 1.0210 | 1.6855 | .63 | 3.65 |
| BCLXL | 0.5% Ethanol | 4 | 1.0000 | 0.00000 | 0.00000 | 1.0000 | 1.0000 | 1.00 | 1.00 |
| | 20µM CT | 4 | .8725 | .13208 | .06604 | .6623 | 1.0827 | .71 | 1.03 |
| | 40µM CT | 4 | 1.2930 | .26056 | .13028 | .8784 | 1.7076 | 1.02 | 1.59 |
| | $10^{-6}$µMVIN | 4 | 1.0100 | .25736 | .12868 | .6005 | 1.4196 | .79 | 1.31 |
| | $10^{-6}$µMVIN+20µM CT | 4 | .8386 | .14213 | .07106 | .6125 | 1.0648 | .66 | 1.00 |
| | $10^{-6}$µMVIN+40µM CT | 4 | 1.4949 | .41008 | .20504 | .8423 | 2.1474 | 1.07 | 2.03 |
| | Total | 24 | 1.0848 | .31895 | .06510 | .9502 | 1.2195 | .66 | 2.03 |

Rn is the reporter signal normalized to the fluorescence signal of ROX (passive reference dye)

ΔRn is Rn minus the baseline
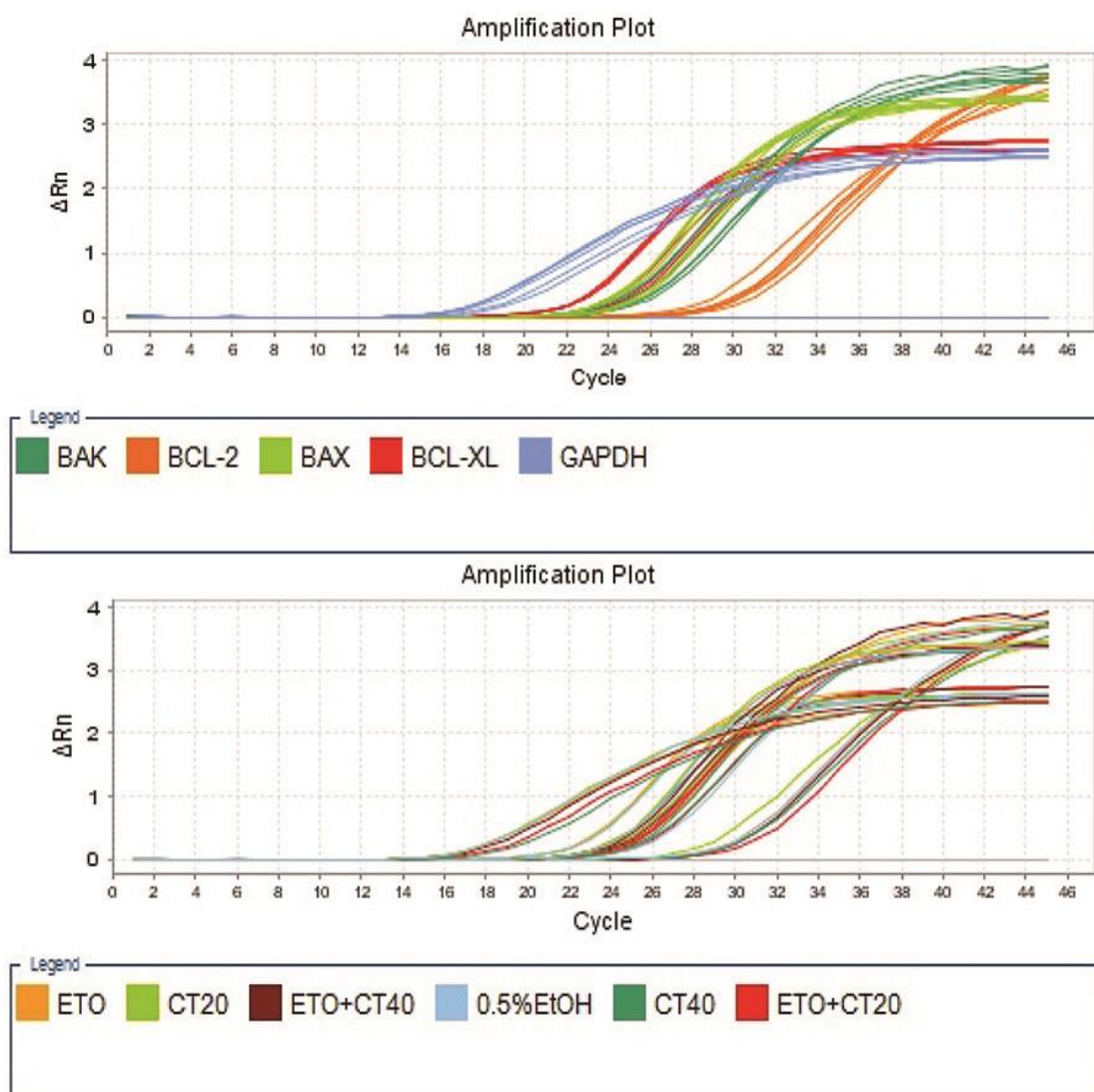
**Figure 36:** Graphical representation by qRT-PCR represented the molecular effect of citral (CT) on the mRNA expression of BCL-2 family proteins induced by etoposide (ETO) in Ramos cells at 18 hours exposure.

**Table 15:** Descriptive data by SPSS of BAX, BAK, BCL-2, and BCL-XL expression, at mRNA level, induced by citral (CT), etoposide (ETO), and their combinations in Ramos cells at 18 hours exposure of four independent experiments (n=4).

| | treatments | N | Mean | Std. Deviation | Std. Error | 95% Confidence Interval for Mean Lower Bound | 95% Confidence Interval for Mean Upper Bound | Minimum | Maximum |
|---|---|---|---|---|---|---|---|---|---|
| BAX | 0.5%Ethanol | 4 | 1.0000 | 0.00000 | 0.00000 | 1.0000 | 1.0000 | 1.00 | 1.00 |
| | 20µM CT | 4 | .7848 | .19381 | .09690 | .4764 | 1.0932 | .61 | 1.02 |
| | 40µM CT | 4 | 1.3386 | .46572 | .23286 | .5975 | 2.0797 | .67 | 1.75 |
| | 5µM ETO | 4 | .6727 | .09219 | .04610 | .5260 | .8194 | .56 | .75 |
| | 5µMETO+20µM CT | 4 | .8151 | .22461 | .11231 | .4577 | 1.1725 | .60 | 1.13 |
| | 5µMETO+40µM CT | 4 | 1.1183 | .09970 | .04985 | .9596 | 1.2769 | 1.01 | 1.25 |
| | Total | 24 | .9549 | .30832 | .06294 | .8247 | 1.0851 | .56 | 1.75 |
| BAK | 0.5%Ethanol | 4 | 1.0000 | 0.00000 | 0.00000 | 1.0000 | 1.0000 | 1.00 | 1.00 |
| | 20µM CT | 4 | 1.7415 | .75507 | .37753 | .5400 | 2.9430 | 1.00 | 2.75 |
| | 40µM CT | 4 | 3.4047 | .84159 | .42080 | 2.0656 | 4.7439 | 2.57 | 4.54 |
| | 5µM ETO | 4 | 2.0348 | .59387 | .29694 | 1.0898 | 2.9798 | 1.23 | 2.64 |
| | 5µM ETO+20µM CT | 4 | 2.7050 | .31762 | .15881 | 2.1996 | 3.2104 | 2.23 | 2.93 |
| | 5µM ETO+40µM CT | 4 | 3.3991 | .47382 | .23691 | 2.6452 | 4.1531 | 2.72 | 3.75 |
| | Total | 24 | 2.3809 | 1.02938 | .21012 | 1.9462 | 2.8155 | 1.00 | 4.54 |
| BCL2 | 0.5%Ethanol | 4 | 1.0000 | 0.00000 | 0.00000 | 1.0000 | 1.0000 | 1.00 | 1.00 |
| | 20µM CT | 4 | 1.0713 | .63174 | .31587 | .0661 | 2.0766 | .68 | 2.01 |
| | 40µM CT | 4 | 1.8089 | .73869 | .36934 | .6335 | 2.9844 | 1.11 | 2.84 |
| | 5µM ETO | 4 | .8753 | .44490 | .22245 | .1674 | 1.5832 | .50 | 1.51 |
| | 5µM ETO+20µM CT | 4 | .7622 | .34153 | .17077 | .2188 | 1.3057 | .46 | 1.25 |
| | 5µM ETO+40µM CT | 4 | 1.5483 | .66847 | .33423 | .4846 | 2.6119 | 1.09 | 2.53 |
| | Total | 24 | 1.1777 | .60755 | .12401 | .9211 | 1.4342 | .46 | 2.84 |
| BCLXL | 0.5%Ethanol | 4 | 1.0000 | 0.00000 | 0.00000 | 1.0000 | 1.0000 | 1.00 | 1.00 |
| | 20µM CT | 4 | .8735 | .13415 | .06708 | .6601 | 1.0870 | .71 | 1.03 |
| | 40µM CT | 4 | 1.3005 | .25716 | .12858 | .8913 | 1.7097 | 1.02 | 1.59 |
| | 5µM ETO | 4 | .5937 | .36173 | .18087 | .0181 | 1.1693 | .29 | 1.01 |
| | 5µM ETO+20µM CT | 4 | .3124 | .14744 | .07372 | .0778 | .5470 | .22 | .53 |
| | 5µM ETO+40µM CT | 4 | .8891 | .42579 | .21290 | .2115 | 1.5666 | .35 | 1.31 |
| | Total | 24 | .8282 | .39406 | .08044 | .6618 | .9946 | .22 | 1.59 |
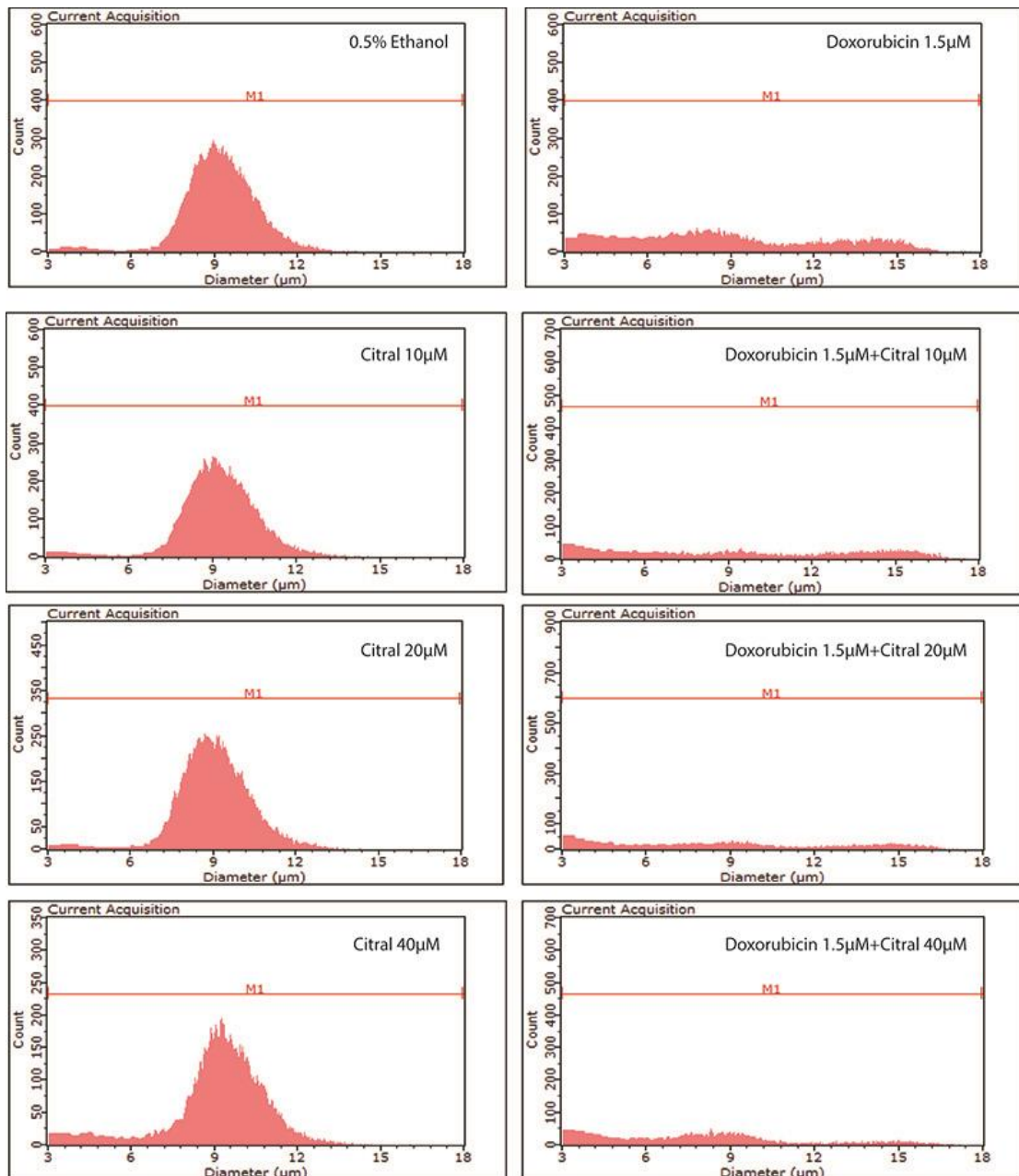
**Figure 37:** The histogram represented the numbers of Ramos cells. The cells were treated with doxorubicin in the absence and presence of citral for 3 hours. The treated cells were washed and further incubated in fresh medium without doxorubicin and citral for 48 hours. Numbers of the treated cells were counted by Scepter™ Handheld Automated Cell Counter.
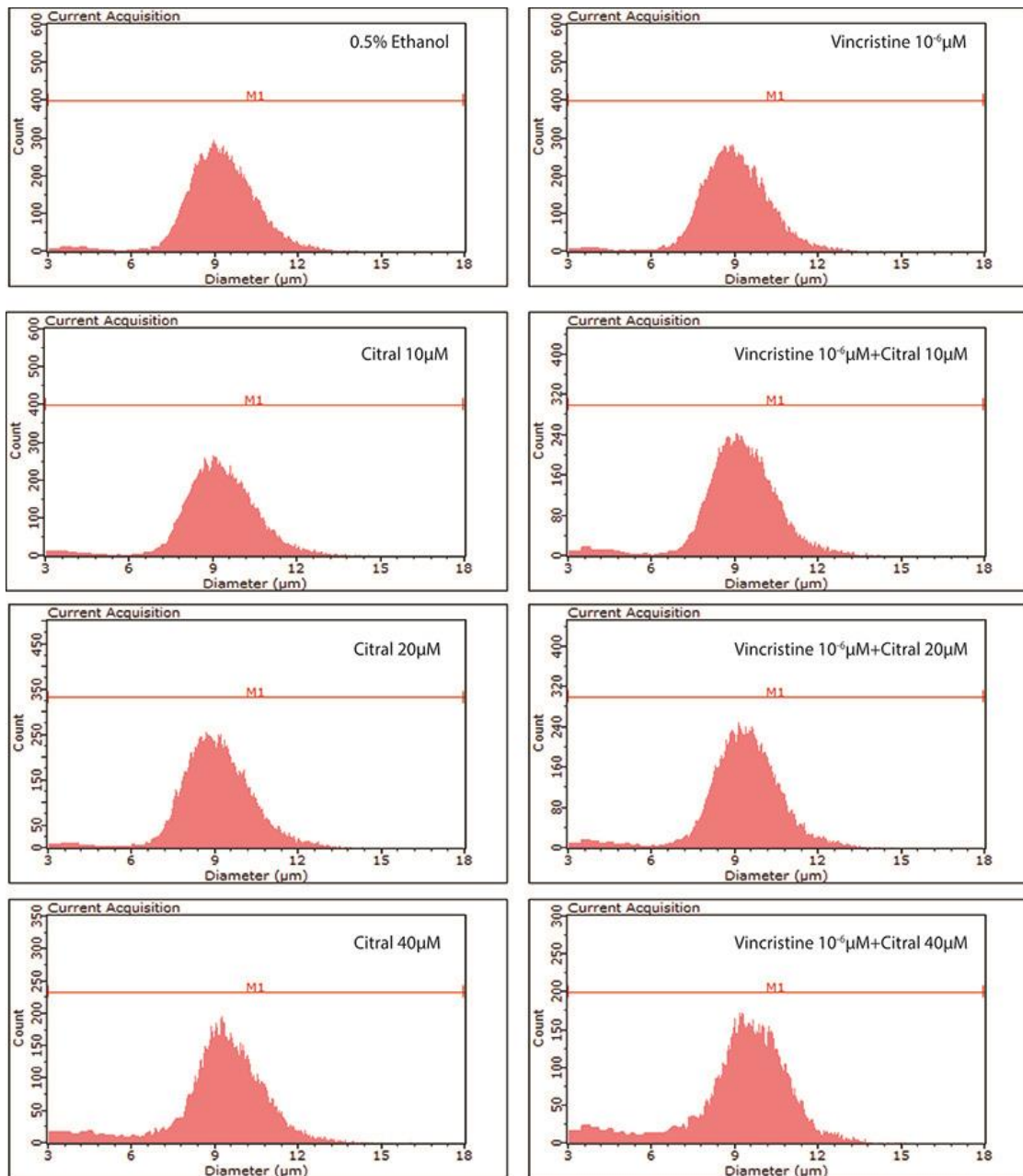
**Figure 38:** The histogram represented the numbers of Ramos cells. The cells were treated with vincristine in the absence and presence of citral for 3 hours. The treated cells were washed and further incubated in fresh medium without vincristine and citral for 48 hours. Numbers of the treated cells were counted by Scepter™ Handheld Automated Cell Counter.
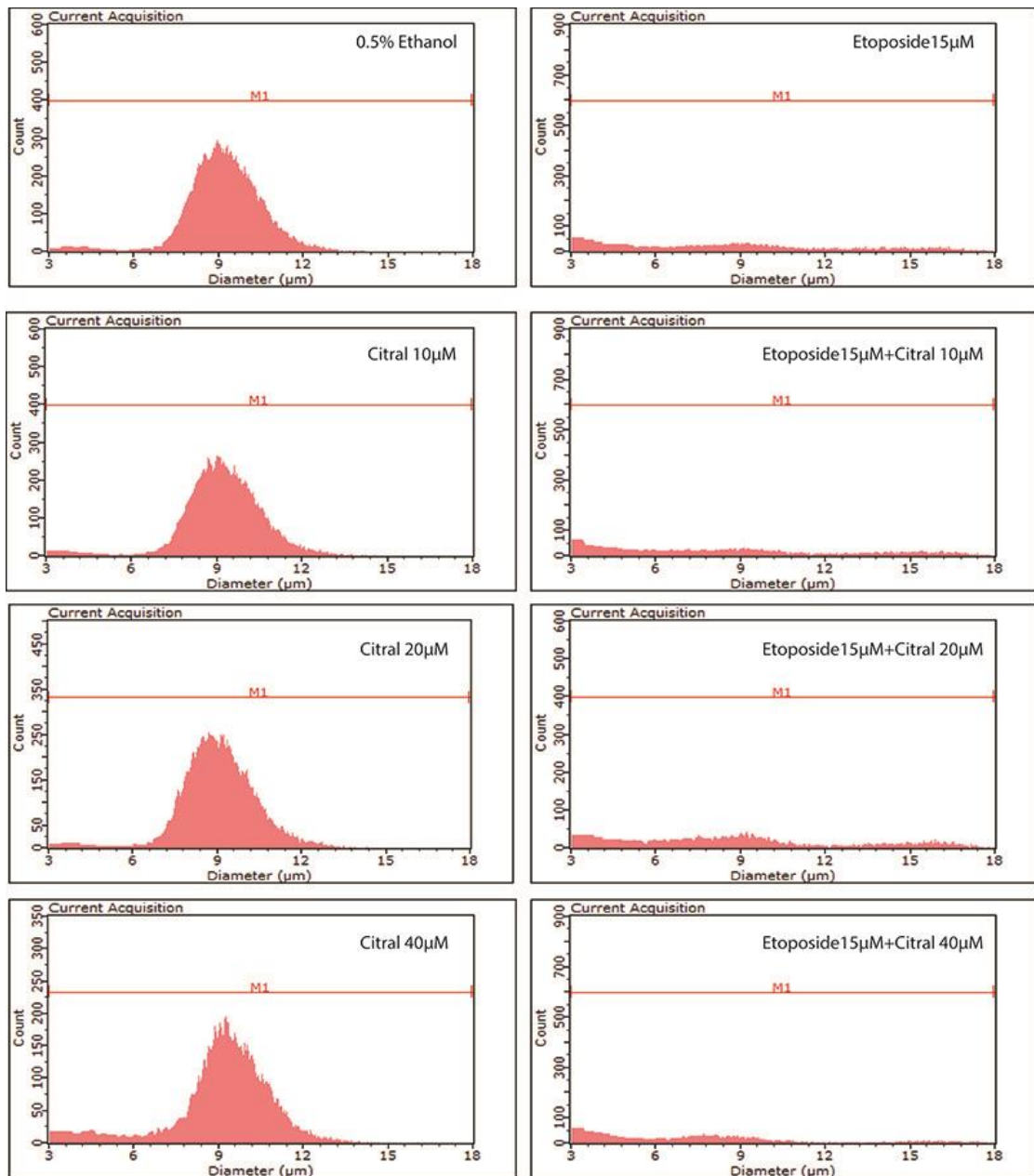
**Figure 39:** The histogram represented the numbers of Ramos cells. The cells were treated with etoposide in the absence and presence of citral for 3 hours. The treated cells were washed and further incubated in fresh medium without etoposide and citral for 48 hours. Numbers of the treated cells were counted by Scepter™ Handheld Automated Cell Counter.

**Table 16:** Descriptive data by SPSS of the percentage inhibition of the cell proliferation by citral (CT), doxorubicin (DOX), vincristine (VIN), and etoposide (ETO), either used alone or combined with citral, on Ramos cells at 48 hours incubation of three independent experiments (n=3).

| treatments | N | Mean | Std. Deviation | Std. Error | 95% Confidence Interval for Mean | | Minimum | Maximum |
|---|---|---|---|---|---|---|---|---|
| | | | | | Lower Bound | Upper Bound | | |
| 0.5% Ethanol | 3 | 100.0000 | .00000 | .00000 | 100.0000 | 100.0000 | 100.00 | 100.00 |
| 10µM CT | 3 | 99.9533 | 1.54053 | .88943 | 96.1264 | 103.7802 | 98.39 | 101.47 |
| 20µM CT | 3 | 96.5300 | 3.05501 | 1.76381 | 88.9409 | 104.1191 | 93.47 | 99.58 |
| 40µM CT | 3 | 76.4300 | 9.48505 | 5.47619 | 52.8678 | 99.9922 | 65.67 | 83.58 |
| 1.5µM DOX | 3 | 47.3867 | 13.10424 | 7.56573 | 14.8339 | 79.9394 | 38.53 | 62.44 |
| 1.5µM DOX+10µM CT | 3 | 39.0667 | 2.72473 | 1.57312 | 32.2981 | 45.8353 | 36.52 | 41.94 |
| 1.5µM DOX+20µM CT | 3 | 38.7600 | 2.97597 | 1.71818 | 31.3673 | 46.1527 | 35.46 | 41.24 |
| 1.5µM DOX+40µM CT | 3 | 34.1567 | 5.41865 | 3.12846 | 20.6960 | 47.6173 | 29.47 | 40.09 |
| 5 µM ETO | 3 | 34.3633 | 5.48881 | 3.16897 | 20.7284 | 47.9983 | 29.51 | 40.32 |
| 5µM ETO+10µM CT | 3 | 37.0100 | 4.42101 | 2.55247 | 26.0276 | 47.9924 | 32.42 | 41.24 |
| 5µM ETO+20µM CT | 3 | 34.7500 | 5.64784 | 3.26078 | 20.7200 | 48.7800 | 30.95 | 41.24 |
| 5µM ETO+40µM CT | 3 | 29.0567 | 4.41502 | 2.54902 | 18.0891 | 40.0242 | 25.89 | 34.10 |
| $10^{-6}$µM VIN | 3 | 98.4133 | 4.94324 | 2.85398 | 86.1336 | 110.6930 | 93.89 | 103.69 |
| $10^{-6}$µM VIN+10µM CT | 3 | 85.4267 | 10.15101 | 5.86069 | 60.2102 | 110.6432 | 73.89 | 92.99 |
| $10^{-6}$µM VIN+20µM CT | 3 | 83.6333 | 4.80422 | 2.77372 | 71.6990 | 95.5677 | 79.58 | 88.94 |
| $10^{-6}$µM VIN+40µM CT | 3 | 69.9633 | 13.42917 | 7.75333 | 36.6034 | 103.3232 | 62.21 | 85.47 |
| Total | 48 | 62.8063 | 28.19277 | 4.06928 | 54.6199 | 70.9926 | 25.89 | 103.69 |

# VITA

Ms. Darinee Dangkong was born on November 02, 1985 in Chumphon, Thailand. She received her Bachelor's degree of Science (Industrial Microbiology) from the Faculty of Sciences, King Mongkut's Institute of Technology Ladkrabang, Bangkok, Thailand in 2008.

Publication

1.    Dangkong D, and Limpanasithikul W. 2013. Potentiating effect of citral on anticancer activities of doxorubicin, vincristine, and etoposide in human B-lymphoma cells. Acta Pharmacologica Sinica. 34 supp:4-4.

Poster Presentation

1.    Dangkong D, and Limpanasithikul W. 2013. Potentiating effect of citral on anticancer activities of doxorubicin, vincristine, and etoposide in human B-lymphoma cells.  The 12th Meeting of the Asia Pacific Federation of Pharmacologists. July 9-13, 2013, Shanghai, China.